CIVIL ENGINEERING STUDIES
STRUCTURAL RESEARCH SERIES NO. 221

ANALYSIS OF STATIC AND DYNAMIC RESPONSE OF SIMPLE-SPAN, MULTIGIRDER HIGHWAY BRIDGES

by
CENAP ORAN
and
A. S. VELETSOS

Issued as a Part
of the
ELEVENTH PROGRESS REPORT
of the
HIGHWAY BRIDGE IMPACT INVESTIGATION

PR Jun 61
11

UNIVERSITY OF ILLINOIS
URBANA, ILLINOIS
JULY 1961

ERRATA

Page	Line	Incorrect	Correct
16	8	$Y_n(\eta)$	$\left\{Y_n(\eta)\right\}$
24	3	$\leq$	$\geq$
43	1	$\sum_{j=0}^{p}$	$\sum_{i=0}^{p}$
70	9	degress	degrees
78	5	porportional	proportional
90	5	Deflection	Moment

ANALYSIS OF STATIC AND DYNAMIC RESPONSE OF SIMPLE-SPAN, MULTIGIRDER HIGHWAY BRIDGES

by

Cenap Oran

and

A. S. Veletsos

Issued as a Part of the Eleventh Progress Report of the
HIGHWAY BRIDGE IMPACT INVESTIGATION

Conducted by
THE ENGINEERING EXPERIMENT STATION
UNIVERSITY OF ILLINOIS

In cooperation with
THE DIVISION OF HIGHWAYS
STATE OF ILLINOIS
and
U. S. DEPARTMENT OF COMMERCE
BUREAU OF PUBLIC ROADS

University of Illinois
Urbana, Illinois
July 1961

TABLE OF CONTENTS

TABLE OF CONTENTS (continued)

LIST OF TABLES

LIST OF FIGURES

LIST OF FIGURES (continued)

LIST OF FIGURES (concluded)

I. INTRODUCTION

1. Object and Scope

The principal objective of this study was to develop a method for the analysis of the dynamic response of simple-span, right, multigirder highway bridges under the action of moving vehicles. In all previous analytical treatments of this problem, the bridge was represented by a beam. In the present study, it is analyzed as a plate continuous over flexible beams.

In the analysis of the beam problem, two different types of approximations have been used. The first refers to the deflection configuration of the beam during vibration, and the second to the mass distribution of the beam.

Inglis[6]*, who was mainly concerned with the study of the effects of pulsating forces, assumed that the beam responded in its fundamental mode of vibration, and expressed the dynamic deflection configuration as a half-sine wave. The same assumption was also made by Looney[7] and by Biggs, Suer, and Louw[1] in connection with "a simplified method" of analysis. The nature of the simplification made by Biggs et al is discussed briefly in Chapter III, Art. 4.3.

In an investigation reported by Hillerborg[3], the deflection configuration of the beam at any time was assumed to be proportional to the static deflection configuration due to the moving load. The same assumption was also made by Tung et al[13], and a modification of this assumption was used by Wen[14] in considering the effects of two-axle loads. All these assumptions amount to considering the bridge as a system having a single degree of freedom. As far as it is known, there has been no systematic study made to evaluate the sensitivity of the response to the assumptions referred to above.

---

* Unless otherwise noted, numbers in parentheses refer to the items in the list of References.

In the studies made by Huang and Veletsos[5] and by Fleming[2], the beam was analyzed as a multi-degree-of-freedom system. The flexibility of the beam was considered to be distributed as in the actual beam, but the distributed mass was replaced by a series of concentrated point masses. The degree of freedom of the mathematical model thus obtained is equal to the number of mass concentrations used.

In the present analysis of the bridge as a plate continuous over beams, both the bending and torsional stiffnesses of the beams are taken into account. The analysis involves two major steps:

(a) The determination of the instantaneous values of the dynamic forces acting on the bridge; these include the interacting forces between the vehicle and the bridge, and the inertia forces of the bridge itself.

(b) The evaluation of the deflections and moments produced in the bridge by these forces.

The second step, which is strictly a problem of statics, is solved by an application of the Rayleigh-Ritz energy procedure. The deflection of the structure is expressed as a series of functions that is capable of approximating any deflection configuration in both the longitudinal and transverse directions.

Although the problem of statics constitutes an indispensable part of the more general dynamic problem, it is discussed separately in this report as it is of interest in itself. In this connection, two computer programs have been developed for the ILLIAC, the digital computer of the University of Illinois. One of these may be used to determine influence surfaces for bending moment and deflection for a specified point of the beams of multigirder bridges, and the other to compute directly the moments and deflections produced in the beams by a three-axle truck loading. A complete description of the method of analysis, and brief descriptions of

the computer programs are presented in Chapter II. Also included in this chapter are comparisons between numerical results obtained with the present method and those obtained by Newmark and Siess[10] using an exact method of analysis.

The method used to evaluate the dynamic forces is essentially an extension of that used for the static problem. In contrast to the expression used to represent the static deflection, however, the dynamic deflection of the bridge is assumed to be a half-sine wave in the direction of the span. This assumption is the same as that used by Inglis[6] for beams. The vehicle is represented by a single-axle loading consisting of a sprung mass and two equal unsprung masses, or wheels. The so-called rolling effect of the vehicle is thus taken into account. The springs are assumed to be linearly elastic. No damping is considered for either the vehicle or the bridge.

The complete dynamic problem, including the determination of the dynamic forces and the computation of the effects produced by these forces in the bridge, has been programmed for the ILLIAC. This program and the method of solution of the dynamic problem are described in Chapter III, in which are also included a brief discussion of the accuracy of the assumptions involved in the analysis and comparisons between theoretical and experimental data. The details of derivation of the equations of motion are given in the Appendix.

A limited number of numerical solutions were obtained to study the influence of those parameters that cannot be considered when the bridge is analyzed as a beam. The results of this effort are presented and discussed in Chapter IV.

A brief summary of the significant results of this investigation is given in Chapter V.

2. Notation

The symbols used in this report are defined in the text when they first appear. For convenience of reference, the important ones are summarized here in alphabetical order. Some of the symbols were assigned more than one meaning; but this was done only when no confusion could arise.

a = span length of bridge, center to center of supports

$\{A_m\}$ = a column matrix of the unknown coefficients α_{mn}, defined in Eq. (2-16)

b = overall width of slab

b_1 = one-half the distance between the wheels of the vehicle model considered in the dynamic analysis.

$\{B_m\}$ = a column matrix of the known load terms β_{mn}, defined in Eq. (2-16)

c = b/a. ratio of sides of bridge

C_d, C_m = influence coefficients for deflection and moment, defined by Eqs. (2-46) and (2-47)

C_d', C_m' = dimensionless coefficients for deflection and moment produced by truck loading; See Eqs. (2-53) and (2-54)

$(C_d)_j$, $(C_m)_j$ = dimensionless coefficients for static values of deflection and moment produced by the interacting force at the j^{th} wheel; See Eqs. (3-79) and (3-80)

D = flexural rigidity of slab

$D_{i,j}$ = deflection produced in the i^{th} beam by the static value of the interacting force at the j^{th} wheel

$D^o_{i,s}$ = deflection produced in the i^{th} beam by the s^{th} component of the inertia forces as defined in Chapter III, Art. 5.3

e_j = dimensionless amplitude of roadway unevenness, defined by Eq. (3-35)

$(E_bI_b)_i$ = flexural rigidity of the i^{th} beam

$(E_bI_b)_{io}$ = flexural rigidity of the reference beam used to define w_o in Eq. (3-1)

$(E_bI_b)_o$ = flexural rigidity of an interior beam

E_bI_b = flexural rigidity of a beam, when all beams are identical

f_b = fundamental natural frequency of the bridge evaluated on the assumption that it acts as a beam

f_v = natural frequency of the vehicle for vertical motion on its springs

f_n = generalized coordinates for the bridge, defined by Eq. (3-1)

$[F_m]$ = symmetric square matrix defined in Eq. (2-16)

$(G_bJ_b)_i$ = torsional rigidity of the i^{th} beam

J = polar moment of inertia of the sprung mass about an axis through its center of gravity and normal to the transverse vertical plane

k = spring constant for one spring; also value of k_i for a bridge with identical beams

$k_i = \frac{(G_bJ_b)_i}{Db}$, dimensionless torsional rigidity factor for the i^{th} beam

k_o, k_1 = dimensionless torsional rigidity factors for an interior and an exterior beam, respectively

$K = (f_v/f_b)^2$

m = one unsprung mass

$(m_b)_i$ = mass per unit length of the i^{th} beam

m_o = number of terms used in the longitudinal direction in the computation of the static effects

m_1 = a positive integer defined in Eq. (3-35)

$M_{i,j}$ = moment corresponding to $D_{i,j}$

$M^o_{i,s}$ = moment corresponding to $D^o_{i,s}$

$\overline{M}_m$, $\overline{M}'_m$ = component moments, defined in Chapter II, Art. 3.2

n_o, n_1, n_2 = numbers of Y_n functions used for various purposes as defined in Chapter III, Art. 5.3

N = total number of integration steps for time required for the vehicle to cross the span; $\Delta\tau = 1/N$

N_1 = number of integration steps between print-outs

p = number of beam spacings

$\overline{p}_m$ = the m^{th} term in the Fourier series expansion of the load, defined by Eq. (2-2)

p_m = a function of η, defined by Eq. (2-2)

$\overline{p}_\mu$ = inertia force due to the mass of the slab

$\overline{p}_i$ = inertia force due to the mass of the i^{th} beam

q_n = generalized coordinate for bridge or vehicle

Q_m, Q'_m = quantities defined by Eqs. (2-45) and (2-52), respectively

$Q_{m,j}$ = quantities defined by Eq. (3-75)

t = time, measured from the instant the vehicle enters the bridge

T = kinetic energy; also shortest natural period of vibration of the system

T_b = $1/f_b$ = fundamental natural period of the bridge evaluated on the assumption that it acts as a beam

T_v = $1/f_v$ = natural period of the vehicle for vertical motion on its springs

u = dynamic rotation of the sprung mass in the transverse vertical plane (See Fig. 3)

U = potential energy of the gravity forces

v = speed of the vehicle

V = strain energy

w = static or dynamic deflection function for the bridge; dynamic deflection is measured from the static position of equilibrium of the bridge under the action of its own weight

w_o = a quantity defined in Eq. (3-1)

w_1 = roadway surface unevenness function, defined in Eq. (3-12)

w_2 = deflection of bridge under the action of its own weight

$\bar{w}_m$ = deflection component associated with load component $\bar{p}_m$

w_m = a function of η, defined in Eq. (2-3)

W = total weight of the dynamic vehicle model

W_1 = total weight of the rear axle of a three-axle truck

x, y = cartesian coordinates, defined in Fig. 1

Y_n = dimensionless functions of η

z = dynamic vertical displacement of the center of gravity of the sprung mass, measured from the static position of equilibrium (See Fig. 3)

z_o = initial dynamic compression of spring

z_s = static compression of spring

$\alpha = \frac{vT_b}{2a}$, dimensionless speed parameter

α_{mn} = unknown coefficients defined in Eq. (2-4)

β_{mn} = elements of the load matrix $\{B_m\}$

γ_i = dimensionless weight parameter for the i^{th} beam, defined by Eq. (3-36)

γ_o, γ_1 = value of γ_i for an interior and an exterior beam, respectively

γ = value of γ_i for a bridge with identical beams

δ_n = dimensionless coefficients defined in Eq. (3-4)

ζ = z/w_o, dimensionless generalized coordinate for the vehicle

ζ_s = z_s/w_o

η = y/b

θ = $u/b_1 w_o$, dimensionless generalized coordinate for the vehicle

λ_i = $(E_b I_b)_i / Db$, dimensionless flexural rigidity factor for the i^{th} beam

λ_{io} = value of λ_i for the reference beam used to define w_o in Eq. (3-1)

λ_o, λ_1 = values of λ_i for an interior and an exterior beam, respectively

λ = value of λ_i for a bridge with identical beams

μ = mass of slab per unit of area

ν = dimensionless weight parameter defined by Eq. (3-36)

ξ = x/a

ρ = dimensionless parameter defined by Eq. (3-43)

τ = $\frac{vt}{a}$, dimensionless time parameter

φ_n = dimensionless generalized coordinate for bridge

ω = dimensionless weight parameter defined by Eq. (3-36)

3. Acknowledgment

This study was made as part of the Illinois Cooperative Highway Research Program Project IHR-9, entitled "Impact on Highway Bridges". The investigation was conducted in the Civil Engineering Department of the University of Illinois in cooperation with the Division of Highways, State of Illinois, and the Bureau of Public Roads, U.S. Department of Commerce.

At the University of Illinois, the project was under the administrative supervision of W. L. Everitt, Dean of the College of Engineering,

Ross J. Martin, Director of the Engineering Experiment Station, N. M. Newmark, Head of the Department of Civil Engineering, and Ellis Danner, Director of the Illinois Cooperative Highway Research Program and Professor of Highway Engineering. At the Division of Highways of the State of Illinois, it was administered by R. R. Bartelsmeyer, Chief Highway Engineer, Theodore F. Morf, Engineer of Research and Planning, and W. E. Chastain, Sr., Engineer of Physical Research.

Guidance to the project staff has been provided by an Advisory Committee composed of the following:

Representing the Illinois Division of Highways:

W. E. Baumann, Engineer of Bridge and Traffic Structures

W. E. Chastain, Sr., Engineer of Physical Research

W. N. Sommer, Bureau of Design

Representing the Bureau of Public Roads:

Harold Allen, Chief, Division of Physical Research

E. L. Erickson, Chief, Bridge Division

Representing the University of Illinois:

S. J. Fenves, Instructor in Civil Engineering

J. E. Stallmeyer, Professor of Civil Engineering

Valuable advice has also been contributed by Fred Kellam, Regional Bridge Engineer, Bureau of Public Roads, and G. S. Vincent, Chief, Bridge Research Branch, Division of Physical Research, Bureau of Public Roads, who participated in the meetings of the Advisory Committee.

This project has been under the general direction of C. P. Siess, Professor of Civil Engineering, who has acted as Project Supervisor and as ex-officio chairman of the Project Advisory Committee. Since March 1956, the immediate supervision of the program has been the responsibility of A. S. Veletsos, Professor of Civil Engineering.

This report was prepared as a doctoral dissertation under the direction of Professor Veletsos.

The authors wish to thank T. Huang, Assistant Professor of Civil Engineering, and W. H. Walker, Research Assistant in Civil Engineering, for having provided helpful comments in the course of this study.

II. ANALYSIS OF STATIC PROBLEM

1. Characteristics of Structure and Assumptions

The structure considered is shown in Fig. 1. It consists of a reinforced concrete slab continuous over a number of parallel steel or reinforced concrete beams spanning in the direction of traffic and simply supported at the ends. The beam spacing may be arbitrary. The dimensions of the beams may vary from one beam to the next, but all beams are assumed to be prismatic. The slab is considered to be isotropic, of constant thickness, and simply supported at the abutments.

The assumptions made in the analysis are those embodied in the ordinary theory of medium-thick, elastic plates and in the ordinary theory of flexure of beams. In addition, it is assumed that:

(1) A beam and the slab over it deflect and rotate alike.

(2) There is no transfer of horizontal shear between the beams and the slab; thus the resultant of the normal stresses acting on a cross section of the slab or a beam is a pure couple. The effect of composite action may be taken into account approximately by modifying the flexural and the torsional stiffnesses of the supporting beams as suggested by Newmark and Siess[10a].

In considering the effect of the torsional resistance of the beams, it is assumed that the Saint-Venant theory of torsion is applicable. Poisson's ratio for the material of the slab is taken equal to zero, except when evaluating the rigidity of the slab.

The span length of the bridge, center to center of supports, is denoted by a, and the overall width of the slab by b. The position of a point on the bridge is specified in terms of dimensionless cartesian coordinates ξ and η, defined by the equations

$$\xi = x/a$$
$$\eta = y/b \qquad (2\text{-}1)$$

where x and y are as shown in Fig. 1.

2. Method of Analysis

2.1 General. The approach used is a combination of the Rayleigh-Ritz energy method, and the Levy method of analysis for rectangular plates simply supported along two opposite edges. The details of the method parallel those of the procedure used by Yamada and Veletsos for the computation of the natural frequencies and modes of vibration of highway bridges[15].

Let the vertical load on the structure, $p(\xi,\eta)$, be represented by a single trigonometric series of the form

$$p(\xi,\eta) = \sum_{m=1}^{\infty} \bar{p}_m = \sum_{m=1}^{\infty} p_m \sin m\pi\xi \qquad (2\text{-}2)$$

in which p_m is a function of η only. The deflection of the structure, $w(\xi,\eta)$, can then be expressed as

$$w(\xi,\eta) = \sum_{m=1}^{\infty} \bar{w}_m = \sum_{m=1}^{\infty} w_m \sin m\pi\xi \qquad (2\text{-}3)$$

where $\bar{w}_m = w_m \sin m\pi\xi$ is the deflection component corresponding to the load component $\bar{p}_m$, and w_m is a function of η only. The problem is then to determine the relationship between w_m and p_m.

In the procedure used, the deflection functions w_m are expressed in the form

$$w_m = \sum_{n} \alpha_{mn} Y_n \qquad (2\text{-}4)$$

where Y_n are known functions of the η-coordinate, and α_{mn} are coefficients which will be evaluated by minimizing the total energy of the system. Let the functions Y_n be dimensionless; then the coefficients α_{mn} have the dimension of length.

In the following development, the functions Y_n are considered to be arbitrary. The specific functions used in this study are presented later.

2.2 Energy of the System. The energy expressions presented in this section correspond to the deflection component $\bar{w}_m = w_m \sin m\pi\xi$ and the associated load component $\bar{p}_m = p_m \sin m\pi\xi$.

Strain Energy. The strain energy of the system, V_m, may be written in the form

$$V_m = (V_m)_s + (V_m)_b \tag{2-5}$$

where $(V_m)_s$ is the strain energy of the slab, and $(V_m)_b$ is the strain energy of the beams. The subscripts m are used as a reminder that these energies correspond to the m^{th} component of the deflection, $\bar{w}_m$. For a value of Poisson's ratio equal to zero, $(V_m)_s$ is given by the equation

$$(V_m)_s = \frac{Dab}{2a^4}\int_0^1\int_0^1 \left[\left(\frac{\partial^2\bar{w}_m}{\partial\xi^2}\right)^2 + \frac{2}{c^2}\left(\frac{\partial^2\bar{w}_m}{\partial\xi\partial\eta}\right)^2 + \frac{1}{c^4}\left(\frac{\partial^2\bar{w}_m}{\partial\eta^2}\right)^2\right] d\xi d\eta \tag{2-6}$$

where $c = b/a$, and D is the flexural rigidity per unit width of the slab. On replacing $\bar{w}_m$ by $w_m \sin m\pi\xi = \sum_n \alpha_{mn} Y_n \sin m\pi\xi$, Eq. (2-6) becomes

$$(V_m)_s = \frac{m^4\pi^4 D}{a^4}\frac{ab}{4}\left[\sum_n\sum_s \alpha_{mn}\alpha_{ms}\int_0^1 Y_n Y_s\, d\eta + \frac{2}{\pi^2(mc)^2}\sum_n\sum_s \alpha_{mn}\alpha_{ms}\int_0^1 Y_n' Y_s'\, d\eta\right.$$

$$\left. + \frac{1}{\pi^4(mc)^4}\sum_n\sum_s \alpha_{mn}\alpha_{ms}\int_0^1 Y_n'' Y_s''\, d\eta\right] \tag{2-7}$$

where a prime denotes one differentiation with respect to η.

The strain energy of the beams, $(V_m)_b$, is given by the equation

$$(V_m)_b = \sum_{i=0}^{p}\left[\frac{(E_bI_b)_i}{2a^3}\int_0^1\left(\frac{\partial^2\bar{w}_m}{\partial\xi^2}\right)_i^2 d\xi + \frac{(G_bJ_b)_i}{2ab^2}\int_0^1\left(\frac{\partial^2\bar{w}_m}{\partial\xi\partial\eta}\right)_i^2 d\xi\right] \tag{2-8}$$

where $(E_bI_b)_i$ and $(G_bJ_b)_i$ denote the flexural rigidity and the torsional rigidity of the i^{th} beam, respectively, and the subscript i associated with

the integrands means "evaluated at the location of the i^{th} beam". By substituting $\bar{w}_m = \sum_n \alpha_{mn} Y_n \sin m\pi\xi$ into Eq. (2-8), multiplying and dividing the right-hand side of the resulting equation by Db, one obtains the equation

$$(V_m)_b = \frac{m^4\pi^4 D}{a^4}\frac{ab}{4}\sum_{i=0}^{p}\left[\lambda_i \sum_n \sum_s \alpha_{mn}\,\alpha_{ms}\,(Y_n)_i\,(Y_s)_i + \frac{k_i}{\pi^2(mc)^2}\sum_n\sum_s \alpha_{mn}\,\alpha_{ms}\,(Y'_n)_i\,(Y'_s)_i\right] \quad (2\text{-}9)$$

in which $(Y_n)_i$ is the ordinate of the function Y_n at the location of the i^{th} beam, and λ_i and k_i are dimensionless rigidity factors defined by the equations

$$\lambda_i = \frac{(E_b I_b)_i}{Db} \quad (2\text{-}10)$$

$$k_i = \frac{(G_b J_b)_i}{Db} \quad (2\text{-}11)$$

The strain energy of the system, V_m, can be rewritten in the condensed form,

$$V_m = \frac{m^4\pi^4 D}{a^4}\frac{ab}{4}\bar{F}_m(\alpha_{mn}\,\alpha_{ms}) \quad (2\text{-}12)$$

where $\bar{F}_m(\alpha_{mn}\,\alpha_{ms})$ is a quadratic form of the unknown coefficients α_{mn}.

Potential Energy of External Forces. The potential energy, U_m, of the load component $\bar{p}_m$ through the associated deflection component $\bar{w}_m$ is given by the equation

$$U_m = -ab\int_0^1\int_0^1 \bar{w}_m\bar{p}_m\,d\xi d\eta = -ab\int_0^1\int_0^1 (w_m \sin m\pi\xi)(p_m \sin m\pi\xi)\,d\xi d\eta \quad (2\text{-}13)$$

By substituting Eq. (2-4) into Eq. (2-13), one obtains

$$U_m = -\frac{ab}{2}\sum_n \alpha_{mn}\int_0^1 p_m Y_n\,d\eta \quad (2\text{-}14)$$

Total Energy of System. The total energy of the system, I_m, is the sum of Eqs. (2-12) and (2-14), i.e.,

$$I_m = \frac{m^4\pi^4 D}{a^4}\frac{ab}{4}\bar{F}_m(\alpha_{mn}\alpha_{ms}) - \frac{ab}{2}\sum_n \alpha_{mn}\int_o^1 p_m Y_n \, d\eta \tag{2-15}$$

2.3 Equations for Computation of α_{mn}. The condition that I_m be a minimum yields a system of linear algebraic equations of the form

$$\{F_m\}\{A_m\} = \{B_m\} \tag{2-16}$$

in which $\{A_m\}$ is a column matrix of the unknown coefficients α_{mn}, $\{B_m\}$ is a column matrix of known load terms, and $[F_m]$ is a symmetric matrix, the order of which is equal to the number of Y_n functions used in Eq. (2-4). As before, the subscript m indicates that these matrices are functions of the integer m. The element $f_{m,ns}$ in the n^{th} row and s^{th} column of the $[F_m]$ matrix is given by the equation

$$f_{m,ns} = \left[\int_o^1 Y_n Y_s \, d\eta + \frac{2}{\pi^2(mc)^2}\int_o^1 Y_n' Y_s' \, d\eta + \frac{1}{\pi^4(mc)^4}\int_o^1 Y_n'' Y_s'' \, d\eta\right]$$

$$+\sum_{i=o}^{P}\left[\lambda_i (Y_n)_i (Y_s)_i + \frac{k_i}{\pi^2(mc)^2}(Y_n')_i (Y_s')_i\right] \tag{2-17}$$

The element β_{mn} in the n^{th} row of the $\{B_m\}$ matrix is

$$\beta_{mn} = \frac{a^3}{m^4\pi^4 Db} ab \int_o^1 p_m Y_n \, d\eta \tag{2-18}$$

For a concentrated force P applied at point $\xi = \xi_1$, $\eta = \eta_1$,

$$b\int_o^1 p_m Y_n \, d\eta = \frac{2P}{a}\sin m\pi\xi_1 \, Y_n(\eta_1) \tag{2-19}$$

and, therefore, Eq. (2-18) becomes

$$\beta_{mn} = \frac{2\,Pa^3}{\pi^4 Db}\frac{\sin m\pi\xi_1}{m^4} Y_n(\eta_1) \tag{2-20}$$

The solution of the system of equations (2-16) gives the values of α_{mn}, which are then used to determine the deflection component $\bar{w}_m = w_m \sin m\pi\xi$. In general, Eqs. (2-16) are solved for as many values of m as may be necessary in a particular application. The total deflection, w, of the structure is then determined from Eq. (2-3) by superposing the component deflections. The latter equation may be rewritten in one of the following forms

$$w = \sum_m \left(\sum_n \alpha_{mn} Y_n \right) \sin m\pi\xi = \sum_m \left\{ A_m \right\} \cdot \left\{ Y_n(\eta) \right\} \sin m\pi\xi \qquad (2\text{-}21)$$

where $Y_n(\eta)$ is a column matrix of the values of the Y_n functions evaluated at the point under consideration, and a dot denotes a scalar product.

It is assumed that the set of Y_n functions are capable of representing any deflection configuration in the interval $0 \leq \eta \leq 1$. The functions Y_{-1}, Y_1, Y_3, ... are considered to be symmetric about $\eta = 1/2$, whereas Y_0, Y_2, Y_4, ... are considered to be antisymmetric.

If Y_n and Y_s represent a pair of symmetric and antisymmetric functions, then

$$\int_0^1 Y_n Y_s \, d\eta = \int_0^1 Y_n' Y_s' \, d\eta = \int_0^1 Y_n'' Y_s'' \, d\eta = 0 \qquad (2\text{-}22)$$

If, in addition, the structure is symmetric about the longitudinal centerline, i.e.

$$\begin{aligned} \eta_i &= 1 - \eta_{p-i} \\ \lambda_i &= \lambda_{p-i} \\ k_i &= k_{p-i} \end{aligned} \qquad (2\text{-}23)$$

for all values of i, then

$$\sum_{i=0}^{p} \lambda_i (Y_n)_i (Y_s)_i = \sum_{i=0}^{p} k_i (Y_n')_i (Y_s')_i = 0 \qquad (2\text{-}24)$$

From Eq. (2-17) it follows that, for such a pair of functions, $f_{m,ns} = 0$ and, therefore, the elements of $[F_m]$ form a checkerboard pattern, with every other element in each row and each column equal to zero. The non-zero elements of $[F_m]$ correspond either to symmetric or to antisymmetric pairs of functions. The matrix $[F_m]$ can, therefore, be split into two submatrices, one formed by the symmetric functions and the other by the antisymmetric functions. The unknown column matrix $\{A_m\}$ in Eq. (2-16) can then be determined more conveniently by solving the two sets of equations separately.

2.4 Reciprocal Relations. From Maxwell's theorem of reciprocal deflections it follows that the deflection of the structure at point 1 (ξ_1, η_1) due to a load P applied at point 2 (ξ_2, η_2) is equal to the deflection at point 2 due to the same load P applied at point 1. Moreover, for a plate having two opposite edges simply-supported, it has been shown[9] that the curvature in the direction of the simply supported span, $\frac{\partial^2 w}{\partial x^2} = \frac{1}{a^2} \frac{\partial^2 w}{\partial \xi^2}$, at point 1 due to a load P applied at point 2 is equal to the corresponding quantity at point 2 due to the same load applied at point 1.

It is the purpose of this section to show that, even for the approximate method of analysis used in this study, these relations hold true regardless of the nature of the Y_n functions considered or the number of functions used.

The coefficients α_{mn} corresponding to a load P at point 1 are obtained as solutions of the equations

$$[F_m]\{A_m\}_1 = \{B_m\}_1 \tag{2-25}$$

which, by making use of Eq. (2-20), can be rewritten as

$$[F_m]\{A_m\}_1 = \frac{2Pa^3}{\pi^4 Db} \frac{\sin m\pi\xi_1}{m^4} \left\{Y_n(\eta_1)\right\} \tag{2-26}$$

The matrix $\{A_m\}_1$ may now be expressed as

$$\{A_m\}_1 = \frac{2Pa^3}{\pi^4 Db} \frac{\sin m\pi\xi_1}{m^4} [G_m] \left\{Y_n(\eta_1)\right\} \tag{2-27}$$

where $[G_m]$ is the inverse of $[F_m]$. The resulting deflection at point 2, $w_{2,1}$, is obtained by substituting Eq. (2-27) into Eq. (2-21),

$$w_{2,1} = \frac{2Pa^3}{\pi^4 Db} \sum_m \frac{1}{m^4} \sin m\pi\xi_1 \sin m\pi\xi_2 [G_m] \left\{Y_n(\eta_1)\right\} \cdot \left\{Y_n(\eta_2)\right\} \tag{2-28}$$

The deflection of the structure at point 1 due to a load P at point 2 may be expressed in similar manner as

$$w_{1,2} = \frac{2Pa^3}{\pi^4 Db} \sum_m \frac{1}{m^4} \sin m\pi\xi_1 \sin m\pi\xi_2 [G_m] \left\{Y_n(\eta_2)\right\} \cdot \left\{Y_n(\eta_1)\right\} \tag{2-29}$$

If A is a symmetric matrix, and X and Y are column matrices, it can readily be shown that

$$AX \cdot Y = AY \cdot X \tag{2-30}$$

Since $[F_m]$ in Eq. (2-25) is symmetric, its inverse, $[G_m]$, is also symmetric. From Eq. (2-30) it follows then that,

$$[G_m]\left\{Y_n(\eta_1)\right\} \cdot \left\{Y_n(\eta_2)\right\} = [G_m]\left\{Y_n(\eta_2)\right\} \cdot \left\{Y_n(\eta_1)\right\} \tag{2-31}$$

Therefore, Eqs. (2-28) and (2-29) are identical, i.e.

$$w_{2,1} = w_{1,2} \tag{2-32}$$

The general expression for the curvature in the ξ-direction, $(\frac{\partial^2 w}{\partial x^2})$, is obtained from Eq. (2-21) by differentiation. Noting that

$$\frac{\partial^2 w}{\partial x^2} = \frac{1}{a^2} \frac{\partial^2 w}{\partial \xi^2} = -\frac{\pi^2}{a^2} \sum_m m^2 \left\{A_m\right\} \cdot \left\{Y_n(\eta)\right\} \sin m\pi\xi \tag{2-33}$$

and making use of Eq. (2-27), one finds that

$$\left(\frac{\partial^2 w}{\partial x^2}\right)_{2,1} = -\frac{2\,Pa}{\pi^2 Db}\sum_m \frac{1}{m^2}\sin m\pi\xi_1 \sin m\pi\xi_2\,[G_m]\left\{Y_n(\eta_1)\right\}\cdot\left\{Y_n(\eta_2)\right\} \tag{2-34}$$

and

$$\left(\frac{\partial^2 w}{\partial x^2}\right)_{1,2} = -\frac{2\,Pa}{\pi^2 Db}\sum_m \frac{1}{m^2}\sin m\pi\xi_1 \sin m\pi\xi_2\,[G_m]\left\{Y_n(\eta_2)\right\}\cdot\left\{Y_n(\eta_1)\right\} \tag{2-35}$$

where the subscripts (2,1) and (1,2) have the same meaning as in Eqs. (2-28) and (2-29). By virtue of Eq. (2-31), it follows now that

$$\left(\frac{\partial^2 w}{\partial x^2}\right)_{2,1} = \left(\frac{\partial^2 w}{\partial x^2}\right)_{1,2} \tag{2-36}$$

2.5 Deflection Functions Used. In the present study, the Y_n functions were taken as follows:

$$Y_n = \begin{cases} 1 & \text{for } n = -1 \\ 0.5 - \eta & \text{for } n = 0 \\ \sin n\pi\eta & \text{for } n \geq 1 \end{cases} \tag{2-37}$$

Note that, Y_{-1}, Y_1, Y_3, ... are symmetric and Y_0, Y_2, Y_4, ... are antisymmetric with respect to the longitudinal centerline of the structure, $\eta = 0.5$.

The elements of $[F_m]$ corresponding to these functions are obtained by substituting Eq. (2-37) into Eq. (2-17). The results for a symmetric structure are summarized in the following table. (See p. 20.)

The elements for the first four symmetric and the first four antisymmetric functions are also tabulated in Tables 1 and 2, given at the end of the text. In the derivation of these equations it has implicitly been assumed that λ_i and k_i are finite quantities.

ELEMENTS $f_{m,ns}$ OF MATRIX $[F_m]$

Values of n and s	Expression for $f_{m,ns}$
(a) Elements Corresponding to Symmetric Functions Y_n	
$n = s = -1$	$1 + \sum_{i=0}^{p} \lambda_i$
$n = -1;\ s \neq -1$	$\frac{2}{\pi s} + \sum_{i=0}^{p} \lambda_i \sin\left(s\pi \frac{i}{p}\right)$
$n = s \neq -1$	$\frac{1}{2}\left[1 + \frac{n^2}{(mc)^2}\right]^2 + \sum_{i=0}^{p} \left[\lambda_i \sin^2\left(n\pi \frac{i}{p}\right) + \frac{n^2 k_i}{(mc)^2} \cos^2\left(n\pi \frac{i}{p}\right)\right]$
$n \neq s \neq -1$	$\sum_{i=0}^{p} \left[\lambda_i \sin\left(n\pi \frac{i}{p}\right) \sin\left(s\pi \frac{i}{p}\right) + \frac{ns\,k_i}{(mc)^2} \cos\left(n\pi \frac{i}{p}\right) \cos\left(s\pi \frac{i}{p}\right)\right]$
(b) Elements Corresponding to Antisymmetric Functions Y_n	
$n = s = 0$	$\left[\frac{1}{12} + \frac{2}{\pi^2 (mc)^2}\right] + \sum_{i=0}^{p} \left[\lambda_i \left(\frac{p-2i}{2p}\right)^2 + \frac{k_i}{\pi^2 (mc)^2}\right]$
$n = 0;\ s \neq 0$	$\frac{1}{s\pi} + \sum_{i=0}^{p} \left[\lambda_i \left(\frac{p-2i}{2p}\right) \sin\left(s\pi \frac{i}{p}\right) - \frac{s k_i}{\pi (mc)^2} \cos\left(s\pi \frac{i}{p}\right)\right]$
$n = s \neq 0$	$\frac{1}{2}\left[1 + \frac{n^2}{(mc)^2}\right]^2 + \sum_{i=0}^{p} \left[\lambda_i \sin^2\left(n\pi \frac{i}{p}\right) + \frac{n^2 k_i}{(mc)^2} \cos^2\left(n\pi \frac{i}{p}\right)\right]$
$n \neq s \neq 0$	$\sum_{i=0}^{p} \left[\lambda_i \sin\left(n\pi \frac{i}{p}\right) \sin\left(s\pi \frac{i}{p}\right) + \frac{ns k_i}{(mc)^2} \cos\left(n\pi \frac{i}{p}\right) \cos\left(s\pi \frac{i}{p}\right)\right]$

3. Problems Considered for Solution on ILLIAC

3.1 General. The method described in the preceding sections has been programmed for the ILLIAC to analyze bridges having from three to seven uniformly spaced prismatic beams. The beams are assumed to be arranged symmetrically with respect to the longitudinal centerline of the structure. All interior beams are considered to be identical. The exterior beams on either side of the bridge are assumed to be located along the edge of the slab and, while identical to one another, they may be different from the interior beams. The characteristics of these bridges are defined in terms of the following dimensionless parameters:

$\mathbf{p}$ = number of beam spacings

$c = b/a$ = ratio of sides of bridge

$\lambda_o = \dfrac{(E_b I_b)_o}{Db}$ = flexural rigidity factor for an interior beam

$\lambda_1 = \dfrac{(E_b I_b)_1}{Db}$ = flexural rigidity factor for an exterior beam

$k_o = \dfrac{(G_b J_b)_o}{Db}$ = torsional rigidity factor for an interior beam

$k_1 = \dfrac{(G_b J_b)_1}{Db}$ = torsional rigidity factor for an exterior beam

Two separate programs have been developed. The first may be used to determine influence surfaces for deflection and bending moment in the beams due to a unit concentrated force applied at various points on the bridge. The second program computes the deflections and bending moments in the beams produced by a three-axle truck loading. The capabilities of these programs and some computational details are described in the following sections.

3.2 Program for Influence Surfaces. This program calculates ordinates of influence surfaces for deflection and bending moment in a beam due to a unit concentrated load located at points directly over the beams and midway between beams along any desired number of equally spaced transverse sections.

These ordinates are determined by application of the reciprocal relations discussed in Art. 2.4. Let point 1 with coordinates (ξ_1, η_1) be located on beam i, and let it be desired to determine the influence ordinate for deflection and bending moment at this point due to a concentrated load applied at some other point 2. These quantities will be denoted by $w_{1,2}$ and $M_{1,2}$, respectively.

By virtue of Eq. (2-32), $w_{1,2}$ may be determined by considering a concentrated unit force at point 1 and evaluating the deflection $w_{2,1}$ produced at point 2. The influence surface for deflection at point 1 may then be constructed by evaluating the deflection $w_{2,1}$ at as many different points 2 as may be needed in a particular application.

In a similar manner, by virtue of Eq. (2-36), the moment $M_{1,2}$ may be expressed as

$$M_{1,2} = - (E_b I_b)_i \left(\frac{\partial^2 w}{\partial x^2}\right)_{2,1} \qquad (2\text{-}38)$$

where $(E_b I_b)_i$ is the flexural rigidity of the beam on which point 1 is located. It should be noted that in the above equation, the moment is defined at point 1, whereas the curvature is defined at point 2. It follows that the

influence ordinates for moment at point 1, just like those for deflection, can be determined in terms of the effects produced by a concentrated unit force applied at that point.

The parameters which must be specified in using this program include the dimensionless parameters summarized in Art. 3.1, the coordinates (ξ_1, η_1) of the point for which the influence surface is desired, the number of equally spaced transverse sections at which the influence ordinates are to be evaluated, the number of Y_a functions used, and the number of terms considered in the Fourier series expansion of the load. The last two parameters have been treated as problem parameters so that they can be varied. The ranges of parameters that may be considered are such as to include most practical structures.

In general, the moments in the beams, M, are computed from the equation

$$M = \sum_{m=1}^{\infty} \bar{M}_m \tag{2-39}$$

by considering a finite number of terms $m = m_o$. In this equation $\bar{M}_m$ represents the moment produced by the component load $\bar{p}_m$. It has been observed that for the beam immediately beneath a concentrated load this series does not converge rapidly and, unless a large number of terms are considered, the result may not be accurate. The convergence of this series may be accelerated, however, by the following procedure.

Let M' be the value of the moment computed on the assumption that the concentrated force is carried entirely by the loaded beam without any

transverse distribution. For a force P applied at $\xi = \xi_1$, the moment at ξ may be expressed either in a closed form, as

$$\begin{aligned} M' &= Pa\ \xi_1(1 - \xi) \quad \text{when } \xi \leq \xi_1 \\ &= Pa\ \xi(1 - \xi_1) \quad \text{when } \xi \leq \xi_1 \end{aligned} \tag{2-40}$$

or in the form of a Fourier series as

$$M' = \sum_{m=1}^{\infty} \bar{M}'_m \tag{2-41}$$

where

$$\bar{M}'_m = \frac{2\ Pa}{m^2\pi^2} \sin m\pi\xi_1 \sin m\pi\xi \tag{2-42}$$

By subtracting the two sides of Eq. (2-41) from the corresponding sides of Eq. (2-39), one obtains the expression

$$M = M' - \sum_{m=1}^{\infty} (\bar{M}'_m - \bar{M}_m) \tag{2-43}$$

where M' is assumed to be determined from Eq. (2-40). Although the series $\Sigma\ \bar{M}'_m$ and $\Sigma\ \bar{M}_m$ individually converge rather slowly, it turns out that their difference converges rapidly. Accordingly, the value of M computed from Eq. (2-43) by considering a finite number of terms $m = m_o$ is closer to the exact value than is the one obtained from Eq. (2-39), using the same number of terms. The computer program has been prepared so as to compute and print out the values obtained both from Eq. (2-39) and from Eq. (2-43).

The fact that, for the higher values of m, the moments $\bar{M}_m$ and $\bar{M}'_m$ are close to one another may be appreciated physically by noting that as m increases the effective span length of the structure, a/m, decreases, and the load component $\bar{p}_m$ tends to be carried by a narrow strip of the structure immediately beneath the load without substantial transverse distribution.

A general flow diagram for the program is shown in Fig. 4. The operations indicated in the first column of this diagram are performed once for each problem, those on the second column are performed once for each value of m, and those on the third column are performed twice for each value of m. The numbers in parentheses above the boxes designate the routines used. Those operations not identified by any numbers are performed by the control routine (1002). In general, the flow diagram is self-explanatory. Some additional details are discussed in the following paragraphs. For a more detailed description of the program the reader is referred to the complete write-up deposited in the ILLIAC Library of the Civil Engineering Department.*

The quantities β_n evaluated by Routine (1003) are defined by the equation

$$\beta_n = \frac{2\lambda_o}{\pi^2} Y_n(\eta_1) \qquad (2\text{-}44)$$

These quantities are proportional to the elements β_{mn} of the load matrix $\{B_m\}$ in Eq. (2-16). For a concentrated force, the elements β_{mn} are given by Eq. (2-20), where P = 1. It should be noted that the quantities β_n are independent of m and are evaluated only once for a given problem.

---

* "ILLIAC Program 1592 - Moments and Deflections of Multigirder I-Beam Highway Bridges", by Cenap Oran, University of Illinois, Civil Engineering Department, July 1960. It should be noted that the symbols λ_o, λ_1, k_o, and k_1 used in this write-up have different meanings from those used in this report.

The elements of $[F_m]$ are evaluated by three different routines. Routine (1005) is used to compute the first row of the submatrix corresponding to symmetrical functions Y_n, routine (1007) computes the first row of the submatrix corresponding to antisymmetric functions, and routine (1008), entered twice for each value of m, computes the remaining rows. For a symmetric load, only the submatrix corresponding to symmetric functions is evaluated.

The quantities Q_m computed with routine (1010) are defined by the equation

$$Q_m = \frac{\sin m\pi\xi_1}{m^2} \sum_n \alpha'_{mn} Y_n(\eta) \qquad (2\text{-}45)$$

They are evaluated for values of

$$\eta = \frac{i}{2p} \text{ , where } i = 0,\ 1,\ 2,\ \ldots\ 2p$$

The coefficients α'_{mn} in Eq. (2-45) are proportional to the coefficient α_{mn} defined by Eq. (2-4). In essence, they represent the solution of Eq. (2-16) with the elements β_{mn} of the load matrix $\{B_m\}$ replaced by β_n.

The influence ordinates for deflection, w, and moment, M, are expressed in the form

$$w = C_d \frac{Pa^3}{(E_b I_b)_o} \qquad (2\text{-}46)$$

$$M = C_m Pa \qquad (2\text{-}47)$$

where C_d and C_m are dimensionless coefficients and $(E_b I_b)_o$ is the flexural rigidity of the interior beam. The coefficients C_d and C_m are related to the quantities Q_m as follows

$$C_d = \frac{1}{\pi^2} \sum_{m=1}^{m_o} \frac{1}{m^2} Q_m \sin m\pi\xi \qquad (2\text{-}48)$$

$$C_m = \frac{\lambda_i}{\lambda_o} \sum_{m=1}^{m_o} Q_m \sin m\pi\xi \qquad (2\text{-}49)$$

where λ_i is the flexural rigidity factor of the beam on which point 1 is located.

It is to be noted that the moment computed from Eq. (2-49) corresponds to that obtained by use of Eq. (2-39). The improved values of moment for the loaded beams are determined by use of Eq. (2-43).

This program utilizes the entire Williams (fast) memory of the ILLIAC which has a capacity of 1024 words. The maximum value of m that can be considered is less than $104/(2p+1)$, this restriction being due to the number of storage locations available in the Williams memory. For a five-girder bridge, this limit corresponds to $m_o = 11$.

The machine time required to obtain a solution depends on such factors as the number of Y_n functions and m-terms used, as well as the number of sections along which the influence ordinates are evaluated. The computation of one complete set of influence surfaces for moment and deflection takes from 0.5 to 1.5 minutes.

3.3 Program for Truck Loading. This program calculates the deflections and bending moments produced in the beams of the structure, along a prescribed transverse section, by a three-axle truck loading. The deflections and moments may be evaluated for any prescribed number of longitudinal positions of the vehicle.

The force exerted by each axle is represented by two equal concentrated forces. It is assumed that the longitudinal centerline of the

truck is parallel to the beams and that the spacing between consecutive axles is the same. For an H-S truck loading, the latter spacing represents the most severe condition for a simply supported bridge.

Let W_1, W_2, and W_3 be the total weights, and ξ_1, ξ_2, and ξ_3 be the ξ-coordinates for the rear, middle and front axles, respectively. For convenience we let

$$W_2 = \omega_2 W_1 \qquad W_3 = \omega_3 W_1$$

$$\xi_2 = \xi_1 + \sigma \qquad \xi_3 = \xi_1 + 2\sigma$$

For this loading, the element β_{mn} of the load matrix $\{B_m\}$ in Eq. (2-16) is obtained from Eq. (2-20) by superimposing the contributions of the six wheel loads. The resulting expression is

$$\beta_{mn} = \frac{W_1 a^3}{\pi^4 Db} \frac{1}{m^4} \left[\sin m\pi\xi_1 + \omega_2 \sin m\pi(\xi_1+\sigma) + \omega_3 \sin m\pi(\xi_1+2\sigma) \right] \left[Y_n(\eta_1) + Y_n(\eta_2) \right] \qquad (2\text{-}50)$$

where η_1 and η_2 are the η-coordinates of the wheels on either side of the truck. For an axle to be located on the structure, the value of the ξ-coordinate for that axle should range between 0 and 1.

The organization of this program is very similar to that described in the preceding article. A general flow diagram is given in Fig. 5 and should be self-explanatory. The quantities β_n' and Q_m' referred to in this program are defined by the following equations

$$\beta_n' = \frac{\lambda_o}{\pi^2} \left[Y_n(\eta_1) + Y_n(\eta_2) \right] \qquad (2\text{-}51)$$

$$Q'_m = \frac{1}{m^2} \sin m\pi\xi \sum_n \alpha''_{mn} Y_n(\eta_i) \qquad (2\text{-}52)$$

where ξ and η_i are the coordinates of the points where the effects are to be evaluated, and the coefficients α''_{mn} represent the solution of Eq. (2-16) with the elements β_{mn} of the load matrix $\{B_m\}$ replaced by β'_n. The subscript i on η denotes that the effects are evaluated only for the beams.

The deflections, w, and moments, M, are expressed in the form

$$w = C'_d \frac{W_1 a^3}{(E_b I_b)_o} \qquad (2\text{-}53)$$

$$M = C'_m W_1 a \qquad (2\text{-}54)$$

where C'_d and C'_m are dimensionless coefficients, and are related to the quantities Q'_m as follows

$$C'_d = \frac{1}{\pi^2} \sum_{m=1}^{m_o} \frac{1}{m^2} Q'_m \left[\sin m\pi\xi_1 + \omega_2 \sin m\pi(\xi_1+\sigma) + \omega_3 \sin m\pi(\xi_1+2\sigma) \right] \qquad (2\text{-}55)$$

$$C'_m = \frac{\lambda_i}{\lambda_o} \sum_{m=1}^{m_o} Q'_m \left[\sin m\pi\xi_1 + \omega_2 \sin m\pi(\xi_1+\sigma) + \omega_3 \sin m\pi(\xi_1+2\sigma) \right] \qquad (2\text{-}56)$$

Note that, in order for the last two equations to be true, the ξ-coordinates for all three axles must range between 0 and 1; this condition is checked by the program, and those axles that may be located outside the bridge are disregarded in Eqs. (2-55) and (2-56).

The program has been written so that after the deflections and moments for the initial position of the truck have been computed and printed out, the truck is advanced in the longitudinal direction by a distance $\Delta x = a\,\Delta\xi$, and the deflections and moments are computed and printed out for this new position of the truck. This operation is continued until the specified number of truck positions have been considered.

The parameters that must be specified for a solution include the six parameters characterizing the structure and summarized in Art. 3.1, the parameters ξ_1, σ, η_1, η_2, ω_2 and ω_3 that define the characteristics and the initial position of the truck, the ξ-coordinate of the transverse section where the effects are to be evaluated, the total number of truck positions and the increment $\Delta\xi$ to be considered, the number of Y_n functions used, and the number of load components used in the longitudinal direction.

This program, like the one described in the preceding article, utilizes the entire William's memory of the ILLIAC. The maximum value of m that can be considered is less than $108/(p + 1)$. For a five-girder bridge, this corresponds to $m_o = 21$. It is important to note, however, that in this program no provision has been made to accelerate the rate of convergence of the moments.

The machine time required to obtain a solution depends on the problem parameters. For the practical ranges of the parameters, the solution of a problem for several positions of the truck takes from 0.5 to 1.5 minutes. This time is affected primarily by the value of m_o and the number of Y_n functions used.

4. Convergence and Accuracy of Method

As an illustration of the accuracy of the method and the rate of convergence of the solutions, there are presented in this section influence coefficients for deflections and bending moments for three different bridges, each having five uniformly spaced, identical beams, as shown in Fig. 2. These solutions, obtained by considering an increasing number of terms in the series expression for the deflection of the structure, are compared with those reported previously by Newmark and Siess[10]. The latter results were obtained by an exact method.

The characteristics of the bridges investigated are defined by the following parameters:*

Bridge 1: $c = 0.4$ $\lambda = 12.5$

Bridge 2: $c = 0.4$ $\lambda = 50$

Bridge 3: $c = 0.8$ $\lambda = 12.5$

The torsional rigidity of the beams was taken equal to zero in all cases.

In tables 3 through 6 are given influence coefficients for deflections and moments for Bridges 1 and 3. These quantities were determined using a constant number of load terms ($m_o = 11$), and a variable number of Y_n functions. The symbol n_o in these tables represents the number of Y_n functions in excess of Y_{-1} and Y_o. The numbers in parentheses were reproduced from Ref. (10).

It can be seen from these tables that the results obtained by the present method, in general, converge quite rapidly with increasing values of n_o. This rapid rate of convergence and the excellent agreement between the

---

* The values of the corresponding parameters used in Ref. (10) in the notation of that reference, are:

Bridge 1: $b/a = 0.1$ $H = 5$
Bridge 2: $b/a = 0.1$ $H = 20$
Bridge 3: $b/a = 0.2$ $H = 10$

present results and those reported in Ref. (10), inspires much confidence in the accuracy of the method employed.*

It is of interest to note that the influence coefficients for Bridge 3 converge less rapidly than those of Bridge 1. This can be explained in terms of the physical characteristics of the two structures. Bridge 1, being a relatively narrow structure with high transverse stiffness, has a fairly smooth and uniform distribution of deflection in the transverse direction. This may be represented by a small number of Y_n functions. Bridge 3, on the other hand, being fairly flexible, requires a much larger number of Y_n terms to specify its transverse configuration.

Influence coefficients for the same two structures were also computed using a constant number of Y_n functions ($n_o = 8$), but a variable number of terms in the trigonometric series expression of the load ($m_o = 1$ to 11). The results, summarized in Tables 7 to 10, converge fairly rapidly with increasing value of m. It is important to note, however, that, of the moments presented in Tables 3 through 10, those for the loaded beams were computed by application of Eq. (2-43). The rate of convergence of these moments is much slower when evaluated in a straightforward manner by use of Eq. (2-39). This is illustrated in Table 11.

As a further measure of the accuracy of the method used, in Tables 12 through 14 are presented additional influence coefficients for deflections and moments, and the results compared with corresponding values reported in Ref. (10). It is seen that the agreement between the two sets of values is for all practical purposes perfect.

---

* See also comparison between experimental and theoretical data reported in Ref. (11).

III. ANALYSIS OF DYNAMIC PROBLEM

1. Characteristics of Structure and Vehicle

The structure analyzed is the same as that considered in the static analysis presented in the preceding chapter. In addition to the assumptions made previously, it is assumed that the mass of the slab is uniformly distributed, and that the mass per unit of length of the beams, although it may vary from one beam to the next, is constant for any one beam.

The vehicle is represented by a single-axle, two-wheel loading consisting of a sprung mass and two equal unsprung masses, as shown in Fig. 3. The center of gravity of the sprung mass is assumed to be located halfway between the supporting springs. The springs are considered to be linearly elastic and to have identical stiffnesses. Damping for both the vehicle and the bridge has been neglected.

2. General Description of Method of Analysis

The analysis of the problem involves:

(a) The determination of the instantaneous values of the interacting forces between the vehicle and the structure, and of the inertia forces due to the mass of the structure, and

(b) The computation of the deflections and bending moments produced in the structure by these forces. The latter step is a problem of statics, and has been discussed in detail in Chapter II. The problem of dynamics, therefore, consists essentially in determining the instantaneous dynamic forces.

The method used to analyze the dynamic problem is an extension of that used in the preceding chapter to study the static problem, and utilizes the approximation employed by Inglis[6] in analyzing the dynamic effects produced by moving loads in simply supported beams.

The dynamic deflection configuration of the structure is expressed as

$$w = w_o \sin \pi\xi \sum_n f_n(t)\, Y_n(\eta) \qquad (3\text{-}1)$$

where w = the deflection of any point of the bridge at any time, due to the static and dynamic effects of the vehicle.

w_o = a quantity with the dimension of deflection, chosen arbitrarily as $Wa^3/(E_bI_b)_{io}$

W = total static weight of the vehicle

$(E_bI_b)_{io}$ = flexural rigidity of a reference beam

$f_n(t)$ = dimensionless coefficients that are functions of time; these are the generalized coordinates for the bridge.

$Y_n(\eta)$ = dimensionless functions of η, as previously discussed.

It should be noted that the instantaneous deflection configuration of the structure in the longitudinal direction (ξ-direction) is assumed to be a half-sine wave. This is the same assumption as that used by Inglis for the beam problem and amounts to considering only the term m = 1 in Eq. (2-21).

On comparing Eqs. (3-1) and (2-21), one observes the following:

1. The assumption made regarding the dynamic deflection configuration in the transverse direction is the same as that used for the static problem.

2. The time-dependent coefficients $f_n(t)$ in Eq. (3-1), correspond to the coefficients α_{1n} in Eq. (2-21).

3. In the special case where a single Y_n function representing a uniform deflection is used, the problem considered here is identical to the

one studied by Inglis[6]. The governing differential equations, obtained and presented later in this chapter, when simplified by using a single Y_n function, yield, in fact, the equations obtained by Inglis; this relationship is discussed in detail in Art. 4.3 of this chapter.

The coordinates used to specify the configuration of the sprung mass are the vertical displacement of the center of gravity of the mass, z, and the rotation of the mass about an axis normal to the transverse vertical plane, u, (see Fig. 3). The vertical positions of the unsprung masses are determined by the configuration of the bridge. Thus the total number of generalized coordinates of the bridge-vehicle system is equal to the number of $f_n(t)$ functions used in Eq. (3-1) plus the two coordinates z and u used for the vehicle.

The vehicle is considered to be attached to a Galilean reference frame that moves along the bridge with a constant velocity, v, in such a way that the unsprung masses and the center of gravity of the sprung mass can move only vertically with respect to the reference frame, and the sprung mass can rotate only about an axis that is parallel to the bridge and passes through the center of gravity of the sprung mass. The restrictions on the motion of the elements of the vehicle represent time-dependent constraints. The system under consideration possesses a time-dependent potential energy function, or a pseudo-potential energy as it is sometimes called, and it is possible to formulate the equations of motion by application of Lagrange's equation

$$\frac{d}{dt}\left(\frac{\partial T}{\partial \dot{q}_n}\right) - \frac{\partial T}{\partial q_n} + \frac{\partial (U+V)}{\partial q_n} = 0 \qquad (3\text{-}2)$$

in which V = the strain energy of the system

U = the potential energy of the gravity forces

T = the kinetic energy of the system

q_n = the n^{th} generalized coordinate of the system

$\dot{q}_n = \frac{dq_n}{dt}$

3. Energy Expressions

The datum of zero energy level for the system is defined by the following conditions: the structure is in an unstressed position, and the springs of the vehicle are undeformed.

Let w_2 represent the deflection configuration of the bridge when loaded with its own weight; this deflection is measured from the unstressed configuration of the bridge. Then the total deflection of the bridge, measured from its unstressed position, is $(w + w_2)$. The dead load deflection configuration, w_2, can be represented in a form analogous to Eq. (2-21) as

$$w_2 = w_o \sum_m \left(\sum_n \delta_{mn} Y_n \right) \sin m\pi\xi \qquad (3\text{-}3)$$

where δ_{mn} are constant dimensionless coefficients. In the following development, only the term m = 1 will be retained. The resulting expression

$$w_2 = w_o \sin \pi\xi \sum_n \delta_n Y_n(\eta) \qquad (3\text{-}4)$$

is then analogous to Eq. (3-1). The higher terms are irrelevant in this case, as they will only increase the energy of the system by a constant.

3.1 Strain Energy. The total strain energy of the system, V, is written in the form

$$V = V_s + V_b + V_{sp} \tag{3-5}$$

where V_s, V_b, and V_{sp} are the strain energies of the slab, of the beams, and of the springs, repsectively.

For zero Poisson's ratio, V_s is given by the equation

$$V_s = \frac{Dab}{2a^4} \int_0^1 \int_0^1 \left[\left(\frac{\partial^2 (w+w_2)}{\partial \xi^2} \right)^2 + \frac{2}{c^2} \left(\frac{\partial^2 (w+w_2)}{\partial \xi \partial \eta} \right)^2 + \frac{1}{c^4} \left(\frac{\partial^2 (w+w_2)}{\partial \eta^2} \right)^2 \right] d\xi d\eta \tag{3-6}$$

Substituting Eqs. (3-1) and (3-4) into Eq. (3-6), gives

$$\begin{aligned} V_s = \frac{Dab}{2a^4} w_o^2 \Bigg[& \pi^4 \sum_n \sum_s (f_n+\delta_n)(f_s+\delta_s) \int_0^1 \sin^2 \pi\xi \, d\xi \int_0^1 Y_n Y_s \, d\eta \\ & + \frac{2\pi^2}{c^2} \sum_n \sum_s (f_n+\delta_n)(f_s+\delta_s) \int_0^1 \cos^2 \pi\xi \, d\xi \int_0^1 Y_n' Y_s' \, d\eta \\ & + \frac{1}{c^4} \sum_n \sum_s (f_n+\delta_n)(f_s+\delta_s) \int_0^1 \sin^2 \pi\xi \, d\xi \int_0^1 Y_n'' Y_s'' \, d\eta \Bigg] \end{aligned} \tag{3-7}$$

where, as before, a prime superscript on Y_n denotes one differentiation with respect to η. Letting

$$A_{ns} = \left[\int_0^1 Y_n Y_s \, d\eta + \frac{2}{\pi^2 c^2} \int_0^1 Y_n' Y_s' \, d\eta + \frac{1}{\pi^4 c^4} \int_0^1 Y_n'' Y_s'' \, d\eta \right] \tag{3-8}$$

and evaluating the integrals involving the ξ-coordinate, one obtains

$$V_s = \frac{\pi^4 D}{a^4} \frac{ab}{4} w_o^2 \sum_n \sum_s A_{ns} (f_n+\delta_n)(f_s+\delta_s) \tag{3-9}$$

Note that $A_{ns} = A_{sn}$

The strain energy of the beams is given by the equation

$$V_b = \sum_{i=o}^{p} \left[\frac{(E_b I_b)_i}{2a^3} \int_o^1 \left(\frac{\partial^2 (w+w_2)}{\partial \xi^2} \right)_i^2 d\xi + \frac{(G_b J_b)_i}{2ab^2} \int_o^1 \left(\frac{\partial^2 (w+w_2)}{d\xi d\eta} \right)_i^2 d\xi \right] \qquad (3\text{-}10)$$

By substituting Eq. (3-1) and (3-4) into Eq. (3-10), one obtains

$$V_b = \frac{\pi^4 D}{a^4} \frac{ab}{4} w_o^2 \sum_{i=o}^{p} \left[\lambda_i \sum_n \sum_s (f_n+\delta_n)(f_s+\delta_s)(Y_n)_i (Y_s)_i + \frac{k_i}{\pi^2 c^2} \sum_n \sum_s (f_n+\delta_n)(f_s+\delta_s)(Y_n')_i (Y_s')_i \right] \qquad (3\text{-}11)$$

where $(Y_n)_i$ is the ordinate of the function Y_n at the location of the i^{th} beam and λ_i and k_i are dimensionless parameters defined previously by Eqs. (2-10) and (2-11).

The strain energy of the springs is given by the equation

$$V_{sp} = \frac{1}{2} k \sum_{j=1}^{2} \left[z+z_s - (w+w_1)_j + (-1)^j ub_1 \right]^2 \qquad (3\text{-}12)$$

in which the bracketed quantity is the total compression in the j^{th} spring, and

k = the spring constant for one spring

z_s = the initial static compression of a spring

z = the dynamic vertical displacement of the center of gravity of the sprung mass, measured from the static position of equilibrium (See Fig. 3)

u = the dynamic rotation of the sprung mass in the transverse vertical plane, measured with respect to the static equilibrium position (See Fig. 3)

w_1 = a deflection function representing the deviation of the deck of the bridge, when loaded with its own weight, from the horizontal plane passing through the supports. It is positive when downward. This quantity is equal to the sum of the dead load deflection configuration and the configuration representing any possible unevenness of the unstressed bridge.

b_1 = one half the distance between the wheels

$(w+w_1)_j$ = $(w+w_1)$ evaluated at wheel j.

Assuming arbitrarily that t = 0 when the vehicle enters the bridge, one can write

$$\xi_j = \frac{vt}{a} \tag{3-13}$$

in which ξ_j = ξ-coordinate of either wheel

v = speed of the vehicle along the bridge

Substituting Eqs. (3-1) and (3-13) into Eq. (3-12), gives

$$V_{sp} = \frac{1}{2} k \sum_{j=1}^{2} \left[z+z_s - (w_1)_j + (-1)^j ub_1 - w_o \sin \frac{\pi vt}{a} \sum_n f_n (Y_n)_j \right]^2 \tag{3-14}$$

3.2 Potential Energy of the Gravity Forces. The potential energy of the gravity forces is written in the form

$$U = U_s + U_b + U_{sp} + U_u \tag{3-15}$$

where U_s, U_b, U_{sp}, and U_u are the potential energies of the slab, of the beams, of the sprung mass, and of the unsprung masses, respectively.

The potential energy of the weight of the slab is given by the equation

$$U_s = -\mu gab \int_0^1 \int_0^1 (w+w_2)\, d\xi d\eta \tag{3-16}$$

in which μ is the mass of the slab per unit of area. By substituting Eqs. (3-1) and (3-4) into Eq. (3-16), one obtains

$$U_s = -\frac{2}{\pi}\mu gab\, w_o \sum_n (f_n+\delta_n)\int_o^1 Y_n d\eta \tag{3-17}$$

The potential energy of the weight of the beams is given by the equation

$$U_b = -ag\int_o^1 \left[\sum_{i=o}^{p}(m_b)_i\,(w+w_2)_i\right] d\xi \tag{3-18}$$

in which $(m_b)_i$ is the mass per unit length of the i^{th} beam. By substituting Eq. (3-1) and (3-4) into Eq. (3-18), one obtains

$$U_b = -\frac{2}{\pi} ag\, w_o \sum_{i=o}^{p}\left[(m_b)_i \sum_n (f_n+\delta_n)(Y_n)_i\right] \tag{3-19}$$

The potential energy of the sprung mass is

$$U_{sp} = -Mg(z+z_s) \tag{3-20}$$

where M = the sprung mass

The potential energy of the unsprung masses is

$$U_u = -mg\sum_{j=1}^{2}(w+w_1)_j \tag{3-21}$$

where m = one unsprung mass. By substituting Eqs. (3-1) and (3-13) into Eq. (3-21), one obtains

$$U_u = -mg\sum_{j=1}^{2}\left[(w_1)_j + w_o \sin\frac{\pi vt}{a}\sum_n f_n(Y_n)_j\right] \tag{3-22}$$

3.3 Kinetic Energy. The total kinetic energy of the system is expressed in the form

$$T = T_s + T_b + T_{sp} + T_u \tag{3-23}$$

where T_s, T_b, T_{sp}, and T_u are the kinetic energies of the slab, of the beams, of the sprung mass, and of the unsprung masses.

The kinetic energy of the slab is

$$T_s = \frac{1}{2}\,\mu ab \int_o^1 \int_o^1 \left(\frac{\partial w}{\partial t}\right)^2 d\xi d\eta \tag{3-24}$$

Noting from Eq. (3-1) that

$$\frac{\partial w}{\partial t} = w_o \sin \pi\xi \sum_n \left(\frac{df_n}{dt}\right) Y_n \tag{3-25}$$

and substituting this equation into Eq. (3-24), one obtains

$$T_s = \frac{1}{4}\,\mu ab\, w_o^2 \sum_n \sum_s f_n'\, f_s' \int_o^1 Y_n\, Y_s\, d\eta \tag{3-26}$$

where $f_n' = \dfrac{df_n}{dt}$.

The kinetic energy of the beams is obtained in a similar manner:

$$T_b = \frac{a}{2} \sum_{i=o}^{p} \int_o^1 (m_b)_i \left(\frac{\partial w}{\partial t}\right)_i^2 d\xi = \frac{1}{4}\, a w_o^2 \sum_{i=o}^{p} (m_b)_i \sum_n \sum_s f_n'\, f_s'\, (Y_n)_i (Y_s)_i \tag{3-27}$$

Note that the kinetic energy of the beams due to their torsional motion is neglected.

The kinetic energy of the sprung mass is given by the equation

$$T_{sp} = \frac{1}{2}\, M \left(\frac{dz}{dt}\right)^2 + \frac{1}{2}\, J \left(\frac{du}{dt}\right)^2 \tag{3-28}$$

in which J is the polar moment of inertia of the sprung mass about an axis through its center of gravity and normal to the transverse vertical plane.

The kinetic energy of the unsprung masses is

$$T_u = \frac{1}{2} m \sum_{j=1}^{2} \left[\frac{d}{dt} (w+w_1)_j\right]^2 \tag{3-29}$$

it is to be noted that

$$\frac{d}{dt} (w+w_1)_j = \left[\left(\frac{\partial w}{\partial t} + \frac{\partial w}{\partial \xi} \frac{d\xi}{dt}\right) + \frac{\partial w_1}{d\xi} \frac{d\xi}{dt}\right]_j \tag{3-30}$$

and that $\frac{d\xi_j}{dt} = \frac{v}{a}$. By substituting these expressions into Eq. (3-29) and using Eq. (3-1), one obtains

$$T_u = \frac{1}{2} m \sum_{j=1}^{2} \left[\frac{v}{a}\left(\frac{\partial w_1}{\partial \xi}\right)_j + w_o \sum_n \left(f_n' \sin \frac{\pi v t}{a} + \frac{\pi v}{a} f_n \cos \frac{\pi v t}{a}\right)(Y_n)_j\right]^2 \tag{3-31}$$

4. Governing Differential Equations

The differential equations governing the motion of the bridge-vehicle system are obtained from Eq. (3-2) by substituting the energy expressions derived in the preceding article. The number of equations thus obtained is equal to the number of generalized coordinates used to define the configuration of the system. The detailed derivation of these equations is presented in the Appendix. The final equations are summarized in the following paragraphs.

4.1 Dimensional Form of Equations. The equation corresponding to the n^{th} generalized coordinate for the bridge, f_n, is

$$w_o \sum_s f_s'' \left[\frac{\mu ab}{2} \int_o^1 Y_n Y_s \, d\eta + \frac{a}{2} \sum_{j=o}^{p} (m_b)_i (Y_n)_i (Y_s)_i + m \sin^2 \frac{\pi v t}{a} \sum_{j=1}^{2} (Y_n)_j (Y_s)_j \right]$$

$$+ w_o \sum_s f_s' \left[2m\left(\frac{\pi v}{a}\right) \sum_{j=1}^{2} (Y_n)_j (Y_s)_j \right] \sin \frac{\pi v t}{a} \cos \frac{\pi v t}{a}$$

$$+ w_o \sum_s f_s \left[\frac{\pi^4 D}{a^4} \frac{ab}{2} \left[A_{ns} + \sum_{i=o}^{p} \lambda_i (Y_n)_i (Y_s)_i + \sum_{i=o}^{p} \frac{k_i}{\pi^2 c^2} (Y_n')_i (Y_s')_i \right] \right.$$

$$\left. + k \sin^2 \frac{\pi v t}{a} \sum_{j=1}^{2} (Y_n)_j (Y_s)_j - m\left(\frac{\pi v}{a}\right)^2 \sin^2 \frac{\pi v t}{a} \sum_{j=1}^{2} (Y_n)_j (Y_s)_j \right]$$

$$- \sin \frac{\pi v t}{a} \sum_{j=1}^{2} (Y_n)_j \left[\frac{gM}{2} + k \left[z - (w_1)_j + (-1)^j u b_1 \right] \right]$$

$$- mg \sin \frac{\pi v t}{a} \sum_{j=1}^{2} (Y_n)_j + m\left(\frac{v}{a}\right)^2 \sin \frac{\pi v t}{a} \sum_{j=1}^{2} (Y_n)_j \left(\frac{\partial^2 w_1}{\partial \xi^2} \right)_j = 0 \qquad (3\text{-}32)$$

The summations on s should extend from s = -1, to s = n_1, the maximum value of n used in Eq. (3-1).

The differential equations for f_{-1}, f_o, ... f_{n_1} are obtained from the above equation by replacing n by -1, 0, ... n_1. There will be a total of $n_1 + 2$ such equations.

The equation corresponding to the z coordinate of the vehicle is

$$Mz'' + k \sum_{j=1}^{2} \left[z - (w_1)_j - w_o \sin \frac{\pi v t}{a} \sum_s f_s (Y_s)_j \right] = 0 \qquad (3\text{-}33)$$

and the one corresponding to the u coordinate is

$$Ju'' + kb_1 \sum_{j=1}^{2} (-1)^j \left[(-1)^j u b_1 - (w_1)_j - w_o \sin \frac{\pi v t}{a} \sum_s f_s (Y_s)_j \right] = 0 \qquad (3\text{-}34)$$

It can be seen that in these equations the roadway surface unevenness function, w_1, appears only as $(w_1)_j$, i.e., with its ordinates evaluated at the transverse location of the wheels. That this should be so is physically apparent.

In what follows, the variation of the functions $(w_1)_j$ in the ξ-direction is assumed to be sinusoidal, i.e.

$$(w_1)_j = w_o e_j \sin m_1 \pi \xi \tag{3-35}$$

where e_j ($j = 1$ or 2) are dimensionless quantities and $w_o e_j$ denotes the amplitude of the unevenness. The quantities e_1 and e_2 may or may not be equal; they may also be positive or negative. The quantity m_1 is a positive integer.

4.2 Dimensionless Form of Equations. Let

$$\nu = \frac{2m + M}{a[\mu b + \sum_{i=o}^{p} (m_b)_i]} = \frac{\text{Total weight of vehicle}}{\text{Total weight of bridge}}$$

$$\omega = \frac{2m}{2m + M} = \frac{\text{Unsprung weight of vehicle}}{\text{Total weight of vehicle}}$$

$$\gamma_i = \frac{(m_b)_i}{\mu b + \sum_{i=o}^{p} (m_b)_i} = \frac{\text{Weight of } i^{th} \text{ beam}}{\text{Total weight of bridge}} \tag{3-36}$$

$$\alpha = \frac{v\, T_b}{2a}$$

$$K = \left(\frac{f_v}{f_b}\right)^2 = \left(\frac{T_b}{T_v}\right)^2$$

in which

f_b = the fundamental natural frequency of the bridge evaluated on the assumption that it acts as a beam

f_v = the natural frequency of the vehicle for vertical motion on its springs

These frequencies are given by the equations

$$f_b^2 = \frac{1}{T_b^2} = \frac{\pi^2}{4a^4} \frac{Db + \sum_{i=o}^{p} (E_b I_b)_i}{\mu b + \sum_{i=o}^{p} (m_b)_i}$$

$$f_v^2 = \frac{1}{T_v^2} = \frac{1}{4\pi^2} \frac{2k}{M} \qquad (3\text{-}37)$$

In addition, let

$$\tau = \frac{vt}{a}$$

$$\varphi_s(\tau) = f_s(t)$$

$$\zeta(\tau) = \frac{z(t)}{w_o} \qquad (3\text{-}38)$$

$$\theta(\tau) = \frac{u(t)b_1}{w_o}$$

By differentiating these equations, one obtains the relations

$$f_s' = \left(\frac{v}{a}\right)\varphi_s' \quad ; \quad f_s'' = \left(\frac{v}{a}\right)^2 \varphi_s''$$

$$\frac{z'}{w_o} = \left(\frac{v}{a}\right)\zeta' \quad ; \quad \frac{z''}{w_o} = \left(\frac{v}{a}\right)^2 \zeta'' \qquad (3\text{-}39)$$

$$\frac{u'b_1}{w_o} = \left(\frac{v}{a}\right)\theta' \quad ; \quad \frac{u''b_1}{w_o} = \left(\frac{v}{a}\right)^2 \theta''$$

in which a prime superscript on f_s, z, and u denotes one differentiation with respect to t, and a prime superscript on φ_s, ζ and θ denotes one differentiation with respect to τ.

Now by multiplying Eq. (3-32) by

$$\frac{T_b^2}{2w_o} \frac{1}{\mu ab + a \sum_{i=o}^{p} (m_b)_i},$$

making use of Eq. (3-35), and introducing the dimensionless quantities defined by Eqs. (3-36) through (3-39) and Eqs. (2-10) and (2-11), one may reduce Eq. (3-32) to the form

$$\sum_s \varphi_s'' (B_{ns} + C_{ns} \sin^2 \pi\tau) + \sum_s \varphi_s' D_{ns} \sin \pi\tau \cos \pi\tau$$

$$+ \sum_s \varphi_s (E_{ns} + F_{ns} \sin^2 \pi\tau) + H_n \sin \pi\tau$$

$$+ L_n (\zeta, \theta, \tau) + R_n \sin \pi\tau \sin m_1 \pi\tau = 0 \qquad (3\text{-}40)$$

where

$$B_{ns} = \alpha^2 \left[\left(1 - \sum_{i=o}^{p} \gamma_i \right) \int_o^1 Y_n Y_s \, d\eta + \sum_{i=o}^{p} \gamma_i (Y_n)_i (Y_s)_i \right]$$

$$C_{ns} = \alpha^2 \nu\omega \sum_{j=1}^{2} (Y_n)_j (Y_s)_j$$

$$D_{ns} = 2\alpha^2 \pi\nu\omega \sum_{j=1}^{2} (Y_n)_j (Y_s)_j$$

$$E_{ns} = \frac{\pi^2}{1 + \sum_{i=o}^{p} \lambda_i} \left[A_{ns} + \sum_{i=o}^{p} \lambda_i (Y_n)_i (Y_s)_i + \frac{1}{\pi^2 c^2} \sum_{i=o}^{p} k_i (Y_n')_i (Y_s')_i \right]$$

$$F_{ns} = \pi^2\nu\left[K(1-\omega) - \alpha^2\omega\right]\sum_{j=1}^{2}(Y_n)_j(Y_s)_j$$

$$H_n = -\frac{1}{\pi^2}\frac{\lambda_{io}}{1+\sum_{i=o}^{p}\lambda_i}\sum_{j=1}^{2}(Y_n)_j$$

$$L_n = -\pi^2 K\nu(1-\omega)\sin\pi\tau\sum_{j=1}^{2}(Y_n)_j\left[\zeta + (-1)^j\theta\right]$$

$$R_n = \pi^2\nu\left[K(1-\omega) - \alpha^2\omega m_1^2\right]\sum_{j=1}^{2}e_j(Y_n)_j$$

The quantity λ_{io} in the expression for H_n represents the flexural rigidity factor of the reference beam used in defining the quantity w_o in Eq. (3-1).

In a similar manner, Eqs. (3-33) and (3-34) may be reduced to the following forms:

$$2\alpha^2\zeta'' + \pi^2 K\left[2\zeta - \sin m_1\pi\tau\sum_{j=1}^{2}e_j - \sin\pi\tau\sum_{s}\varphi_s\sum_{j=1}^{2}(Y_s)_j\right] = 0 \qquad (3\text{-}41)$$

and

$$2\alpha^2\rho\theta'' + \pi^2 K\left[2\theta - \sin m_1\pi\tau\sum_{j=1}^{2}(-1)^j e_j - \sin\pi\tau\sum_{s}\varphi_s\sum_{j=1}^{2}(-1)^j(Y_s)_j\right] = 0 \qquad (3\text{-}42)$$

where

$$\rho = \frac{J}{Mb_1^2} \qquad (3\text{-}43)$$

Eqs. (3-41) is obtained from Eq. (3-33) by multiplying it by $T_b^2/(Mw_o)$, and Eq. (3-42) is obtained from Eq. (3-34) by multiplying it by $T_b^2/(b_1 Mw_o)$.

Equations (3-40) through (3-42) form a system of second order, linear differential equations with variable coefficients, the number of equations being equal to $(n_1 + 4)$, the number of generalized coordinates used.

4.3 Reduction of Governing Equations to Equations for Beams. Since a beam has no transverse dimension, in Eq. (3-1) it is only necessary to consider the function $Y_{-1} = 1$ and the corresponding generalized coordinate f_{-1}; therefore, the summation sign on s may be deleted in this equation and in all other equations derived therefrom. Note also that $Y'_{-1} = Y''_{-1} = 0$. For convenience in writing, the dimensionless generalized coordinate φ_{-1} corresponding to f_{-1} will be denoted by φ. Since the vehicle also has no width,

$$\theta = \theta' = \theta'' = 0$$

Consider the special case in which the surface of the beam is initially level, i.e.

$$e_1 = e_2 = 0$$

Then the quantities B_{ns} through R_n in Eq. (3-40) reduce to

$$B_{ns} = \alpha^2$$

$$C_{ns} = 2\alpha^2 \nu\omega$$

$$D_{ns} = 4\alpha^2 \pi\nu\omega$$

$$E_{ns} = \pi^2$$

$$F_{ns} = 2\pi^2 \nu \left[K(1-\omega) - \alpha^2\omega\right]$$

$$H_n = -\frac{2}{\pi^2} \frac{\lambda_{io}}{1 + \sum_{i=o}^{p} \lambda_i}$$

$$L_n = -2\pi^2 K\nu (1-\omega)\, \zeta \sin \pi\tau$$

$$R_n = 0$$

It is to be recalled that, in defining the quantity w_o in Eq. (3-1) the flexural stiffness of the reference beam, $(E_b I_b)_{io}$, was used; if instead, the total flexural stiffness of the structure, $EI = Db + \sum_{i=o}^{p} (E_b I_b)_i$ (i.e. that of the idealized beam) is used, then the quantity H_n becomes

$$H_n = - \frac{2}{\pi^2}$$

and Eq. (3-40) reduces to

$$\varphi'' \left[\alpha^2 + 2\alpha^2 \nu\omega \sin^2 \pi\tau \right] + \varphi' \left[4\alpha^2 \pi\nu\omega \sin \pi\tau \cos \pi\tau \right]$$

$$+ \varphi \left[\pi^2 + 2\pi^2 \nu \left(K(1-\omega) - \alpha^2\omega \right) \sin^2 \pi\tau \right] - \frac{2}{\pi^2} \sin \pi\tau$$

$$- 2\pi^2 K\nu (1-\omega)\zeta \sin \pi\tau = 0 \qquad (3\text{-}44)$$

In a similar manner it can be shown that Eq. (3-41) reduces to

$$\alpha^2 \zeta'' + \pi^2 K (\zeta - \varphi \sin \pi\tau) = 0 \qquad (3\text{-}45)$$

In the following, these equations will be compared to those derived by Inglis[6], and by Biggs, Suer, and Louw[1].

Inglis' equations for the same case*, expressed in his own notation, are

---

* Inglis' equations include also the effects of a moving alternating force and of damping. These factors are omitted here. It should be noted, however, that the effects of the gravity forces are not taken into account in Inglis' equations.

$$\frac{d^2f}{dt^2}\left(M_G + M_u - M_u \cos 4\pi nt\right) + 2\pi \frac{df}{dt}\left(2n\, M_u \sin 4\pi nt\right)$$

$$+ 4\pi^2 f\left(n_o^2 M_G - n^2 M_u + n^2 M_u \cos 4\pi nt\right)$$

$$= -2M_s \frac{d^2z}{dt^2} \sin 2\pi nt \qquad (3\text{-}46)$$

and

$$\frac{d^2z}{dt^2} + 4\pi^2 n_s^2 z = 4\pi^2 n_s^2 f \sin 2\pi nt \qquad (3\text{-}47)$$

The relationship between the notation used by Inglis and that used in this report is shown in the following table. (See page 51).

Equation (3-44) can be transformed into Eq. (3-46) by taking $H_n = 0$ (this means that the gravity forces are not taken into account), making use of Eq. (3-45), multiplying Eq. (3-44) by $4f_b^2 M_b$, and changing notation. The identity of Eqs. (3-45) and (3-47) can be shown simply by multiplying Eq. (3-45) by $4f_b^2$ and changing notation.

By assuming arbitrarily that

$$D_{ns} = 0$$

$$F_{ns} = 2\pi^2 \nu K (1 - \omega) \qquad (3\text{-}48)$$

Equations (3-44) and (3-45) can be transformed into the equations derived by Biggs, Suer, and Louw[1]. This assumption amounts to neglecting the effect of the translational motion of the unsprung mass on its vertical acceleration; in Ref. (1), this was assumed implicitly. It is to be noted that Eqs. (3-48) are exact if the unsprung mass is equal to zero.

Present Notation	Inglis' Notation
$M_b = \mu ab + a\sum_{i=o}^{p} (m_b)_i$	M_G
M	M_s
$2m$	M_u
a	ℓ
$\frac{v}{2a}$	n
f_b^2	$n_o^2 = \frac{\pi^2}{4\ell^4} \frac{EI\ell}{M_G}$
f_v^2	$n_s^2 = \frac{1}{4\pi^2} \frac{k_s}{M_s}$
$k_v = 2k$	k_s
α	$\frac{n}{n_o}$
$K = (\frac{f_v}{f_b})^2$	$(\frac{n_s}{n_o})^2$
τ	$2nt$
$w_o\Phi$	f
$(\frac{v}{a}) w_o\Phi'$	$\frac{df}{dt}$
$(\frac{v}{a})^2 w_o\Phi''$	$\frac{d^2f}{dt^2}$
$\nu(1 - \omega)$	$\frac{M_s}{M_G}$
$\nu\omega$	$\frac{M_u}{M_G}$
$z = w_o\zeta$	z

5. Computation of Response

The procedure used to evaluate the dynamic response of the bridge-vehicle system may be summarized briefly as follows: First, the governing differential equations of motion are solved to determine the values of the generalized coordinates and of their first two derivatives. Next, the interacting forces between the vehicle and the bridge, and the inertia forces of the bridge are evaluated. Finally, the dynamic deflections and bending moments induced in the bridge are determined from the dynamic forces acting on the bridge, instead of directly from the generalized coordinates computed in the first step.

5.1 Solution of Governing Differential Equations. The system of Eqs. (3-40) through (3-42) are solved by means of a step-by-step method of numerical integration. The time required for the vehicle to cross the span, $0 < \tau < 1$, is divided into a number of small intervals, and the governing equations are "satisfied" only at the ends of these intervals.

Let q_n represent a dimensionless generalized coordinate - it may refer to the bridge or the vehicle - , and $\dot{q}_n$ and $\ddot{q}_n$ represent its first and second derivatives with respect to τ. The values of these quantities at $\tau = \tau_r$ will be identified with the subscript r separated from the subscript n by a comma. Let it be assumed that the values of $q_{n,r}$, $\dot{q}_{n,r}$ and $\ddot{q}_{n,r}$ are known for each generalized coordinate of the system, and that it is desired to find the corresponding values at $\tau = \tau_{r+1} = \tau_r + \Delta\tau$ in which $\Delta\tau$ is a short interval. The following procedure may be used. Suppose that an assumption is made regarding the manner in which the second derivatives vary within the interval from τ_r to τ_{r+1}. Then the quantities q_{r+1} and $\dot{q}_{r+1}$ may be expressed in terms of the known $q_{n,r}$, $\dot{q}_{n,r}$ and $\ddot{q}_{n,r}$, and the still unknown $\ddot{q}_{n,r+1}$. These quantities may then be substituted into the differential

equations of motion to obtain a system of linear algebraic equations involving the quantities $\ddot{q}_{n,r+1}$ as the only unknowns. The number of unknowns will be equal to the number of generalized coordinates used. The solution of these equations will yield the values of $\ddot{q}_{n,r+1}$. However, the resulting equations are in general fairly involved, and in this study an iterative procedure was used to integrate the equations within each time interval.

The variation of $\ddot{q}_n$ within the time interval $\Delta\tau$ was considered to be linear; with this assumption, the expressions for $\dot{q}_{n,r+1}$ and $q_{n,r+1}$ become

$$\dot{q}_{n,r+1} = \dot{q}_{n,r} + \frac{1}{2}(\Delta\tau)(\ddot{q}_{n,r} + \ddot{q}_{n,r+1}) \tag{3-49}$$

$$q_{n,r+1} = q_{n,r} + (\Delta\tau)\dot{q}_{n,r} + \frac{1}{3}(\Delta\tau)^2 \ddot{q}_{n,r} + \frac{1}{6}(\Delta\tau)^2 \ddot{q}_{n,r+1} \tag{3-50}$$

The iterative procedure may now be summarized as follows:

1. Assume that the second derivatives of the generalized coordinates at the end of the time interval are the same as those at the beginning of the interval, i.e. take $\ddot{q}_{n,r+1} = \ddot{q}_{n,r}$, and by application of Eqs. (3-49) and (3-50) evaluate $\dot{q}_{n,r+1}$ and $q_{n,r+1}$.

2. Substitute the values of $\dot{q}_{n,r+1}$ and $q_{n,r+1}$ thus obtained into the governing differential equations, and by solving the resulting system of algebraic equations, obtain improved values for $\ddot{q}_{n,r+1}$.

3. From Eqs. (3-49) and (3-50) calculate the values of $\dot{q}_{n,r+1}$ and $q_{n,r+1}$ corresponding to the values of $\ddot{q}_{n,r+1}$ just determined.

4. Repeat Step 2 by using the latest available values of $\dot{q}_{n,r+1}$ and $q_{n,r+1}$.

5. For each generalized coordinate compare the newly derived value of $\ddot{q}_{n,r+1}$ with the previously available value. If the difference between the two values for each coordinate exceeds a prescribed tolerance,

repeat Steps 3 through 5, until all differences are less than the prescribed tolerance. The algebraic equations are then considered to be solved, and the integration for the time interval from τ_r to τ_{r+1} completed. If desired, the values of the dynamic forces acting on the bridge, and the effects produced in the bridge by these forces may be calculated at this stage before proceeding to the next time interval.

Initial Conditions. The initial values of q_n and $\dot{q}_n$ must be known for each generalized coordinate so that the integration procedure may be started. The initial values of the second derivatives $\ddot{q}_n$ are determined from the governing differential equations by substituting the specified values of q_n and $\dot{q}_n$ for $\tau = 0$ and solving for $\ddot{q}_n$.

Choice of Time Interval. The time interval $\Delta\tau$ used in the numerical procedure should be small enough so that successive cycles of iteration converge and the solution be stable. For the particular procedure used, it has been shown[8] that both the convergence and the stability criteria are satisfied if

$$\Delta t = \frac{a}{v}\Delta\tau < 0.389\ T \qquad (3\text{-}51)$$

where T is the shortest natural period of vibration of the system; the system, here, is the bridge-vehicle combination, idealized in the manner described in the preceding sections. Numerical values for the natural periods of vibration of multigirder bridges have been reported in Ref. (15).

5.2 Computation of Dynamic Forces Acting on Bridge. The static value of the interacting force for each wheel is obviously one-half the total weight of the "vehicle" or W/2. The dynamic increment of the interacting force for the j^{th} wheel may conveniently be stated in the form $\Delta_j \frac{W}{2}$ where Δ_j is a dimensionless factor. Now let

$$\Delta_j = (\Delta_1)_j + (\Delta_2)_j \tag{3-52}$$

where $(\Delta_1)_j$ = the component of Δ_j due to the dynamic increment of the compression in the spring.

$(\Delta_2)_j$ = the component of Δ_j due to the vertical acceleration of the unsprung mass j.

These quantities may be determined as follows:

The change of force in the j^{th} spring is

$$(\Delta_1)_j \frac{W}{2} = k[z + (-1)^j ub_1 - (w_1+w)_j] \tag{3-53}$$

By substituting into this equation the dimensionless quantities defined by Eqs. (3-36) through (3-39), and noting that

$$kw_o = \pi^4 K\nu(1 - \omega) \frac{1 + \sum_{i=o}^{p} \lambda_i}{\lambda_{io}} \frac{W}{2}$$

one obtains

$$(\Delta_1)_j = \pi^4 K\nu(1-\omega) \frac{1 + \sum_{i=o}^{p} \lambda_i}{\lambda_{io}} \left[\zeta + (-1)^j\theta - e_j \sin m_1\pi\tau - \sin \pi\tau \sum_s \varphi_s(Y_s)_j\right] \tag{3-54}$$

The inertia force of the unsprung mass j is given by the equation

$$(\Delta_2)_j \frac{W}{2} = - m \left[\left(\frac{d^2w}{dt^2}\right)_j + \left(\frac{v}{a}\right)^2 \left(\frac{\partial^2 w_1}{\partial \xi^2}\right)_j\right] \tag{3-55}$$

in which the bracketed quantity represents the vertical acceleration of the j^{th} unsprung mass; this quantity is positive when downward. By substituting into Eq. (3-55) the dimensionless quantities defined by Eqs. (3-36) through (3-39), and noting that

$$mw_o \left(\frac{v}{a}\right)^2 = \pi^2\alpha^2\nu\omega \frac{1 + \sum_{i=o}^{p} \lambda_i}{\lambda_{io}} \frac{W}{2}$$

one finds that

$$(\Delta_2)_j = -\pi^2\alpha^2 w \frac{1+\sum_{i=o}^{p}\lambda_i}{\lambda_{io}}\left[\sum_s (Y_s)_j(\varphi_s'' \sin\pi\tau + 2\pi\varphi_s' \cos\pi\tau - \pi^2\varphi_s \sin\pi\tau) - e_j m_1^2\pi^2 \sin m_1\pi\tau\right] \quad (3\text{-}56)$$

The intensity of the inertia force $\bar{p}_\mu$ due to the mass of the slab is given by the equation

$$\bar{p}_\mu = -\mu\left(\frac{\partial^2 w}{\partial t^2}\right) = -\mu w_o \sin\pi\xi \sum_s f_s'' Y_s \quad (3\text{-}57)$$

The inertia force due to the mass of a beam is a line load. The intensity of this force for the i^{th} beam is given by the equation

$$\bar{p}_i = -(m_b)_i\left(\frac{\partial^2 w}{\partial t^2}\right)_i = -(m_b)_i w_o \sin\pi\xi \sum_s f_s''(Y_s)_i \quad (3\text{-}58)$$

In terms of the dimensionless quantities given in Eqs. (3-36) through (3-39), Eqs. (3-57) and (3-58) may be expressed as follows:

$$\bar{p}_\mu = -\left[\left(1-\sum_{i=o}^{p}\gamma_i\right)\alpha^2\pi^2 \frac{1+\sum_{i=o}^{p}\lambda_i}{\lambda_{io}} \sum_s \varphi_s'' Y_s\right]\left(\frac{W}{ab}\right)\sin\pi\xi \quad (3\text{-}59)$$

and

$$\bar{p}_i = -\left[\gamma_i\alpha^2\pi^2 \frac{1+\sum_{i=o}^{p}\lambda_i}{\lambda_{io}} \sum_s \varphi_s''(Y_s)_i\right]\left(\frac{W}{a}\right)\sin\pi\xi \quad (3\text{-}60)$$

5.3 Computation of Dynamic Increments of Deflections and Moments in Bridge. As previously noted, the instantaneous values of the dynamic forces acting on the bridge are treated as static forces, and the effects of these forces are evaluated in the manner described in Chapter II.

Let $D_{i,j}$ = the deflection produced at a specified point of the i^{th} beam by a concentrated force W/2 applied at the position of the j^{th} wheel, and

$M_{i,j}$ = the bending moment corresponding to $D_{i,j}$

Then the deflection and bending moment produced at the same point by the dynamic increment of the interacting forces are given by

$$\sum_{j=1}^{2} D_{i,j}\,\Delta_j \qquad \text{and} \qquad \sum_{j=1}^{2} M_{i,j}\,\Delta_j$$

respectively.

In order to evaluate the corresponding effects of the inertia forces of the bridge, it is first necessary to determine the load matrix $\{B_m\}$ in Eq. (2-16). Since the distribution of these forces in the longitudinal direction is sinusoidal, only the term m = 1 need be considered.

The n^{th} element of $\{B_1\}$ is obtained from Eq. (2-18) by substituting Eqs. (3-59) and (3-60). Thus

$$\beta_{mn} = \beta_{1n} = \frac{a^4}{\pi^4 Db}\,\frac{1 + \sum_{i=o}^{p} \lambda_i}{\lambda_{io}}\,\alpha^2\pi^2 \left[\sum_{i=o}^{p} \gamma_i (Y_n)_i \sum_{s} \varphi_s''(Y_s)_i + \left(1 - \sum_{i=o}^{p} \gamma_i\right) \sum_{s} \varphi_s'' \int_o^1 Y_n\, Y_s\, d\eta\right] \frac{W}{a} \tag{3-61}$$

or

$$\beta_{1n} = \sum_{s} \beta_{ns}^{o}\, \varphi_s'' \tag{3-62}$$

where

$$\beta_{ns}^{o} = -\frac{\alpha^2}{\pi^2}\left(1 + \sum_{i=o}^{p} \lambda_i\right)\left[\sum_{i=o}^{p} \gamma_i (Y_s)_i (Y_n)_i + \left(1 - \sum_{i=o}^{p} \gamma_i\right)\int_o^1 Y_n\, Y_s\, d\eta\right] w_o \tag{3-63}$$

Note that $\beta_{ns}^{o} = \beta_{sn}^{o}$.

Now let $D^{o}_{i,s}$ = the deflection produced at a given point of beam i by a static load which is distributed as a sine wave in the longitudinal direction, and for which the n^{th} element of the load matrix $\{B_1\}$ is given by Eq. (3-63).

$M^{o}_{i,s}$ = the bending moment corresponding to $D^{o}_{i,s}$

The dynamic increment of deflection for beam i, $(\Delta D)_i$, can now be expressed in the form

$$(\Delta D)_i = \sum_{j=1}^{2} D_{i,j}\,\Delta_j + \sum_{s} D^{o}_{i,s}\,\varphi''_s \qquad (3\text{-}64)$$

and the corresponding increment for moment as

$$(\Delta M)_i = \sum_{j=1}^{2} M_{i,j}\,\Delta_j + \sum_{s} M^{o}_{i,s}\,\varphi''_s \qquad (3\text{-}65)$$

It is important to note that the quantities, $D_{i,j}$ and $M_{i,j}$, $D^{o}_{i,s}$ and $M^{o}_{i,s}$ are independent of the solution of the governing differential equations of motion. Furthermore, in evaluating these quantities, the number of Y_n functions used need <u>not</u> be the same as that considered in the differential equations of motion. It is for this reason that the maximum value of n used in the computation of the static effects has been denoted by n_o, whereas the value used in the equations of motion has been denoted by n_1. In fact, one of the important features of the method used is that the value of n_o may be much larger than n_1. The maximum value of s to be considered in Eqs. (3-64) and (3-65) may differ both from n_o and n_1, and it will be designated by n_2. Obviously, n_2 cannot be larger than n_1. It should finally be noted that, whereas the deflection configuration of the bridge in the longitudinal direction, was

assumed to be sinusoidal in the formulation of the equations of motion, this assumption was not retained in evaluating the deflections and moments produced in the bridge by the interacting forces.

6. Correlation Between Dynamic Increments for Deflection and Moment

The dynamic increments of the effects produced in the bridge consist of a component due to the inertia forces of the structure, and a component due to the dynamic increments of the interacting forces.

Let ΔD be the dynamic increment of deflection at a prescribed point of beam i, for any time t, and ΔM be the corresponding quantity for moment. These quantities may be written as:

$$\begin{aligned} \Delta D &= (\Delta D)_1 + (\Delta D)_2 \\ \Delta M &= (\Delta M)_1 + (\Delta M)_2 \end{aligned} \tag{3-66}$$

where the subscripts 1 and 2 refer to the first and second components of the effects.

Since the inertia forces of the structure and, consequently, the resulting effects vary as a half sine wave in the longitudinal direction, the quantities $(\Delta D)_1$, and $(\Delta M)_1$ are related by the equation

$$(\Delta M)_1 = \frac{\pi^2}{a^2} (E_b I_b)_i (\Delta D)_1 \tag{3-67}$$

whence

$$\frac{(\Delta M)_1}{Wa} = \frac{(\Delta D)_1}{Wa^3/\pi^2 (E_b I_b)_i} \tag{3-68}$$

The effects due to the dynamic increments of the interacting forces can be expressed as

$$(\Delta D)_2 = \sum_m (\Delta D)_{2,m}$$

$$(\Delta M)_2 = \sum_m (\Delta M)_{2,m}$$

where $(\Delta D)_{2,m}$ and $(\Delta M)_{2,m}$ are the deflection and moment produced by the m^{th} term in a Fourier series expansion of the instantaneous values of the interacting forces. By considering only the first term in this series, one obtains

$$(\Delta D)_2 \approx (\Delta D)_{2,1}$$

$$(\Delta M)_2 \approx (\Delta M)_{2,1} \tag{3-69}$$

and, by analogy to Eq. (3-68), one concludes that

$$\frac{(\Delta M)_2}{Wa} \approx \frac{(\Delta D)_2}{Wa^3/\pi^2(E_b I_b)_i} \tag{3-70}$$

From Eqs. (3-66), (3-68) and (3-70), it now follows that

$$\frac{\Delta M}{Wa} \approx \frac{\Delta D}{Wa^3/\pi^2(E_b I_b)_i} \tag{3-71}$$

Numerical solutions presented later in this report show that Eq. (3-71) is generally quite accurate.

7. Problem Considered for Solution on ILLIAC

7.1 General. The computer program has been developed for the class of bridges considered in Art. 3 of Chapter II. The roadway surface unevenness is represented by a trigonometric function in the longitudinal direction, as discussed in Art. 4.1. The load unit may consist of one or two wheels.

The program provides results for the complete history of the response of the system, by printing out the crawl or static values of the deflections and moments in the beams at midspan, the corresponding dynamic increments, and the dynamic increments of the wheel reactions.

7.2 Summary of Problem Parameters. The following dimensionless parameters are used to define a problem.

Bridge Parameters

1. The ratio of sides, c. This is the ratio of the overall width of the structure, b, to the span length, a.

2. The number of beams, p + 1.

3. The flexural rigidity factors, λ_o and λ_1, for the interior and exterior beams, respectively.

4. The torsional rigidity factors, k_o and k_1, for the interior and exterior beams, respectively.

5. The dimensionless mass parameters, γ_o and γ_1, for the interior and exterior beams, respectively.

6. The roadway surface unevenness parameters, m_1, e_1, and e_2, defined by Eq. (3-35).

Vehicle Parameters

7. The transverse position of the vehicle on the bridge, as specified by the η-coordinates of the wheels, η_1 and η_2.

8. The parameter ρ for the moment of inertia of the sprung mass, defined by Eq. (3-43).

9. The weight parameter ω, defined by Eq. (3-36).

Bridge-Vehicle Parameters

10. The speed parameter α, defined by Eq. (3-36).

11. The weight ratio ν, defined by Eq. (3-36).

12. The frequency parameter K, defined by Eq. (3-36).

Parameters Related to Method of Solution

13. The parameter m_o which specifies the maximum number of half-sine waves considered in the longitudinal direction in the computation of the static effects.

14. The parameters n_o, n_1 and n_2; these specify the numbers of Y_n functions used for various purposes: (See Art. 5.3).

15. The number of integration steps, N, and the number of steps between print-outs, N_1.

Initial Conditions

16. The initial values of φ_s, ζ, and θ, and of φ_s', ζ', and θ'.

For a bridge cambered so that, under the action of its own weight, its surface is horizontal, the quantities $e_1 = e_2 = 0$. If the bridge is not cambered, the effect of the dead load deflection of the structure may be considered approximately as follows. The deflection in the longitudinal direction may be represented by the first term in a Fourier series expansion, and the configuration in the transverse direction may be considered as uniform. Then

$$m_1 = 1$$

and

$$e_1 = e_2 = \frac{1}{w_o} \frac{4a^4}{\pi^5} \frac{g[\mu b + \sum_{i=o}^{p} (m_b)_i]}{Db + \sum_{i=o}^{p} (E_b I_b)_i}$$

In terms of the dimensionless quantities defined in Eqs. (3-36) to (3-39), the latter equation becomes

$$e_1 = e_2 = \frac{4}{\pi^5 \nu} \frac{\lambda_o}{1 + \sum_{i=o}^{p} \lambda_i} \tag{3-72}$$

The initial dynamic displacement of the sprung mass of the vehicle in the vertical direction, z_o, is usually expressed as a fraction of the static value of the deflection of the mass, z_s. The initial value of the dimensionless coordinate ζ may then be determined from the equation

$$\zeta = \left(\frac{z_o}{z_s}\right) \zeta_s \tag{3-73}$$

where

$$\zeta_s = \frac{z_s}{w_o} = \frac{gM}{2kw_o} = \frac{1}{K\nu\pi^4} \frac{\lambda_o}{1 + \sum_{i=o}^{p} \lambda_i} \tag{3-74}$$

The initial value of the dimensionless coordinate θ can be determined in a similar manner.

7.3 Description of Computer Program. A general flow diagram for the complete program is shown in Fig. 6. The operations listed in the first column of this diagram are performed once for each problem, those listed in the second column are performed once every time the response of the bridge is to be printed out, and the operations in the third column are performed once in each step of integration. The sequence of the major operations involved and the routines used are described briefly in the following paragraphs with the aid of additional flow diagrams. The complete write-up of the program will be placed in the ILLIAC Library of the Department of Civil Engineering.

As indicated in Fig. 6, the first major task of the program is to evaluate the quantities $Q_{m,j}$ which are used to evaluate the deflections and bending moments in the beams at midspan. These are defined by the equation

$$Q_{m,j} = \frac{1}{m^2} \sin \frac{m\pi}{2} \sum_{n=-1}^{n_o} \alpha'_{mn,j} Y_n(\eta_i) \tag{3-75}$$

in which the subscript j refers to the j^{th} wheel and can take on the values of 1 and 2. The coefficients $\alpha'_{mn,j}$ represent solutions of Eq. (2-16) with the elements β_{mn} of the load matrix $\{B_m\}$ replaced by $\beta_{n,j}$, where

$$\beta_{n,j} = \frac{\lambda_\bullet}{\pi^2} Y_n(\eta_j) \tag{3-76}$$

As before, the subscript j refers to the j^{th} wheel. Equations (3-75) and (3-76) are entirely analogous to Eqs. (2-45) and (2-44) for the static problem.

The operations involved in the computation of $Q_{m,j}$ are indicated in Fig. 7. This flow diagram is similar to that presented in Fig. 4 for the static problem. In the present case, however, only the odd values of m are considered, since the even terms do not contribute to the deflections and moments at midspan. The quantities $Q_{m,j}$ are stored on the magnetic drum, and they are recalled to the Williams memory whenever needed.

The deflections, $D_{i,j}$, and moments, $M_{i,j}$, are related to the quantities $Q_{m,j}$ as follows.

$$D_{i,j} = (C_d)_j \frac{Wa^3}{(E_b I_b)_o} \tag{3-77}$$

$$M_{i,j} = (C_m)_j Wa \tag{3-78}$$

Then

$$(C_d)_j = \frac{1}{\pi^2} \sum_{m=1,3..}^{m_o} \frac{1}{m^2} Q_{m,j} \sin m\pi\tau \qquad (3\text{-}79)$$

$$(C_m)_j = \frac{\lambda_i}{\lambda_o} \sum_{m=1,3..}^{m_o} Q_{m,j} \sin m\pi\tau \qquad (3\text{-}80)$$

These equations may be obtained from Eqs. (2-48) and (2-49) by replacing Q_m by $Q_{m,j}$ and ξ by τ. The quantity λ_i represents the value of λ for the beam where C_m is evaluated.

It is to be recalled that $D_{i,j}$ and $M_{i,j}$ represent the static effects due to the j^{th} wheel only.

The operations involved in the computation of the quantities $D^o_{i,s}$ and $M^o_{i,s}$ for the inertia forces of the bridge are indicated in the flow diagram presented in Fig. 8. These operations are similar to those used to calculate $D_{i,j}$ and $M_{i,j}$, with the important exception that they are performed for m = 1 only, since the distribution of the inertia forces in the longitudinal direction is sinusoidal.

The quantities $D^o_{i,s}$ and $M^o_{i,s}$, together with the quantities $Q_{m,j}$, are stored on the drum, and are played back to the Williams memory only when the deflections and moments are to be computed.

The constant coefficients referred to in the first column of the flow diagram in Fig. 6 are the coefficients on the left-hand sides of Eqs. (3-40) that are independent of τ and of the generalized coordinates. It should be noted that the number of these depends on the number of generalized coordinates used for the bridge. Since the routines that are needed to evaluate these constants cannot all be retained in the Williams memory, they are stored on the magnetic drum, and they are recalled in successive groups.

Before starting the integration of the differential equations, the second derivatives of the generalized coordinates $\ddot{q}_n$ (i.e., φ_s'', ζ'', and θ''), the interacting forces, and the deflections and moments in the bridge are evaluated for $\tau = 0$. A detailed flow diagram of the operations involved is given in Fig. 9. The significance of the S6 parameter referred to in this figure is explained in the detailed program write-up referred to previously in Art. 7.3.

A flow diagram for the integration procedure is given in Fig. 10; this is believed to be self-explanatory.

In Fig. 10 it should be noted that the interacting forces and the effects in the bridge are not evaluated at each step of integration, but only when they are to be printed out. The interval between print-outs is specified by means of the problem parameter N_1.

This program utilizes the entire Williams memory of the ILLIAC, and approximately 3200 locations of its magnetic drum memory. Certain parts of the program, including the main control routine (MC), blocks of constant quantities, the library routine (T5) for sines and cosines, the library routine (Y1) which is used to transfer blocks of instructions between the Williams memory and the drum, and the problem parameters which are read in from the data tape at the beginning of each problem, are retained in the Williams memory. The remaining parts of the program are recorded on the drum, and are transferred to the Williams memory whenever needed.

In the following are listed some of the limitations of the computer program:

$$m_o + 1 \leq 160/(p+1); \quad 2 \leq n_o \leq 8; \quad n_2 \leq n_1 \leq 2$$

where m_o, n_o, n_1, n_2 are integers defined in Arts. 7.3 and 5.3. For a five-girder bridge, the limitation on m_o becomes $m_o \leq 31$. It should be remembered that the range of the n-quantities is -1, 0, 1, ...

A single-wheel loading is treated as a two-wheel loading for which $\eta_1 = \eta_2$. The program is so arranged that it does not have to consider Eq. (3-42) in this case.

The program may be used also to determine the response of a beam by considering only the function Y_{-1} in the differential equations of motion. This amounts to assuming that the bridge does not deflect in the transverse direction. The interacting forces and the inertia forces in the bridge will then be identical to those for the beam. The deflection and bending moments for each of the supporting beams of the bridge will not be the same, however, because of the limitation on the minimum value of n_o that may be considered in the static problem. The moment in the single beam may be evaluated by taking the sum of the moments in the beams and in the slab of the bridge.

With the maximum possible values of n_1, n_2, n_o and m_o, and with $N = 100$ and $N_1 = 2$, the machine time required to calculate and print out the history of the response for a five-girder bridge is about nine minutes.

8. Discussion of Assumptions

8.1 General. In the formulation of the equations of motion of the system, the instantaneous distribution of the dynamic deflection of the bridge in the longitudinal direction was assumed to vary as a half-sine wave, and the distribution in the transverse direction was expressed as a linear combination of Y_n functions, each multiplied by a time-dependent coefficient.

The adequacy of the first assumption was investigated indirectly by obtaining numerical solutions for the special case of a beam, and comparing the results with those obtained by application of other methods. It has already been noted that, as applied to a beam, the present method reduces to Inglis' method. The sensitivity of the response to the number of Y_n functions considered in the equation of motion was studied by obtaining solutions for several five-girder bridges for an increasing number of Y_n functions.

8.2 Comparison of Beam Solutions. In Figs. 11 through 14 are given solutions for the response of a beam for a fairly wide range of values of the parameters involved. The curves in Figs. 11 and 12 are for a smoothly moving load, whereas those in Figs. 13 and 14 are for an initially oscillating load. The upper curves in each of these figures represent dynamic increments of moment at midspan. The solutions shown in solid lines and identified as "Procedure 1" were obtained with the aid of the computer program developed in the present investigation. Only the Y_{-1} function was used in the dynamic equations. As noted in Art. 4.3 of this chapter, this amounts to solving Eqs. (3-44) and (3-45). The moments were computed as the sum of the moments in the beams of a five-beam bridge with $c = 0.8$ and $\lambda = 25$. A solution was also obtained by using $c = 0.4$ and $\lambda = 12.5$. As would be expected, the interacting forces computed for these two sets of parameters were identical. The sum of moments in the beams differed by about 1.5%, the difference being due to the change of moment in the slab. The solutions referred to as "Procedure 2" and "Procedure 3" were obtained by use of the computer programs reported in Refs. (14) and (5) respectively. Wen's method, which is a modification of Hillerborg's method and which, in turn is a modification of

Inglis' method, involves the assumption that the instantaneous configuration of the dynamic deflection of the beam is proportional to the static deflection configuration produced by the combined effect of the moving load and the weight of the beam itself. In the Huang-Veletsos method, the beam is analyzed as a multi-degree-of-freedom system, with the mass of the beam concentrated at a finite number of points. The solutions included here were obtained by considering only three concentrated masses.

It can be seen from Figs. 11 through 14 that the results obtained by the three methods are generally in very good agreement. This favorable comparison inspires much confidence in the adequacy of the assumption that the instantaneous distribution of the dynamic deflection along the beam is a half-sine wave. In addition, these solutions have served to provide an independent check on the correctness of the computer program that has been developed.

8.3 Effect of Number of Dynamic Degrees of Freedom for Bridge. This problem was studied by means of numerical solutions for three five-girder bridges having the following dimensions:

$c = 0.4$ $\quad\quad$ $\lambda = 12.5$

$c = 0.4$ $\quad\quad$ $\lambda = 50$

$c = 0.8$ $\quad\quad$ $\lambda = 25$

The torsional rigidity of the beams was taken equal to zero in all cases. The first two bridges are the same as those considered for the static solutions presented in Chapter II. The vehicle was idealized as a single-wheel load without any unsprung mass, and it was considered to move along the edge beam. In each case, three solutions were obtained by treating the bridge as a system with two, three, and four degrees of freedom, respectively.

In Figs. 15 through 21 are presented the time histories of the interacting forces and of the dynamic increments of deflections of the beams at midspan. The values of the various parameters are indicated on the figures. It can be seen that the solutions for $c = 0.4$ and $\lambda = 12.5$ - a structure with a relatively high transverse rigidity - differ only slightly from one another. Those for $c = 0.8$ and $\lambda = 25$ - a fairly flexible structure in the transverse direction - are very much different. The results for the intermediate structure ($c = 0.4$, $\lambda = 50$) are in fairly good agreement, especially the solutions obtained by analyzing the bridge as a system with three and four degress of freedom.

On the basis of these data, and from a study of the natural modes of vibration of the three structures that were investigated[15], it appears that in the formulation of the equations of motion, one must consider a sufficiently large number of Y_n functions so that the first two symmetric and the first two antisymmetric natural modes of vibration of the structure are approximated fairly accurately. The relative importance of the higher modes cannot be evaluated, since these cannot be considered in the computer program. The indications are, however, that their contribution to the total response may be important only for very flexible structures for which the natural frequencies of the first four modes are close to each other. It is also anticipated that the contribution of these modes will be less significant for a two-wheel loading than for a single-wheel loading.

8.4 Effect of Time Interval of Integration. The natural periods of vibration, T, of a multigirder bridge may be stated as

$$T = \frac{T_b}{\sqrt{K_o}} \qquad (3\text{-}81)$$

where K_o is a dimensionless coefficient dependent on the geometric and physical characteristics of the bridge and on the order of the period under consideration. Numerical values of K_o for various structures have been reported in Ref. (15)*.

The criterion for convergence and stability of the integration procedure (see Eq. 3-51), can now be written as

$$\frac{a}{v}\,\frac{1}{N} < 0.389\,\frac{T_b}{\sqrt{K_o}}$$

or, noting that $\alpha = \frac{vT_b}{2a}$, as

$$N > 1.285\,\frac{\sqrt{K_o}}{\alpha} \qquad (3\text{-}82)$$

The value of K_o in this equation should correspond to the lowest period of the mathematical model used in the analysis. The bridge as analyzed here, has four natural modes of vibration, two of which are symmetric and the other two antisymmetric about the longitudinal center line. The relevant period is the one corresponding to the second antisymmetric mode.

For a five-girder bridge with $c = 0.4$, $\lambda = 25$, $k = 0$, and $\gamma = 0.05$, the value** of K_o corresponding to the second antisymmetrical mode is $K_o = 12.1$; for a value of $\alpha = 0.15$, Eq. (3-82) gives

$$N > 30$$

---

* The meanings of the symbols λ and γ used in Ref. (15) and the present report are different.

** This is the value obtained by considering more than four degrees of freedom. Strictly speaking, one should use the value computed for the four-degree-of-freedom system.

The response of this bridge under a smoothly moving load was evaluated on the basis of four different values of N. The maximum values of the response are summarized in Table 15 together with the values of the problem parameters. It can be seen from this table that the differences between the results corresponding to different values of N are generally very small. For the numerical results presented in this report a constant value N = 100 was used.

9. Comparison of Theoretical and Experimental Results

The theoretical predictions have also been compared with experimental data obtained from dynamic tests conducted on an all-aluminum, five-girder I-beam bridge model; the characteristics of this model and the conditions of the tests have been described in Ref. (12). The results for the two test runs that were considered are presented in Figs. 21 through 24. The experimental results included were reproduced from Ref. (4).

The theoretical solutions were obtained for the following values of the parameters: $c = 0.4$, $\lambda_o = \lambda_1 = 14.5$, $k_o = k_1 = 5$, $\gamma_o = \gamma_1 = 0.12$, $e_j = 0.0076$, $\omega = 0.09$, $\nu = 0.34$, $f_v/f_b = 0.55$, $\alpha = 0.16$. Both the bridge and the vehicle were assumed to be initially in their static positions of equilibrium.

In Fig. 21 are given history curves for total deflections (i.e. sum of static value and dynamic increment) at midspan of beams A, B, and C, produced by a single wheel load moving over beam C. In Fig. 22 are shown the same results, expressed in the form of history curves for dynamic increments. The corresponding curves for dynamic increments of strains at midspan are given in Fig. 23. Included in Figs. 22 and 23 are the experimental curves for beams D and E. It is seen that, although the structure and the loading are presumably symmetric with respect to the longitudinal

center line, the experimental results for the responses of the symmetric beams are not identical. These differences, which are generally small, may be considered as measures of the uncertainties about the properties of the system and the reliability of the experimental data. The agreement between the theoretical and experimental curves presented in Figs. 21 through 23 is generally satisfactory.

In Fig. 24 are given history curves for the dynamic increments of strains produced at midspan of the beams by the same load running over beam A. The agreement between theoretical and experimental data, although not as good as in the previous case, is still satisfactory.

IV. NUMERICAL STUDIES

1. General

The aim of the numerical results presented herein is to provide information which may lead to a better understanding of the dynamic behavior of simple-span multigirder bridges. The parameters that were varied in this study are those that cannot be considered when the bridge is analyzed as a beam. Most solutions were obtained for a single-wheel loading. The solutions presented are of a limited number, and the conclusions drawn therefrom are generally of qualitative nature. A more complete study of the effects of the various parameters involved would require a much greater number of solutions.

The structures analyzed are of the same type as those considered in the static solutions presented in Chapter II (see Fig. 2). As before, the torsional stiffness of the beams is taken equal to zero. The vehicle is represented either as a single-wheel load or a two-wheel load without any unsprung mass. In all the solutions, the parameters α, ν, and f_v/f_b are kept constant, so that the solution obtained by considering the bridge as a beam is the same in all cases. The mass and the flexural rigidity of the equivalent beam are assumed to be the same as those for the total structure. This approach has been used by previous investigators, and amounts to considering a uniform transverse distribution of deflections. The major parameters varied are the flexural rigidity of the beams relative to that of the slab, the ratio of sides, and the transverse location of the loads.

The dimensionless weight parameter for the beams is taken as $\gamma = 0.05$. In all the solutions, the bridge deck is assumed to be initially smooth and horizontal, and the sprung mass is assumed to be at its position of static equilibrium when it enters the span.

Unless otherwise stated, it is to be understood that all solutions were obtained by using four Y_n functions in Eq. 3-1, i.e. by analyzing the bridge as a system with four degrees of dynamic freedom ($n_1 = 2$). In evaluating the effects of the instantaneous inertia forces and of the interacting forces, the transverse deflection configuration of the bridge was represented by means of eight Y_n functions (i.e. $n_o = 6$). In computing the effects of the interacting forces, fifteen load components were considered in the longitudinal direction (i.e. $m_o = 15$).

The dynamic response of the bridge-vehicle system is depicted in terms of history curves for interacting forces and for dynamic increments of moment and/or deflection for the individual beams. In addition, curves for the sum of the dynamic increments of moments in the beams are presented. The latter curves and those for the interacting forces are compared with the corresponding curves determined by use of the beam theory. The concept of the sum of dynamic increments of moments has been introduced in an attempt to relate the results obtained by the present method of analysis to those predicted by the beam theory.

2. Solutions for Symmetric Loading

2.1 Typical Response Curves and Effects of Transverse Flexibility.

The solutions presented in this section were obtained by considering a single-wheel load moving over beam C.

In Figs. 25 to 27 are presented history curves for the interacting force and for the sum of dynamic increments of moments in the beams for eight structures characterized by different sets of values of λ and c. It may be recalled that the greater the values of λ and c the greater is the

flexibility of the structure in the transverse direction. In Figs. 25 and 26 the ratio of sides is kept constant and λ is varied, whereas in Fig. 27 the quantity $H = \lambda c$ is kept constant and the effect of varying c is investigated. Included in each of these figures are also the results of the beam theory obtained by using only the Y_{-1} function in the dynamic equations.

It can be seen from these figures that the response curves for the bridge have essentially the same shape as those obtained by the beam theory. It is important to note, however, that the peak values of the response for the bridge are consistently larger than those predicted by the beam theory, the difference generally increasing with increasing flexibility of the structure in the transverse direction, or increasing values of λ and c. For the most flexible structures considered, the absolute maximum value of the sum of dynamic increments of moment in the beams is about twice as large as that predicted by the beam theory.

An attempt was made to relate the peak values of the sum of the dynamic increments of moments in the beams to the value of the maximum static deflection produced in the loaded beam by the load at midspan. The results of this study are summarized in Table 16, and they are also plotted in Fig. 28 in a normalized form. It is noteworthy that the results plot almost on a straight line.

In Figs. 25 to 27 it is interesting to note that at the instant that the sum of the dynamic increments of moments attain their peak values, the value of the interacting force is relatively small. This indicates that the response of the bridge is primarily due to the inertia forces of the structure, and that the contribution of the interacting force is relatively minor.

In Figs. 29 and 30 are given the time histories of dynamic increments of moment for the individual beams of some of the structures considered previously in Figs. 25 and 26. For clarity, only the solutions corresponding to the extreme values of λ are presented. As would be expected from the data presented in Figs. 25 and 26, the maximum response of the loaded beam increases with increasing transverse flexibility of the structure (i.e. increasing values of λ and c).

2.2 Relationship Between Dynamic Increments for Deflection and Moment. As a check on the accuracy of Eq. (3-71), in Fig. 31 the dynamic increments for moment in the beams of a particular structure are compared with the corresponding increments for moment. The characteristics of the system analyzed are defined on the figure. The ordinates for moment are expressed in terms of Wa, and those for deflection in terms of $Wa^3/\pi^2 E_b I_b$.

It can be seen that, except for some minor differences in the curves for the loaded beam, the two sets of curves are almost identical. For beams A and B only the solid line is shown as the dotted curve could not be differentiated when plotted on the same scale. This agreement, typical of a large number of similar comparisons that have been made, substantiates the accuracy of Eq. (3-71). Another comparison for a load applied over beam A is given in Fig. 42. Since the dynamic increments for moment and deflection are for all practical purposes proportional, in the remaining part of this report, solutions will be presented either for moment only, or for deflection only.

2.3 Transverse Distribution of Dynamic Effects. The instantaneous transverse distribution of the dynamic increments of moments in the beams are presented in Fig. 32 for three structures having a common ratio of sides, $c = 0.8$, but different values of λ.

It can be seen from this figure that the distribution of dynamic effects is not constant, but varies with time. It follows that the bridge does not respond as a system having a single degree of freedom in the transverse direction. In particular, the transverse distribution of effects is neither uniform nor porportional to that of the static effects. A comparison of the distributions of static effects and dynamic increments is given in Table 17. The peak values of the dynamic increments of moment in the beams for all the structures investigated are listed in this table as percent of the maximum value of their sum. Similarly the maximum static moments in the beams are listed as percent of the corresponding sum.

It is convenient to think of the response of the bridge as being made up of two components, one arising from the variation of the interacting force, and a component arising from the inertia forces of the bridge itself. The first component, which is proportional to the static effects, is not very significant, at least for the cases considered, since the variation of the interacting force is relatively small. The second component is essentially the sum of the contributions of the natural modes of vibration of the mathematical bridge model analyzed. It may be recalled that the bridge is analyzed as a system with four degrees of dynamic freedom, and that for motions that are symmetric about the longitudinal center line it has only two degrees of freedom. Both modes contribute to the response of the systems considered.

The degree of participation of the various modes in the total response depends, among other factors, on the relative ordinates of the various modes at the transverse position of the load or loads. For example, if the path of travel of the load is a node line for a particular mode, that mode cannot be excited.

In an effort to explore this possibility, solutions were obtained for a structure with $c = 0.8$ and $\lambda = 25$, and a two-wheel loading.

The results are presented in Figs. 33 through 37 in the form of time histories of interacting forces, dynamic increments for moment in the individual beams, sum of dynamic increments, and instantaneous distributions of dynamic increments. The results presented in Figs. 33 and 34 were obtained with the wheels over beams B and D, and those presented in Figs. 35 and 36 were obtained with the wheels over beams A and E.

From Fig. 33 it can be seen that, when the wheels move over beams B and D, the time histories of the dynamic increments for all the beams are in phase, and that the effects in the edge beams are a small fraction of those in the center beam. In this case the bridge responds primarily in the first symmetric, or fundamental mode of vibration. This may be seen clearly from the second column of Fig. 37 which shows that the transverse distribution of dynamic increments does not vary appreciably with time; also this distribution corresponds to the fundamental mode, as reported in Ref. (15).

In Fig. 34 it is of interest to note that the sum of dynamic increments of moments in the beams is very similar to the beam solution except for a phase shift which may be explained by the fact that the natural frequency of the bridge is actually less than that of the beam[15]. The relatively insignificant contribution of the second symmetric mode is due to the fact that the node lines of this mode are close to beams B and D.

When the wheels are over beams A and E, the fundamental mode is not excited appreciably, since the relative ordinates of this mode at beams A and E are small. As may be seen from Figs. 35, 36 and 37(c), in this case, the major contribution to the response arises from the second symmetric mode.

3. Solutions for Eccentric Loading

The solutions presented in this section parallel those presented in the previous section for symmetric loading.

3.1 Typical Response Curves and Effects of Transverse Flexibility. In Figs. 38 and 39 are given history curves for the interacting forces and for the sum of dynamic increments of moments in the beams of the structures considered previously, produced by a single-wheel load moving over beam A. The results of the beam theory are also included for comparison.

It is noted from these figures that the actual interacting force curves have no resemblance to the curve determined from the beam theory. However, they all are characterized by high frequency oscillations superimposed on a low frequency main curve which is practically the same for all cases. The predominant period of the high-frequency oscillations ranges approximately between the periods of the first and second antisymmetrical modes of the corresponding structure.

On comparing Figs. 38 and 39 to Figs. 25 and 26, it is seen that for a given structure the magnitude of the interacting force is larger when the load moves along beam A than when it moves along beam C. There appear to be two factors that contribute to this result: (1) Since the static or crawl deflection of the point of application of the load is greater when the load moves over an edge beam than when it moves over the center beam, the resulting excitation of the vehicle is greater in the former case. This factor seems to be responsible for the large ordinates of the main curve. (2) Since the high-frequency waves are numerous, the chances are great that one of these will combine with a large ordinate of the main low frequency curve to yield a higher maximum than could otherwise be obtained.

It is also seen from these figures that, in contrast to the observation made for the case of a load applied over beam C, the shapes of the curves for the sum of the dynamic increments of moments are different from the one obtained by the beam theory; furthermore, the peak value of the sum does not increase with increasing flexibility of the structure. In particular, the linear relationship presented in Fig. 28 is not applicable in this case.

In Figs. 40 and 41 history curves are presented for the dynamic increments of moments in the individual beams of the same structures as were considered previously in Figs. 29 and 30. It is seen from these figures that the shapes of the curves are different for the different beams. This result indicates that several modes of vibration contribute to the response to a comparable extent. The contribution of the antisymmetric modes is most clearly seen on the curves for beam E, where the predominant period of oscillations ranges between the periods of the first and second antisymmetric modes of the structure. Note that the predominant period increases with increasing transverse flexibility, as would be expected.

3.2 Transverse Distribution of Dynamic Effects. The instantaneous transverse distribution of the dynamic increments of moments in the beams is presented in Fig. 43. The structures considered here are the same as those in Fig. 32 where the distribution of the effects due to a load on beam C was presented.

It is seen that, in this case, the antisymmetric modes of vibration are excited to a rather pronounced extent. It should be noted, however, that the structures considered in this figure are fairly flexible in the transverse direction. For stiffer structures, the participation of the higher modes are not likely to be as important. This may be appreciated by referring to

Figs. 15 through 20 and noting that, for the stiffer structures, the response of the system is not sensitive to the number of Y_n functions used in the dynamic equations.

V. SUMMARY

A method and a computer program have been developed for the computation of the dynamic response of simple-span, multigirder highway bridges under a moving vehicle. The bridge was analyzed as a plate continuous in one direction over flexible beams. The vehicle was idealized as a single-axle, sprung load having one or two wheels. The torsional stiffness of the beams was taken into account, but the effects of damping in the bridge and the vehicle were not considered.

An exploratory set of numerical solutions were obtained for a group of five-girder bridges in order to study the response characteristics of these bridges and to compare the predictions of the present analysis with those determined by treating the bridge as a beam, a simplification used in all previous investigations of this problem. In these solutions, a total of four generalized coordinates were used to express the dynamic configuration of the bridge in the transverse direction. The majority of the solutions were for a single-wheel load.

The results were presented in the form of history curves for interacting forces, for dynamic increments of deflection and moment in the individual beams, and for the sum of dynamic increments for moment in the beams. The latter quantity was used as a means of relating the results of the present study to those predicted on the basis of the beam theory.

The principal findings may be summarized as follows:

(1) For a load moving along the center beam, the time histories for the sum of the dynamic increments for moment in the beams are similar to those determined by the beam theory, but the magnitudes of these effects are generally larger. For some of the more flexible structures considered, the absolute maximum value of this sum was about twice as large as that predicted by the beam theory.

(2) For a load moving over the edge beam, no correlation could be found between the sum of dynamic increments for moment in the beams and the prediction of the beam theory. In general, the first torsional or antisymmetrical mode of vibration was found to contribute significantly to the total response. Since the contributions of the antisymmetrical modes are not reflected in the sum of the dynamic increments, this lack of correlation should not be surprising. It is possible, however, that a better correlation between the two approaches may be obtained upon comparing the sum of the strain energies of the beams of the actual structure to the energy of the substitute beam.

(3) The transverse distribution of dynamic increments is neither uniform nor proportional to the static effects; it is essentially a combination of the various natural modes. It is to be noted that, even for the fundamental mode of vibration, the transverse distribution of effects may be quite non-uniform.

(4) The degree of participation of the various modes depends both on the properties of the bridge and on the positions of the wheel paths relative to the node lines of the various natural modes of vibration. Broadly speaking, the greater the transverse stiffness of the bridge, the smaller is the contribution of the higher modes.

It is important to note that these conclusions may not be valid beyond the range of parameters considered in this study. For example, it is likely that the differences between the response of the actual bridge and of the substitute beam may not be as significant for multiple-wheel loads as it is for the single-wheel loads considered in the majority of the solutions that have been presented.

As a part of this investigation, the analysis of bridges for static loads was considered, and two computer programs were developed for the computation of influence surfaces for deflection and moment, and for the effects produced by a three-axle truck loading.

REFERENCES

1. Biggs, J. M., Suer, H. S., and Louw, J. M., "Vibration of Simple-Span Highway Bridges," Transactions, ASCE, Paper No. 2979, 1959, pp. 291-318.

2. Fleming, J. F., "The Effect of Load Characteristics and the Bridge Geometry upon Highway Bridge Impact," Ph.D Thesis, Carnegie Institute of Technology, 1960.

3. Hillerborg, A., "Dynamic Influences of Smoothly Running Loads on Simply Supported Girders," Institution of Structural Engineering and Bridge Building of the Royal Institute of Technology, Stockholm, Sweden, 1951.

4. Huang, C. L., and Walker, W. H., "Analysis of Data Obtained from Tests on a Highway Bridge Model," Part D, Tenth Progress Report, Highway Bridge Impact Investigation, University of Illinois, 1960.

5. Huang, T., and Veletsos, A. S., "Dynamic Response of Three-Span Continuous Highway Bridges," Civil Engineering Studies, Structural Research Series No. 190, University of Illinois, 1960.

6. Inglis, C. E., "A Mathematical Treatise on Vibration in Railway Bridges," Cambridge University Press, 1934.

7. Looney, C. T. G., "High-Speed Computer Applied to Bridge Impact," Proceedings, ASCE, Paper 1759, September 1958.

8. Newmark, N. M., "A Method of Computation of Structural Dynamics," Journal of Engineering Mechanics Division, Proceedings, ASCE, July 1959, pp. 67-94.

9. Newmark, N. M., "A Distribution Procedure for the Analysis of Slabs Continuous Over Flexible Beams," University of Illinois Engineering Experiment Station, Bulletin 304, 1938.

10. Newmark, N. M., and Siess, C. P., "Moments in I-Beam Bridges," University of Illinois Engineering Experiment Station, Bulletin 336, 1942. (a) p. 28.

11. Oran, C., "Comparison Between Measured and Computed Static Effects in an I-Beam Bridge Model," Part C, Ninth Progress Report, Highway Bridge Impact Investigation, University of Illinois, 1959.

12. Prince-Alfaro, J., and Veletsos, A. S., "Dynamic Behavior of an I-Beam Bridge Model Under a Smoothly Rolling Load," Civil Engineering Studies, Structural Research Series No. 167, University of Illinois, 1958.

13. Tung, T. P., Goodman, L. E., Chen, T. Y., and Newmark, N. M., "Highway Bridge Impact Problems," Highway Research Board, Bulletin 124, 1956, p. 111.

14. Wen, R. K. L., "Dynamic Behavior of Simple-Span Highway Bridges Traversed by Two-Axle Vehicles," Civil Engineering Studies, Structural Research Series No. 142, University of Illinois, 1957.

15. Yamada, Y., and Veletsos, A. S., "Free Vibration of Simple Span I-Beam Bridges," Part B, Eighth Progress Report, Highway Bridge Impact Investigation, University of Illinois, 1958.

TABLES

TABLE 1. MATRIX $[F_m]$ CORRESPONDING TO SYMMETRIC FUNCTIONS Y_n

$1+\sum\lambda_i$	$\frac{2}{\pi}+\sum\lambda_i \sin\left(\pi\frac{i}{p}\right)$	$\frac{2}{3\pi}+\sum\lambda_i \sin\left(3\pi\frac{i}{p}\right)$	$\frac{2}{5\pi}+\sum\lambda_i \sin\left(5\pi\frac{i}{p}\right)$
	$\frac{1}{2}\left[1+\frac{1}{(mc)^2}\right]^2+$ $\sum\left[\lambda_i \sin^2\left(\pi\frac{i}{p}\right)\right.$ $\left.+\frac{k_i}{(mc)^2}\cos^2\left(\pi\frac{i}{p}\right)\right]$	$\sum\left[\lambda_i \sin\left(\pi\frac{i}{p}\right)\sin\left(3\pi\frac{i}{p}\right)\right.$ $\left.+\frac{3k_i}{(mc)^2}\cos\left(\pi\frac{i}{p}\right)\cos\left(3\pi\frac{i}{p}\right)\right]$	$\sum\left[\lambda_i \sin\left(\pi\frac{i}{p}\right)\sin\left(5\pi\frac{i}{p}\right)\right.$ $\left.+\frac{5k_i}{(mc)^2}\cos\left(\pi\frac{i}{p}\right)\cos\left(5\pi\frac{i}{p}\right)\right]$
Symmetric about Diagonal		$\frac{1}{2}\left[1+\frac{9}{(mc)^2}\right]^2+$ $\sum\left[\lambda_i \sin^2\left(3\pi\frac{i}{p}\right)\right.$ $\left.+\frac{9k_i}{(mc)^2}\cos^2\left(3\pi\frac{i}{p}\right)\right]$	$\sum\left[\lambda_i \sin\left(3\pi\frac{i}{p}\right)\sin\left(5\pi\frac{i}{p}\right)\right.$ $\left.+\frac{15k_i}{(mc)^2}\cos\left(3\pi\frac{i}{p}\right)\cos\left(5\pi\frac{i}{p}\right)\right]$
Symbol $\sum$ denotes $\sum_{i=0}^{p}$			$\frac{1}{2}\left[1+\frac{25}{(mc)^2}\right]^2+$ $\sum\left[\lambda_i \sin^2\left(5\pi\frac{i}{p}\right)\right.$ $\left.+\frac{25k_i}{(mc)^2}\cos^2\left(5\pi\frac{i}{p}\right)\right]$

TABLE 2. MATRIX $[F_m]$ CORRESPONDING TO ANTISYMMETRIC FUNCTIONS Y_n

$\left[\frac{1}{12} + \frac{2}{\pi^2(mc)^2}\right] +$ $\sum\left[\lambda_i \left(\frac{p-2i}{2p}\right)^2 + \frac{k_i}{\pi^2(mc)^2}\right]$	$\frac{1}{2\pi} + \sum\left[\lambda_i\left(\frac{p-2i}{2p}\right)\sin\left(2\pi\frac{i}{p}\right)\right.$ $\left. - \frac{2k_i}{\pi(mc)^2}\cos\left(2\pi\frac{i}{p}\right)\right]$	$\frac{1}{4\pi} + \sum\left[\lambda_i\left(\frac{p-2i}{2p}\right)\sin\left(4\pi\frac{i}{p}\right)\right.$ $\left. - \frac{4k_i}{\pi(mc)^2}\cos\left(4\pi\frac{i}{p}\right)\right]$	$\frac{1}{6\pi} + \sum\left[\lambda_i\left(\frac{p-2i}{2p}\right)\sin\left(6\pi\frac{i}{p}\right)\right.$ $\left. - \frac{6k_i}{\pi(mc)^2}\cos\left(6\pi\frac{i}{p}\right)\right]$
	$\frac{1}{2}\left[1 + \frac{4}{(mc)^2}\right]^2 +$ $\sum\left[\lambda_i \sin^2\left(2\pi\frac{i}{p}\right)\right.$ $\left. + \frac{4k_i}{(mc)^2}\cos^2\left(2\pi\frac{i}{p}\right)\right]$	$\sum\left[\lambda_i \sin\left(2\pi\frac{i}{p}\right)\sin\left(4\pi\frac{i}{p}\right)\right.$ $\left. + \frac{8k_i}{(mc)^2}\cos\left(2\pi\frac{i}{p}\right)\cos\left(4\pi\frac{i}{p}\right)\right]$	$\sum\left[\lambda_i \sin\left(2\pi\frac{i}{p}\right)\sin\left(6\pi\frac{i}{p}\right)\right.$ $\left. + \frac{12k_i}{(mc)^2}\cos\left(2\pi\frac{i}{p}\right)\cos\left(6\pi\frac{i}{p}\right)\right]$
	Symmetric about Diagonal	$\frac{1}{2}\left[1 + \frac{16}{(mc)^2}\right]^2 +$ $\sum\left[\lambda_i \sin^2\left(4\pi\frac{i}{p}\right)\right.$ $\left. + \frac{16k_i}{(mc)^2}\cos^2\left(4\pi\frac{i}{p}\right)\right]$	$\sum\left[\lambda_i \sin\left(4\pi\frac{i}{p}\right)\sin\left(6\pi\frac{i}{p}\right)\right.$ $\left. + \frac{24k_i}{(mc)^2}\cos\left(4\pi\frac{i}{p}\right)\cos\left(6\pi\frac{i}{p}\right)\right]$
Symbol $\sum$ denotes $\sum_{i=0}^{p}$			$\frac{1}{2}\left[1 + \frac{36}{(mc)^2}\right]^2 +$ $\sum\left[\lambda_i \sin^2\left(6\pi\frac{i}{p}\right)\right.$ $\left. + \frac{36k_i}{(mc)^2}\cos^2\left(6\pi\frac{i}{p}\right)\right]$

TABLE 3. INFLUENCE COEFFICIENTS FOR DEFLECTION OF BEAMS AT MIDSPAN--EFFECT OF n_o

Five-Girder Bridge; $c = 0.4$; $\lambda = 12.5$; $k = 0$; $m_o = 11$; Y_n = Functions Used: $n = -1$ through n_o

To obtain deflections, the tabulated coefficients are to be multiplied by the quantity Pa^3/E_bI_b

Beam	Longit. Position of Load	n_o	Values of Deflection Coefficient, Cd — Transverse Location of Load								
			A	AB	B	BC	C	CD	D	DE	E
A	Quarter	2	0.00887	0.00665	0.00463	0.00293	0.00163	0.00067	-0.00002	-0.00054	-0.00098
		4	0.00887	0.00665	0.00462	0.00294	0.00163	0.00067	-0.00002	-0.00054	-0.00098
		6	0.00887	0.00665	0.00462	0.00294	0.00163	0.00067	-0.00002	-0.00054	-0.00098
		8	0.00887	0.00665	0.00462	0.00294	0.00163	0.00067	-0.00002	-0.00054	-0.00098
			(0.00887)*	(0.00674)	(0.00462)	(0.00294)	(0.00163)	(0.00067)	(-0.00002)	(-0.00063)	(-0.00098)
	Center	2	0.01307	0.00967	0.00661	0.00412	0.00225	0.00094	0.00000	-0.00074	-0.00139
		4	0.01308	0.00964	0.00659	0.00413	0.00229	0.00095	-0.00003	-0.00076	-0.00138
		6	0.01308	0.00965	0.00658	0.00413	0.00229	0.00094	-0.00002	-0.00076	-0.00138
		8	0.01308	0.00966	0.00658	0.00414	0.00229	0.00095	-0.00002	-0.00076	-0.00138
			(0.01308)	(0.00966)	(0.00658)	(0.00414)	(0.00229)	(0.00095)	(-0.00003)	(-0.00076)	(-0.00138)
B	Quarter	8	0.00462	0.00472	0.00459	0.00409	0.00332	0.00245	0.00157	0.00076	-0.00002
			(0.00462)	(0.00472)	(0.00459)	(0.00409)	(0.00332)	(0.00245)	(0.00157)	(0.00076)	(-0.00002)
	Center	8	0.00658	0.00700	0.00694	0.00608	0.00477	0.00345	0.00221	0.00106	-0.00002
			(0.00658)	(0.00700)	(0.00695)	(0.00608)	(0.00477)	(0.00345)	(0.00221)	(0.00107)	(-0.00003)
C	Quarter	2	0.00163	0.00257	0.00337	0.00390	0.00409	0.00390	0.00337	0.00257	0.00163
		4	0.00163	0.00251	0.00333	0.00393	0.00416	0.00393	0.00333	0.00251	0.00163
		6	0.00163	0.00252	0.00333	0.00393	0.00417	0.00393	0.00332	0.00252	0.00163
		8	0.00163	0.00252	0.00333	0.00393	0.00417	0.00393	0.00332	0.00252	0.00163
			(0.00163)	(0.00252)	(0.00332)	(0.00393)	(0.00417)	(0.00393)	(0.00332)	(0.00252)	(0.00163)
	Center	2	0.00225	0.00371	0.00494	0.00577	0.00606	0.00577	0.00494	0.00371	0.00225
		4	0.00229	0.00351	0.00479	0.00587	0.00631	0.00587	0.00479	0.00351	0.00229
		6	0.00229	0.00355	0.00477	0.00586	0.00633	0.00586	0.00477	0.00355	0.00229
		8	0.00229	0.00355	0.00477	0.00585	0.00634	0.00585	0.00477	0.00355	0.00229
			(0.00229)	(0.00355)	(0.00477)	(0.00585)	(0.00634)	(0.00585)	(0.00477)	(0.00355)	(0.00229)

* Numbers in parentheses were reproduced from Ref. (10).

TABLE 4. INFLUENCE COEFFICIENTS FOR MOMENT IN BEAMS AT MIDSPAN--EFFECT OF n_o

m_o = 11; Y_n Functions Used: n = -1 through n_o

Five-Girder Bridge; c = 0.4; λ = 12.5; k = 0

To obtain moments, the tabulated coefficients are to be multiplied by the quantity Pa

Beam	Longit. Position of Load	n_o	Values of Deflection Coefficient, C_m Transverse Location of Load								
			A	AB	B	BC	C	CD	D	DE	E
A	Quarter	2	0.0725	0.0581	0.0437	0.0298	0.0173	0.0069	-0.0007	-0.0059	-0.0095
		4	0.0723	0.0587	0.0442	0.0295	0.0165	0.0066	-0.0002	-0.0052	-0.0097
		6	0.0723	0.0585	0.0442	0.0295	0.0165	0.0068	-0.0002	-0.0053	-0.0097
		8	0.0723	0.0585	0.0442	0.0295	0.0165	0.0068	-0.0002	-0.0053	-0.0097
			(0.072)*	(0.059)	(0.044)	(0.030)	(0.017)	(0.007)	(0.000)	(-0.005)	(-0.010)
	Center	2	0.1711	0.1121	0.0690	0.0381	0.0192	0.0088	0.0017	-0.0057	-0.0142
		4	0.1717	0.1095	0.0672	0.0394	0.0220	0.0095	-0.0002	-0.0077	-0.0136
		6	0.1717	0.1100	0.0670	0.0395	0.0221	0.0092	-0.0003	-0.0075	-0.0136
		8	0.1717	0.1100	0.0670	0.0395	0.0221	0.0092	-0.0003	-0.0075	-0.0136
			(0.172)	(0.111)	(0.067)	(0.040)	(0.022)	(0.009)	(0.000)	(-0.008)	(-0.014)
B	Quarter	8	0.0442	0.0373	0.0325	0.0319	0.0305	0.0244	0.0159	0.0076	-0.0002
			(0.044)	(0.037)	(0.033)	(0.032)	(0.031)	(0.024)	(0.016)	(0.008)	(0.000)
	Center	8	0.0670	0.0898	0.1073	0.0786	0.0504	0.0329	0.0213	0.0104	-0.0003
			(0.067)	(0.091)	(0.107)	(0.080)	(0.050)	(0.033)	(0.021)	(0.010)	(0.000)
C	Quarter	2	0.0173	0.0231	0.0280	0.0313	0.0323	0.0313	0.0280	0.0231	0.0173
		4	0.0165	0.0259	0.0304	0.0301	0.0290	0.0301	0.0304	0.0259	0.0165
		6	0.0165	0.0251	0.0305	0.0304	0.0289	0.0304	0.0305	0.0251	0.0165
		8	0.0165	0.0251	0.0305	0.0304	0.0289	0.0304	0.0305	0.0251	0.0165
			(0.017)	(0.025)	(0.031)	(0.030)	(0.029)	(0.030)	(0.031)	(0.025)	(0.017)
	Center	2	0.0192	0.0416	0.0605	0.0731	0.0860	0.0731	0.0605	0.0416	0.0192
		4	0.0220	0.0299	0.0510	0.0784	0.0998	0.0784	0.0510	0.0299	0.0220
		6	0.0221	0.0339	0.0504	0.0768	0.1006	0.0768	0.0504	0.0339	0.0221
		8	0.0221	0.0337	0.0504	0.0764	0.1006	0.0764	0.0504	0.0337	0.0221
			(0.022)	(0.034)	(0.050)	(0.077)	(0.101)	(0.077)	(0.050)	(0.034)	(0.022)

* Numbers in parentheses were reproduced from Ref. (10).

TABLE 5. INFLUENCE COEFFICIENTS FOR DEFLECTION OF BEAMS AT MIDSPAN--EFFECT OF n_o

m_o = 11; Y_n Functions Used: n = -1 through n_o

Five-Girder Bridge; ϵ = 0.8; λ = 12.5, k = 0

To obtain deflections, the tabulated coefficients are to be multiplied by the quantity Pa^3/E_bI_b

Beam	Longit. Position of Load	n_o	Values of Deflection Coefficient, Cd — Transverse Location of Load: A	AB	B	BC	C	CD	D	DE	E
A	Quarter	2	0.01200	0.00696	0.00291	0.00043	-0.00052	-0.00049	-0.00015	0.00002	-0.00005
		4	0.01204	0.00678	0.00276	0.00051	-0.00031	-0.00040	-0.00030	-0.00016	-0.00001
		6	0.01205	0.00683	0.00273	0.00052	-0.00028	-0.00044	-0.00030	-0.00016	-0.00002
		8	0.01205	0.00684	0.00273	0.00053	-0.00028	-0.00043	-0.00030	-0.00015	-0.00001
			(0.01204)*	(0.00684)	(0.00273)	(0.00054)	(-0.00028)	(-0.00043)	(-0.00030)	(-0.00015)	(-0.00001)
	Center	2	0.01752	0.01010	0.00416	0.00055	-0.00080	-0.00069	-0.00018	0.00005	-0.00009
		4	0.01759	0.00979	0.00391	0.00070	-0.00044	-0.00056	-0.00042	-0.00024	-0.00002
		6	0.01760	0.00988	0.00388	0.00071	-0.00040	-0.00062	-0.00043	-0.00022	-0.00002
		8	0.01760	0.00989	0.00387	0.00073	-0.00040	-0.00060	-0.00043	-0.00022	-0.00002
			(0.01760)	(0.00990)	(0.00387)	(0.00074)	(-0.00040)	(-0.00060)	(-0.00043)	(-0.00022)	(-0.00002)
B	Quarter	8	0.00273	0.00632	0.00794	0.00635	0.00344	0.00135	0.00024	-0.00020	-0.00030
			(0.00273)	(0.00631)	(0.00795)	(0.00634)	(0.00344)	(0.00135)	(0.00024)	(-0.00020)	(-0.00030)
	Center	8	0.00387	0.00929	0.01178	0.00929	0.00488	0.00187	0.00033	-0.00028	-0.00043
			(0.00387)	(0.00926)	(0.01178)	(0.00927)	(0.00487)	(0.00188)	(0.00033)	(-0.00027)	(-0.00043)
C	Quarter	2	-0.00052	0.00211	0.00435	0.00584	0.00637	0.00584	0.00435	0.00211	-0.00052
		4	-0.00031	0.00112	0.00354	0.00631	0.00756	0.00631	0.00354	0.00112	-0.00031
		6	-0.00028	0.00130	0.00344	0.00624	0.00770	0.00624	0.00344	0.00130	-0.00028
		8	-0.00028	0.00129	0.00344	0.00623	0.00771	0.00623	0.00344	0.00129	-0.00028
			(-0.00028)	(0.00130)	(0.00344)	(0.00622)	(0.00771)	(0.00622)	(0.00344)	(0.00130)	(-0.00028)
	Center	2	-0.00080	0.00307	0.00634	0.00853	0.00929	0.00853	0.00634	0.00307	-0.00080
		4	-0.00044	0.00145	0.00503	0.00928	0.01123	0.00928	0.00503	0.00145	-0.00044
		6	-0.00040	0.00180	0.00488	0.00914	0.01144	0.00914	0.00488	0.00180	-0.00040
		8	-0.00040	0.00179	0.00488	0.00912	0.01144	0.00912	0.00488	0.00179	-0.00040
			(-0.00040)	(0.00179)	(0.00487)	(0.00910)	(0.01145)	(0.00910)	(0.00487)	(0.00179)	(-0.00040)

*** Numbers in parentheses were reproduced from Ref. (10).**

TABLE 6. INFLUENCE COEFFICIENTS FOR MOMENT IN BEAMS AT MIDSPAN--EFFECT OF n_o

m_o = 11; Y_n Functions Used: n = -1 through n_o

Five-Girder Bridge; c = 0.8; λ = 12.5, k = 0

To obtain moments, the tabulated coefficients are to be multiplied by the quantity Pa

Beam	Longit. Position of Load	n_o	Values of Moment Coefficient, C_m — Transverse Location of Load								
			A	AB	B	BC	C	CD	D	DE	E
A	Quarter	2	0.1027	0.0613	0.0274	0.0058	-0.0036	-0.0047	-0.0025	-0.0007	-0.0002
		4	0.1027	0.0609	0.0270	0.0059	-0.0030	-0.0043	-0.0029	-0.0014	-0.0001
		6	0.1028	0.0610	0.0268	0.0060	-0.0027	-0.0044	-0.0030	-0.0015	-0.0002
		8	0.1028	0.0610	0.0268	0.0061	-0.0028	-0.0043	-0.0030	-0.0015	-0.0001
			(0.103)*	(0.061)	(0.027)	(0.006)	(-0.003)	(-0.004)	(-0.003)	(-0.002)	(0.000)
	Center	2	0.2161	0.1160	0.0437	0.0018	-0.0113	-0.0070	0.0007	0.0026	-0.0016
		4	0.2175	0.1089	0.0390	0.0057	-0.0044	-0.0057	-0.0041	-0.0019	-0.0002
		6	0.2176	0.1090	0.0386	0.0059	-0.0040	-0.0058	-0.0042	-0.0021	-0.0002
		8	0.2176	0.1089	0.0386	0.0058	-0.0041	-0.0059	-0.0042	-0.0022	-0.0002
			(0.218)	(0.109)	(0.039)	(0.006)	(-0.004)	(-0.006)	(-0.004)	(-0.002)	(0.000)
B	Quarter	8	0.0268	0.0522	0.0629	0.0539	0.0336	0.0144	0.0024	-0.0022	-0.0030
			(0.027)	(0.052)	(0.063)	(0.054)	(0.034)	(0.014)	(0.002)	(-0.002)	(-0.003)
	Center	8	0.0386	0.1108	0.1591	0.1087	0.0487	0.0168	0.0032	-0.0024	-0.0042
			(0.039)	(0.110)	(0.159)	(0.108)	(0.049)	(0.017)	(0.003)	(-0.002)	(-0.004)
C	Quarter	2	-0.0036	0.0187	0.0376	0.0502	0.0545	0.0502	0.0376	0.0187	-0.0036
		4	-0.0030	0.0147	0.0345	0.0522	0.0594	0.0522	0.0345	0.0147	-0.0030
		6	-0.0027	0.0141	0.0336	0.0525	0.0606	0.0525	0.0336	0.0141	-0.0027
		8	-0.0028	0.0141	0.0336	0.0525	0.0606	0.0525	0.0336	0.0141	-0.0028
			(-0.003)	(0.014)	(0.034)	(0.052)	(0.061)	(0.052)	(0.034)	(0.014)	(-0.003)
	Center	2	-0.0113	0.0351	0.0745	0.1007	0.1184	0.1007	0.0745	0.0351	-0.0113
		4	-0.0044	0.0058	0.0533	0.1141	0.1533	0.1141	0.0533	0.0058	-0.0044
		6	-0.0040	0.0166	0.0487	0.1097	0.1557	0.1097	0.0487	0.0166	-0.0040
		8	-0.0041	0.0157	0.0487	0.1073	0.1557	0.1073	0.0487	0.0157	-0.0041
			(-0.004)	(0.016)	(0.049)	(0.106)	(0.156)	(0.106)	(0.049)	(0.016)	(-0.004)

* Numbers in parentheses were reproduced from Ref. (10).

TABLE 7. INFLUENCE COEFFICIENTS FOR DEFLECTION OF BEAMS AT MIDSPAN--EFFECT OF m_o

Five-Girder Bridge; c = 0.4; λ = 12.5; k = 0; n_o = 8; m = 1 through m_o

To obtain deflections, the tabulated coefficients are to be multiplied by the quantity Pa^3/E_bI_b

Beam	Longit. Position of Load	m_o	Values of Deflection Coefficient, Cd — Transverse Locations of Load								
			A	AB	B	BC	C	CD	D	DE	E
A	Quarter	1	0.00905	0.00674	0.00464	0.00293	0.00163	0.00067	-0.00002	-0.00054	-0.00098
		3	0.00888	0.00666	0.00462	0.00294	0.00163	0.00067	-0.00002	-0.00054	-0.00098
		5	0.00886	0.00665	0.00462	0.00294	0.00163	0.00067	-0.00002	-0.00054	-0.00098
		7	0.00887	0.00665	0.00462	0.00294	0.00163	0.00067	-0.00002	-0.00054	-0.00098
		9	0.00887	0.00665	0.00462	0.00294	0.00163	0.00067	-0.00002	-0.00054	-0.00098
		11	0.00887	0.00665	0.00462	0.00294	0.00163	0.00067	-0.00002	-0.00054	-0.00098
	Center	1	0.01280	0.00953	0.00656	0.00415	0.00230	0.00095	-0.00002	-0.00076	-0.00138
		3	0.01303	0.00964	0.00658	0.00414	0.00229	0.00095	-0.00003	-0.00076	-0.00138
		5	0.01307	0.00965	0.00658	0.00414	0.00229	0.00095	-0.00002	-0.00076	-0.00138
		7	0.01307	0.00965	0.00658	0.00414	0.00229	0.00095	-0.00002	-0.00076	-0.00138
		9	0.01308	0.00965	0.00658	0.00414	0.00229	0.00095	-0.00002	-0.00076	-0.00138
		11	0.01308	0.00966	0.00658	0.00414	0.00229	0.00095	-0.00002	-0.00076	-0.00138
C	Quarter	1	0.00163	0.00251	0.00335	0.00403	0.00432	0.00403	0.00335	0.00251	0.00163
		3	0.00163	0.00251	0.00332	0.00394	0.00419	0.00394	0.00332	0.00251	0.00163
		5	0.00163	0.00252	0.00332	0.00392	0.00416	0.00392	0.00332	0.00252	0.00163
		7	0.00163	0.00252	0.00332	0.00393	0.00417	0.00393	0.00332	0.00252	0.00163
		9	0.00163	0.00252	0.00332	0.00393	0.00417	0.00393	0.00332	0.00252	0.00163
		11	0.00163	0.00252	0.00332	0.00393	0.00417	0.00393	0.00332	0.00252	0.00163
	Center	1	0.00230	0.00355	0.00473	0.00570	0.00611	0.00570	0.00473	0.00355	0.00230
		3	0.00229	0.00355	0.00477	0.00583	0.00629	0.00583	0.00477	0.00355	0.00229
		5	0.00229	0.00355	0.00477	0.00584	0.00632	0.00584	0.00477	0.00355	0.00229
		7	0.00229	0.00355	0.00477	0.00585	0.00633	0.00585	0.00477	0.00355	0.00229
		9	0.00229	0.00355	0.00477	0.00585	0.00633	0.00585	0.00477	0.00355	0.00229
		11	0.00229	0.00355	0.00477	0.00585	0.00633	0.00585	0.00477	0.00355	0.00229

TABLE 8. INFLUENCE COEFFICIENTS FOR MOMENT IN BEAMS AT MIDSPAN--EFFECT OF m_o

$n_o = 8$; m = 1 through m_o

Five-Girder Bridge; c = 0.4; λ = 12.5, k = 0

To obtain moments, the tabulated coefficients are to be multiplied by the quantity Pa

Beam	Longit. Position of Load	m_o	Values of Moment Coefficient, C_m Transverse Position of Load								
			A	AB	B	BC	C	CD	D	DE	E
A	Quarter	1	0.0710	0.0665	0.0458	0.0289	0.0160	0.0066	-0.0002	-0.0053	-0.0097
		3	0.0722	0.0595	0.0443	0.0294	0.0164	0.0068	-0.0002	-0.0053	-0.0097
		5	0.0724	0.0572	0.0442	0.0297	0.0165	0.0067	-0.0002	-0.0053	-0.0097
		7	0.0723	0.0582	0.0442	0.0296	0.0165	0.0068	-0.0002	-0.0053	-0.0097
		9	0.0723	0.0588	0.0442	0.0295	0.0165	0.0068	-0.0002	-0.0053	-0.0097
		11	0.0723	0.0585	0.0442	0.0295	0.0165	0.0068	-0.0002	-0.0053	-0.0097
	Center	1	0.1737	0.0940	0.0647	0.0409	0.0227	0.0094	-0.0002	-0.0075	-0.0136
		3	0.1720	0.1039	0.0668	0.0403	0.0221	0.0092	-0.0003	-0.0075	-0.0136
		5	0.1718	0.1072	0.0670	0.0399	0.0221	0.0092	-0.0003	-0.0075	-0.0136
		7	0.1717	0.1087	0.0670	0.0397	0.0221	0.0092	-0.0003	-0.0075	-0.0136
		9	0.1717	0.1096	0.0670	0.0396	0.0221	0.0092	-0.0003	-0.0075	-0.0136
		11	0.1717	0.1100	0.0670	0.0395	0.0221	0.0092	-0.0003	-0.0075	-0.0136
C	Quarter	1	0.0160	0.0248	0.0330	0.0398	0.0243	0.0398	0.0330	0.0248	0.0160
		3	0.0164	0.0249	0.0307	0.0317	0.0285	0.0317	0.0307	0.0249	0.0164
		5	0.0165	0.0254	0.0304	0.0285	0.0290	0.0285	0.0304	0.0254	0.0165
		7	0.0165	0.0252	0.0305	0.0301	0.0289	0.0301	0.0305	0.0252	0.0165
		9	0.0165	0.0251	0.0305	0.0310	0.0288	0.0310	0.0305	0.0251	0.0165
		11	0.0165	0.0251	0.0305	0.0304	0.0289	0.0304	0.0305	0.0251	0.0165
	Center	1	0.0227	0.0351	0.0467	0.0562	0.1076	0.0562	0.0467	0.0351	0.0227
		3	0.0221	0.0349	0.0500	0.0677	0.1017	0.0677	0.0500	0.0349	0.0221
		5	0.0221	0.0342	0.0504	0.0721	0.1009	0.0721	0.0504	0.0342	0.0221
		7	0.0221	0.0339	0.0504	0.0743	0.1008	0.0743	0.0504	0.0339	0.0221
		9	0.0221	0.0338	0.0504	0.0756	0.1007	0.0756	0.0504	0.0338	0.0221
		11	0.0221	0.0337	0.0504	0.0764	0.1006	0.0764	0.0504	0.0337	0.0221

TABLE 9. INFLUENCE COEFFICIENTS FOR DEFLECTION OF BEAMS AT MIDSPAN--EFFECT OF m_o

$n_o = 8$; $m = 1$ through m_o

Five-Girder Bridge; $c = 0.8$; $\lambda = 12.5$; $k = 0$

To obtain deflections, the tabulated coefficients are to be multiplied by the quantity Pa^3/E_bI_b

Beam	Longit. Position of Load	m_o	Values of Deflection Coefficient, C_d — Transverse Position of Load								
			A	AB	B	BC	C	CD	D	DE	E
A	Quarter	1	0.01224	0.00691	0.00274	0.00052	-0.00028	-0.00043	-0.00030	-0.00015	-0.00001
		3	0.01206	0.00684	0.00273	0.00053	-0.00028	-0.00043	-0.00030	-0.00015	-0.00001
		5	0.01204	0.00684	0.00273	0.00053	-0.00028	-0.00043	-0.00030	-0.00015	-0.00001
		7	0.01204	0.00684	0.00273	0.00053	-0.00028	-0.00043	-0.00030	-0.00015	-0.00001
		9	0.01205	0.00684	0.00273	0.00053	-0.00028	-0.00043	-0.00030	-0.00015	-0.00001
		11	0.01205	0.00684	0.00273	0.00053	-0.00028	-0.00043	-0.00030	-0.00015	-0.00001
	Center	1	0.01731	0.00978	0.00387	0.00074	-0.00040	-0.00061	-0.00043	-0.00022	-0.00002
		3	0.01756	0.00988	0.00387	0.00073	-0.00040	-0.00060	-0.00043	-0.00022	-0.00002
		5	0.01759	0.00989	0.00387	0.00073	-0.00040	-0.00060	-0.00043	-0.00022	-0.00002
		7	0.01760	0.00989	0.00387	0.00073	-0.00040	-0.00060	-0.00043	-0.00022	-0.00002
		9	0.01760	0.00989	0.00387	0.00073	-0.00040	-0.00060	-0.00043	-0.00022	-0.00002
		11	0.01760	0.00989	0.00387	0.00073	-0.00040	-0.00060	-0.00043	-0.00022	-0.00002
C	Quarter	1	-0.00028	0.00128	0.00345	0.00633	0.00789	0.00633	0.00345	0.00128	-0.00028
		3	-0.00028	0.00129	0.00344	0.00624	0.00772	0.00624	0.00344	0.00129	-0.00028
		5	-0.00028	0.00129	0.00344	0.00622	0.00770	0.00622	0.00344	0.00129	-0.00028
		7	-0.00028	0.00129	0.00344	0.00623	0.00770	0.00623	0.00344	0.00129	-0.00028
		9	-0.00028	0.00129	0.00344	0.00623	0.00771	0.00623	0.00344	0.00129	-0.00028
		11	-0.00028	0.00129	0.00344	0.00623	0.00771	0.00623	0.00344	0.00129	-0.00028
	Center	1	-0.00040	0.00181	0.00488	0.00896	0.01116	0.00896	0.00488	0.00181	-0.00040
		3	-0.00040	0.00179	0.00488	0.00910	0.01140	0.00910	0.00488	0.00179	-0.00040
		5	-0.00040	0.00179	0.00488	0.00911	0.01143	0.00911	0.00488	0.00179	-0.00040
		7	-0.00040	0.00179	0.00488	0.00911	0.01144	0.00911	0.00488	0.00179	-0.00040
		9	-0.00040	0.00179	0.00488	0.00912	0.01144	0.00912	0.00488	0.00179	-0.00040
		11	-0.00040	0.00179	0.00488	0.00912	0.01144	0.00912	0.00488	0.00179	-0.00040

TABLE 10. INFLUENCE COEFFICIENTS FOR MOMENT IN BEAMS AT MIDSPAN--EFFECT OF m_o

$n_o = 8$; m = 1 through m_o

Five-Girder Bridge; c = 0.8; λ = 12.5; k = 0

To obtain moments, the tabulated coefficients are to be multiplied by the quantity Pa

Beam	Longit. Position of Load	m_o	Values of Moment Coefficient, C_m — Transverse Position of Load								
			A	AB	B	BC	C	CD	D	DE	E
A	Quarter	1	0.1025	0.0682	0.0270	0.0052	-0.0028	-0.0042	-0.0030	-0.0015	-0.0001
		3	0.1028	0.0620	0.0268	0.0059	-0.0028	-0.0043	-0.0030	-0.0015	-0.0001
		5	0.1029	0.0603	0.0268	0.0061	-0.0028	-0.0043	-0.0030	-0.0015	-0.0001
		7	0.1028	0.0609	0.0268	0.0061	-0.0028	-0.0043	-0.0030	-0.0015	-0.0001
		9	0.1028	0.0611	0.0268	0.0060	-0.0028	-0.0044	-0.0030	-0.0015	-0.0001
		11	0.1028	0.0610	0.0268	0.0061	-0.0028	-0.0043	-0.0030	-0.0015	-0.0001
	Center	1	0.2182	0.0965	0.0382	0.0073	-0.0040	-0.0060	-0.0042	-0.0021	-0.0002
		3	0.2177	0.1053	0.0385	0.0062	-0.0041	-0.0058	-0.0042	-0.0022	-0.0002
		5	0.2176	0.1077	0.0386	0.0060	-0.0041	-0.0058	-0.0042	-0.0022	-0.0002
		7	0.2176	0.1086	0.0386	0.0059	-0.0041	-0.0058	-0.0042	-0.0022	-0.0002
		9	0.2176	0.1089	0.0386	0.0058	-0.0041	-0.0059	-0.0042	-0.0022	-0.0002
		11	0.2176	0.1089	0.0386	0.0058	-0.0041	-0.0059	-0.0042	-0.0022	-0.0002
C	Quarter	1	-0.0028	0.0126	0.0340	0.0625	-0.0596	0.0625	0.0340	0.0126	-0.0028
		3	-0.0028	0.0139	0.0337	0.0538	0.0606	0.0538	0.0337	0.0139	-0.0028
		5	-0.0028	0.0142	0.0336	0.0511	0.0607	0.0511	0.0336	0.0142	-0.0028
		7	-0.0028	0.0141	0.0336	0.0522	0.0607	0.0522	0.0336	0.0141	-0.0028
		9	-0.0028	0.0141	0.0336	0.0528	0.0606	0.0528	0.0336	0.0141	-0.0028
		11	-0.0028	0.0141	0.0336	0.0525	0.0606	0.0525	0.0336	0.0141	-0.0028
	Center	1	-0.0040	0.0178	0.0481	0.0884	0.1575	0.0884	0.0481	0.0178	-0.0040
		3	-0.0041	0.0160	0.0487	0.1007	0.1561	0.1007	0.0487	0.0160	-0.0041
		5	-0.0041	0.0157	0.0487	0.1045	0.1559	0.1045	0.0487	0.0157	-0.0041
		7	-0.0041	0.0156	0.0487	0.1062	0.1558	0.1062	0.0487	0.0156	-0.0041
		9	-0.0041	0.0156	0.0487	0.1069	0.1557	0.1069	0.0487	0.0156	-0.0041
		11	-0.0041	0.0157	0.0487	0.1073	0.1557	0.1073	0.0487	0.0157	-0.0041

TABLE 11. COMPARISON OF INFLUENCE COEFFICIENTS FOR MOMENT IN LOADED BEAM AT MIDSPAN COMPUTED BY TWO DIFFERENT PROCEDURES

Five-Girder Bridge; $n_o = 8$; m = 1 through m_o

To obtain moments, the tabulated coefficients are to be multiplied by the quantity Pa

Longit. Position of Load	m_o	e = 0.4; λ = 1.5; k = 0				e = 0.8; λ = 1.5; k = 0			
		Values of Moment Coefficient, C_M, for Beam							
		A		C		A		C	
		From Eq. (2-39)	From Eq. (2-43)	From Eq. (2-39)	From Eq. (2-43)	From Eq. (2-39)	From Eq. (2-43)	From Eq. (2-39)	From Eq. (2-43)
Quarter	1	0.0893	0.0710	0.0426	0.0243	0.1208	0.1025	0.0779	0.0596
	3	0.0746	0.0722	0.0309	0.0285	0.1052	0.1028	0.0629	0.0606
	5	0.0730	0.0724	0.0297	0.0290	0.0995	0.1029	0.0573	0.0607
	7	0.0729	0.0723	0.0295	0.0289	0.1024	0.1028	0.0602	0.0607
	9	0.0726	0.0725	0.0294	0.0288	0.1042	0.1028	0.0620	0.0606
	11	0.0725	0.0723	0.0293	0.0289	0.1030	0.1028	0.0608	0.0606
Center	1	0.1663	0.1737	0.0603	0.1076	0.1708	0.2182	0.1101	0.1575
	3	0.1472	0.1720	0.0768	0.1017	0.1929	0.2177	0.1313	0.1561
	5	0.1551	0.1718	0.0842	0.1009	0.2009	0.2176	0.1391	0.1559
	7	0.1591	0.1717	0.0882	0.1008	0.2050	0.2176	0.1432	0.1558
	9	0.1616	0.1717	0.0906	0.1007	0.2075	0.2176	0.1457	0.1557
	11	0.1633	0.1717	0.0922	0.1006	0.2092	0.2176	0.1473	0.1557

TABLE 12. INFLUENCE COEFFICIENTS FOR DEFLECTION OF BEAMS AT QUARTER-POINT OF SPAN

$m_o = 11$; $n_o = 8$

Five-Girder Bridge; $c = 0.4$; $\lambda = 12.5$; $k = 0$

To obtain deflections, the tabulated coefficients are to be multiplied by the quantity Pa^3/E_bI_b

Beam	Longit. Position of Load	Values of Deflection Coefficient, C_d — Transverse Position of Load								
		A	AB	B	BC	C	CD	D	DE	E
A	1/4	0.00764 * (0.00764)	0.00545 (0.00545)	0.00353 (0.00353)	0.00211 (0.00212)	0.00112 (0.00112)	0.00044 (0.00044)	-0.00004 (-0.00004)	-0.00039 (-0.00039)	-0.00069 (-0.00069)
	Center	0.00887 (0.00887)	0.00665 (0.00674)	0.00462 (0.00462)	0.00294 (0.00294)	0.00163 (0.00163)	0.00067 (0.00067)	-0.00002 (-0.00002)	-0.00054 (-0.00063)	-0.00098 (-0.00098)
	3/4	0.00544 (0.00544)	0.00421 (0.00421)	0.00305 (0.00305)	0.00202 (0.00202)	0.00117 (0.00117)	0.00051 (0.00051)	0.00001 (0.00001)	-0.00037 (-0.00037)	-0.00069 (-0.00069)
B	1/4	0.00353 (0.00353)	0.00408 (0.00408)	0.00421 (0.00421)	0.00362 (0.00362)	0.00269 (0.00269)	0.00184 (0.00184)	0.00113 (0.00113)	0.00052 (0.00052)	-0.00004 (-0.00004)
	Center	0.00462 (0.00462)	0.00472 (0.00472)	0.00459 (0.00459)	0.00409 (0.00409)	0.00332 (0.00332)	0.00245 (0.00245)	0.00157 (0.00157)	0.00076 (0.00076)	-0.00002 (-0.00002)
	3/4	0.00305 (0.00305)	0.00292 (0.00292)	0.00274 (0.00274)	0.00246 (0.00246)	0.00208 (0.00208)	0.00161 (0.00161)	0.00108 (0.00108)	0.00055 (0.00055)	0.00001 (0.00001)
C	1/4	0.00112 (0.00112)	0.00189 (0.00189)	0.00269 (0.00269)	0.00349 (0.00349)	0.00388 (0.00389)	0.00349 (0.00349)	0.00269 (0.00269)	0.00189 (0.00189)	0.00112 (0.00112)
	Center	0.00163 (0.00163)	0.00252 (0.00252)	0.00332 (0.00332)	0.00393 (0.00393)	0.00417 (0.00417)	0.00393 (0.00393)	0.00332 (0.00332)	0.00252 (0.00252)	0.00163 (0.00163)
	3/4	0.00117 (0.00117)	0.00166 (0.00166)	0.00208 (0.00208)	0.00236 (0.00236)	0.00245 (0.00245)	0.00236 (0.00236)	0.00208 (0.00208)	0.00166 (0.00166)	0.00117 (0.00117)

* Numbers in parentheses were reproduced from Ref. (10).

TABLE 13. INFLUENCE COEFFICIENTS FOR MOMENT IN BEAMS AT QUARTER-POINT OF SPAN

$m_o = 11$; $n_o = 8$

Five-Girder Bridge; $c = 0.4$; $\lambda = 12.5$; $k = 0$

To obtain moments, the tabulated coefficients are to be multiplied by the quantity Pa.

Beam	Longit. Position of Load	Values of Moment Coefficient, C_m — Transverse Position of Load								
		A	AB	B	BC	C	CD	D	DE	E
A	1/4	0.1403 (0.140)*	0.0820 (0.083)	0.0432 (0.043)	0.0213 (0.021)	0.0100 (0.010)	0.0032 (0.003)	-0.0012 (-0.001)	-0.0043 (-0.004)	-0.0069 (-0.007)
	Center	0.0723 (0.072)	0.0585 (0.059)	0.0442 (0.044)	0.0295 (0.030)	0.0165 (0.017)	0.0068 (0.007)	-0.0002 (0.000)	-0.0053 (-0.005)	-0.0097 (-0.010)
	3/4	0.0314 (0.031)	0.0281 (0.028)	0.0239 (0.024)	0.0183 (0.018)	0.0120 (0.012)	0.0061 (0.006)	0.0009 (0.001)	-0.0032 (-0.003)	-0.0068 (-0.007)
B	1/4	0.0432 (0.043)	0.0719 (0.073)	0.0935 (0.094)	0.0658 (0.067)	0.0374 (0.037)	0.0206 (0.021)	0.0114 (0.011)	0.0046 (0.005)	-0.0012 (-0.001)
	Center	0.0442 (0.044)	0.0373 (0.037)	0.0325 (0.033)	0.0319 (0.032)	0.0305 (0.031)	0.0244 (0.024)	0.0159 (0.016)	0.0076 (0.008)	-0.0002 (0.000)
	3/4	0.0239 (0.024)	0.0179 (0.018)	0.0139 (0.014)	0.0128 (0.013)	0.0130 (0.013)	0.0122 (0.012)	0.0098 (0.010)	0.0058 (0.006)	0.0009 (0.001)
C	1/4	0.0100 (0.010)	0.0208 (0.021)	0.0374 (0.037)	0.0643 (0.065)	0.0893 (0.089)	0.0643 (0.065)	0.0374 (0.037)	0.0208 (0.021)	0.0100 (0.010)
	Center	0.0165 (0.017)	0.0251 (0.025)	0.0305 (0.031)	0.0304 (0.030)	0.0289 (0.029)	0.0304 (0.030)	0.0305 (0.031)	0.0251 (0.025)	0.0165 (0.017)
	3/4	0.0120 (0.012)	0.0130 (0.013)	0.0130 (0.013)	0.0120 (0.012)	0.0114 (0.011)	0.0120 (0.012)	0.0130 (0.013)	0.0130 (0.013)	0.0120 (0.012)

*** Numbers in parentheses were reproduced from Ref. (10).**

TABLE 14. INFLUENCE COEFFICIENTS FOR DEFLECTION AND MOMENT OF BEAMS AT MIDSPAN

Five-Girder Bridge; $c = 0.4$; $\lambda = 50$; $k = 0$, $m_o = 11$; $n_o = 8$
To obtain deflections and moments, the tabulated coefficients are to be multiplied by the quantities Pa^3/E_bI_b and Pa, respectively.

Beam	Longit. Position of Load	Values of Influence Coefficients — Transverse Location of Load								
		A	AB	B	BC	C	CD	D	DE	E
					(a) Deflections, C_d					
A	Quarter	0.01105 (0.01106)*	0.00720 (0.00719)	0.00391 (0.00391)	0.00164 (0.00163)	0.00029 (0.00028)	-0.00036 (-0.00036)	-0.00056 (-0.00055)	-0.00053 (-0.00054)	-0.00041 (-0.00042)
	Center	0.01619 (0.01620)	0.01042 (0.01041)	0.00555 (0.00555)	0.00228 (0.00227)	0.00040 (0.00040)	-0.00050 (-0.00051)	-0.00078 (-0.00078)	-0.00075 (-0.00077)	-0.00059 (-0.00059)
B	Quarter	0.00391 (0.00391)	0.00536 (0.00536)	0.00599 (0.00600)	0.00528 (0.00528)	0.00381 (0.00380)	0.00233 (0.00233)	0.00110 (0.00110)	0.00018 (0.00018)	-0.00056 (-0.00055)
	Center	0.00555 (0.00555)	0.00796 (0.00794)	0.00900 (0.00901)	0.00778 (0.00778)	0.00542 (0.00542)	0.00325 (0.00326)	0.00155 (0.00155)	0.00027 (0.00026)	-0.00078 (-0.00078)
C	Quarter	0.00029 (0.00028)	0.00206 (0.00206)	0.00381 (0.00380)	0.00537 (0.00536)	0.00606 (0.00607)	0.00537 (0.00536)	0.00381 (0.00380)	0.00206 (0.00206)	0.00029 (0.00028)
	Center	0.00040 (0.00040)	0.00286 (0.00288)	0.00542 (0.00542)	0.00791 (0.00790)	0.00909 (0.00910)	0.00791 (0.00790)	0.00542 (0.00542)	0.00286 (0.00288)	0.00040 (0.00040)
					(b) Moments, C_m					
A	Quarter	0.0930	0.0642	0.0382	0.0172	0.0030	-0.0037	-0.0055	-0.0052	-0.0041
	Center	0.2037 (0.204)	0.1170 (0.118)	0.0555 (0.055)	0.0205 (0.021)	0.0037 (0.004)	-0.0047 (-0.005)	-0.0077 (-0.008)	-0.0075 (-0.008)	-0.0058 (-0.006)
B	Quarter	0.0382	0.0421	0.0439	0.0431	0.0367	0.0243	0.0111	0.0016	-0.0055
	Center	0.0555 (0.055)	0.1016 (0.102)	0.1313 (0.131)	0.0964 (0.097)	0.0548 (0.055)	0.0294 (0.030)	0.0149 (0.015)	0.0031 (0.003)	-0.0077 (-0.008)
C	Quarter	0.0030	0.0220	0.0367	0.0437	0.0449	0.0437	0.0367	0.0220	0.0030
	Center	0.0037 (0.004)	0.0250 (0.025)	0.0548 (0.055)	0.0982 (0.099)	0.1318 (0.132)	0.0982 (0.099)	0.0548 (0.055)	0.0250 (0.025)	0.0037 (0.004)

*** Numbers in parentheses were reproduced from Ref. (10).**

TABLE 15. COMPARISON OF RESULTS OBTAINED BY USING DIFFERENT NUMBERS OF INTEGRATION STEPS

Five-Girder Bridge; Load over Beam A

$c = 0.4$; $\lambda = 25$; $k = 0$; $\gamma = 0.05$; $\nu = 0.2$; $\omega = 0$; $\alpha = 0.15$; $f_v/f_b = 0.7$

Max. Dyn. Increment for	Beam	N = Number of Integration Steps*			
		50	100	150	200
Interacting Force		0.177	0.178	0.178	0.178
Deflection at Midspan in Terms of Wa^3/E_bI_b	0	0.00251	0.00254	0.00254	0.00254
	1	0.00140	0.00150	0.00150	0.00150
	2	0.00071	0.00069	0.00069	0.00069
	3	0.00096	0.00091	0.00089	0.00088
	4	0.00135	0.00136	0.00136	0.00136
Moment at Midspan in Terms of Wa	0	0.0267	0.0262	0.0262	0.0262
	1	0.0139	0.0148	0.0148	0.0148
	2	0.0070	0.0068	0.0068	0.0068
	3	0.0095	0.0090	0.0088	0.0087
	4	0.0133	0.0134	0.0134	0.0134

*Minimum number of integration steps required by stability and convergence criterion is N = 30.
No solution could be obtained for N = 25.

TABLE 16. RELATIONSHIP BETWEEN PEAK VALUES OF RESPONSE FOR ACTUAL STRUCTURE AND EQUIVALENT BEAM

Five-Girder Bridge; Load over Beam C

$k = 0$; $\gamma = 0.05$; $\nu = 0.2$, $\omega = 0$; $\alpha = 0.15$; $f_v/f_b = 0.7$

All deflections are expressed in terms of Wa^3/E_bI_b, and moments in terms of Wa

c	λ	Max. Static Deflection in Loaded Beam	Max. Sum of Dyn. Incr. for Moment in Beams
0.4	12.5	0.00634	0.0471
	25	0.00761	0.0533
	50	0.00909	0.0599
0.6	16.67	0.00977	0.0617
0.8	6.25	0.00955	0.0608
	12.5	0.01144	0.0695
	25	0.01341	0.0744
1.0	10	0.01288	0.0720
Beam Solution		0.00416	0.0388

TABLE 17. COMPARISON OF STATIC AND DYNAMIC DISTRIBUTIONS OF MOMENT IN BEAMS ACROSS MIDSPAN

Five-Girder Bridge; Load over Beam C

$k = 0$; $\gamma = 0.05$; $\nu = 0.2$; $\omega = 0$, $\alpha = 0.15$; $f_v/f_b = 0.7$

All moments are expressed in terms of Wa

c	λ	H= λc	Max. Value of Sum of Moments in Beams		Moment in Beam in Percent of Corresponding Maximum Value of Sum					
					Static			Dynamic Increment		
			Static	Dyn. Incr.	A	B	C	A	B	C
0.4	12.5	5	0.24	0.047	9	21	40	17	21	24
	25	10	0.24	0.053	5	22	46	17	22	25
	50	20	0.24	0.060	1	23	52	14	23	27
0.6	16.67	10	0.24	0.064	0	22	56	15	22	26
0.8	6.25	5	0.24	0.061	1	21	56	15	22	26
	12.5	10	0.24	0.070	-2	20	64	16	22	25
	25	20	0.24	0.074	-3	18	70	16	22	26
1.0	10	10	0.24	0.072	-2	17	70	16	22	25

FIGURAS

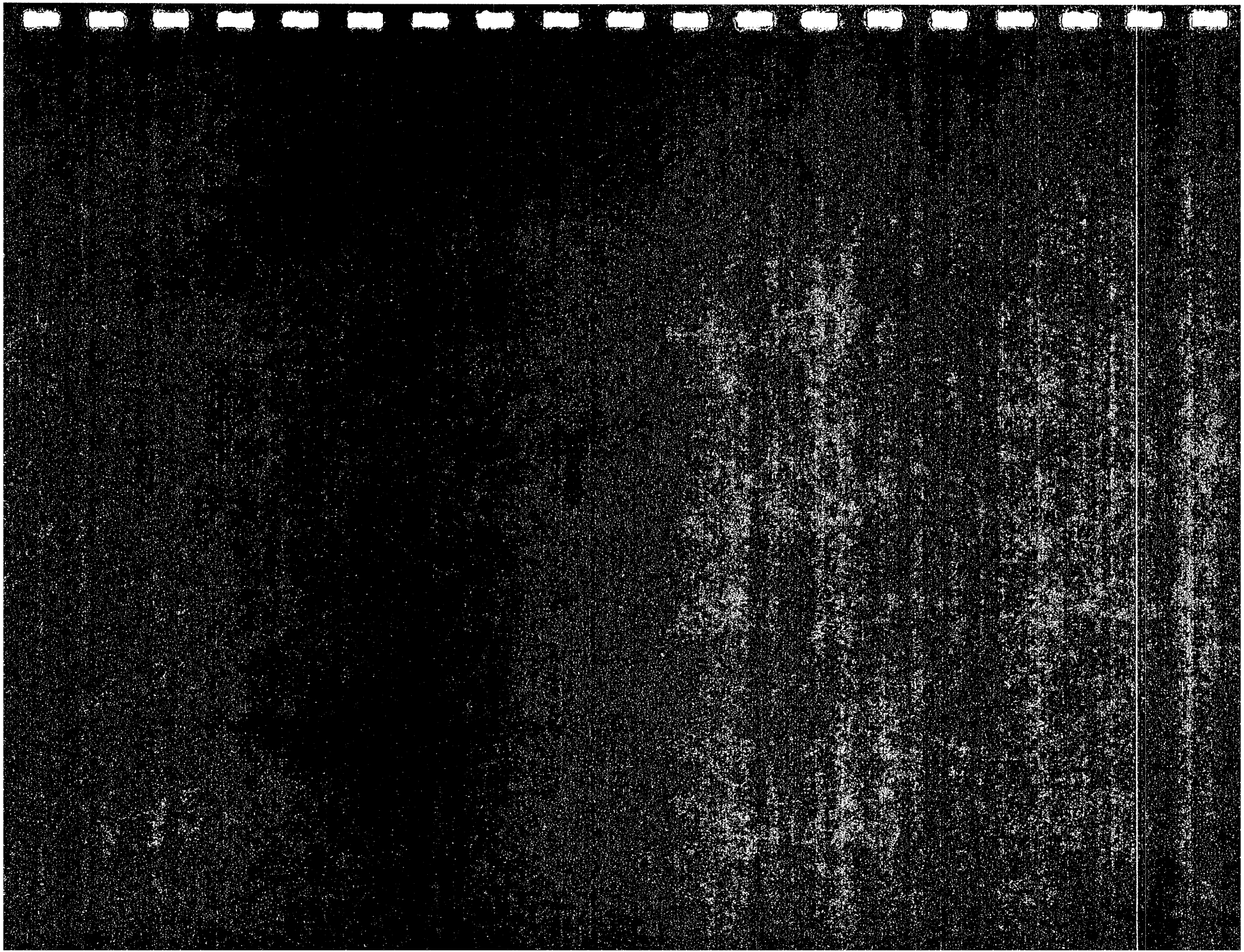

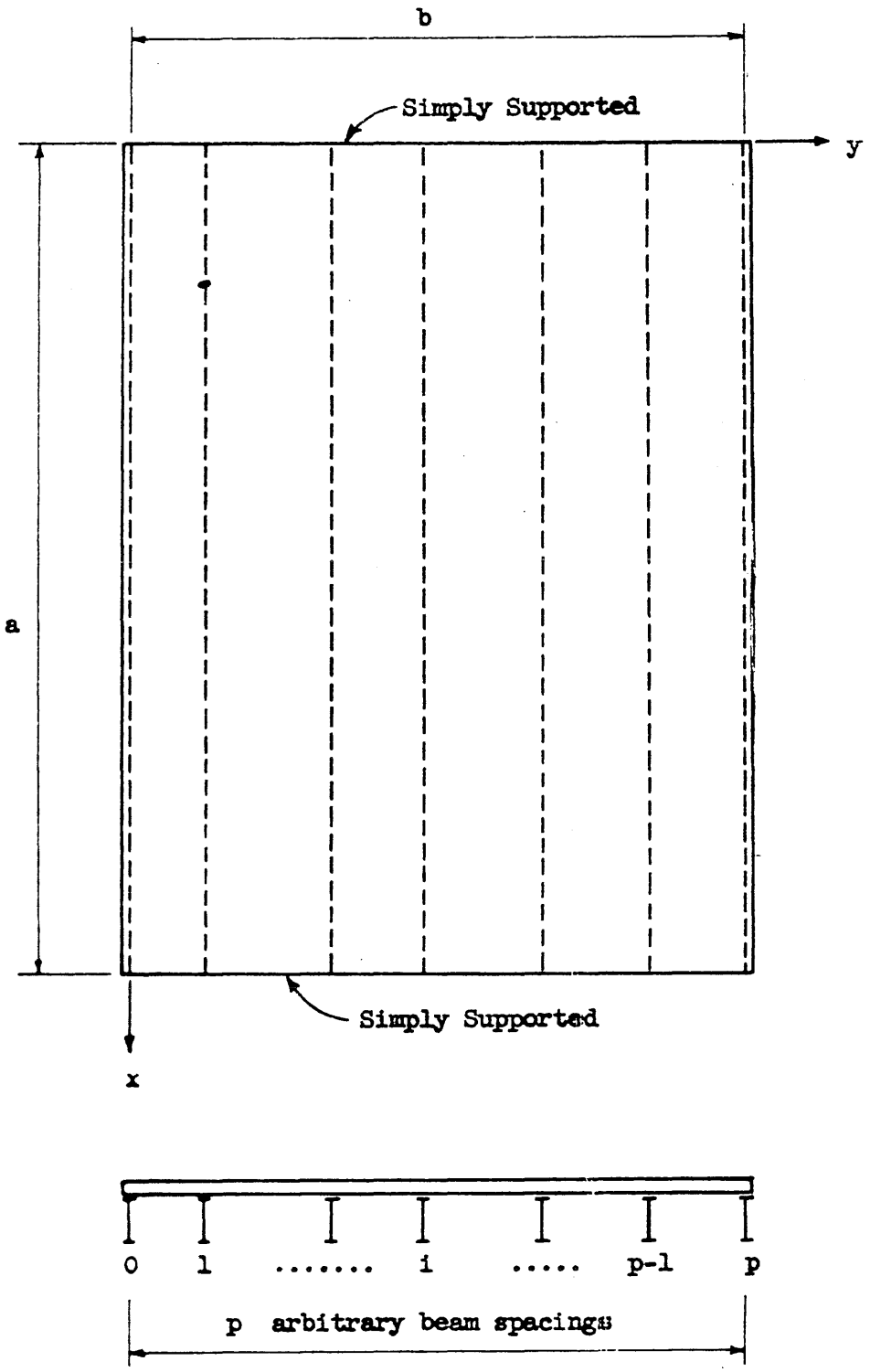

FIG. 1 CHARACTERISTICS OF STRUCTURE INVESTIGATED

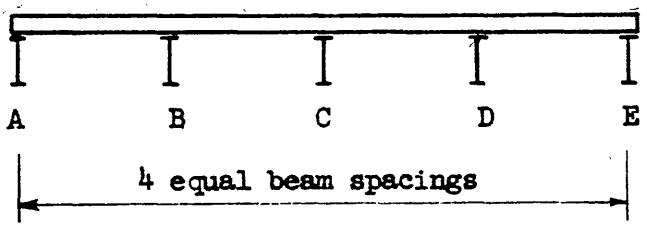

FIG. 2 CROSS-SECTION OF FIVE-GIRDER BRIDGE CONSIDERED IN NUMERICAL SOLUTIONS

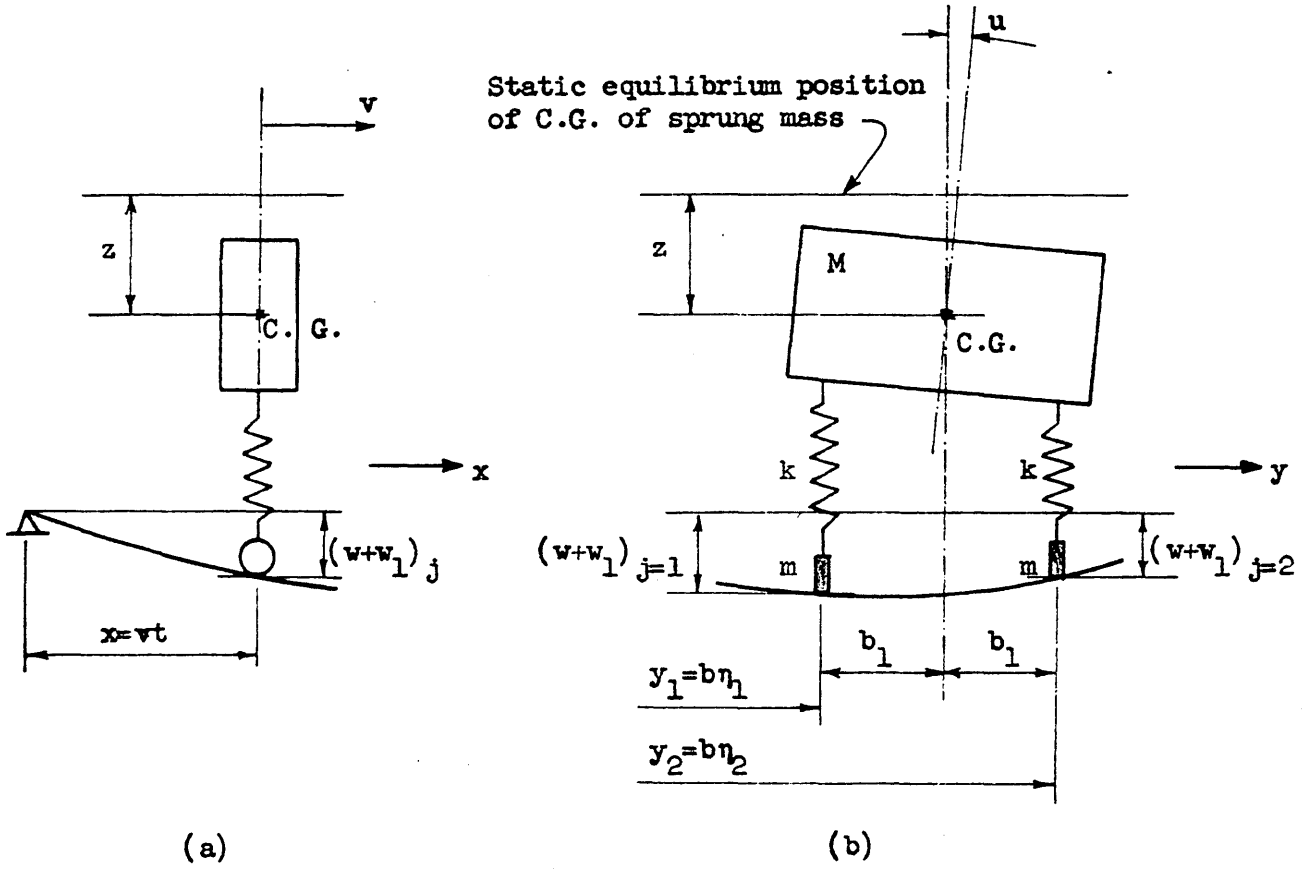

FIG. 3 VEHICLE MODEL

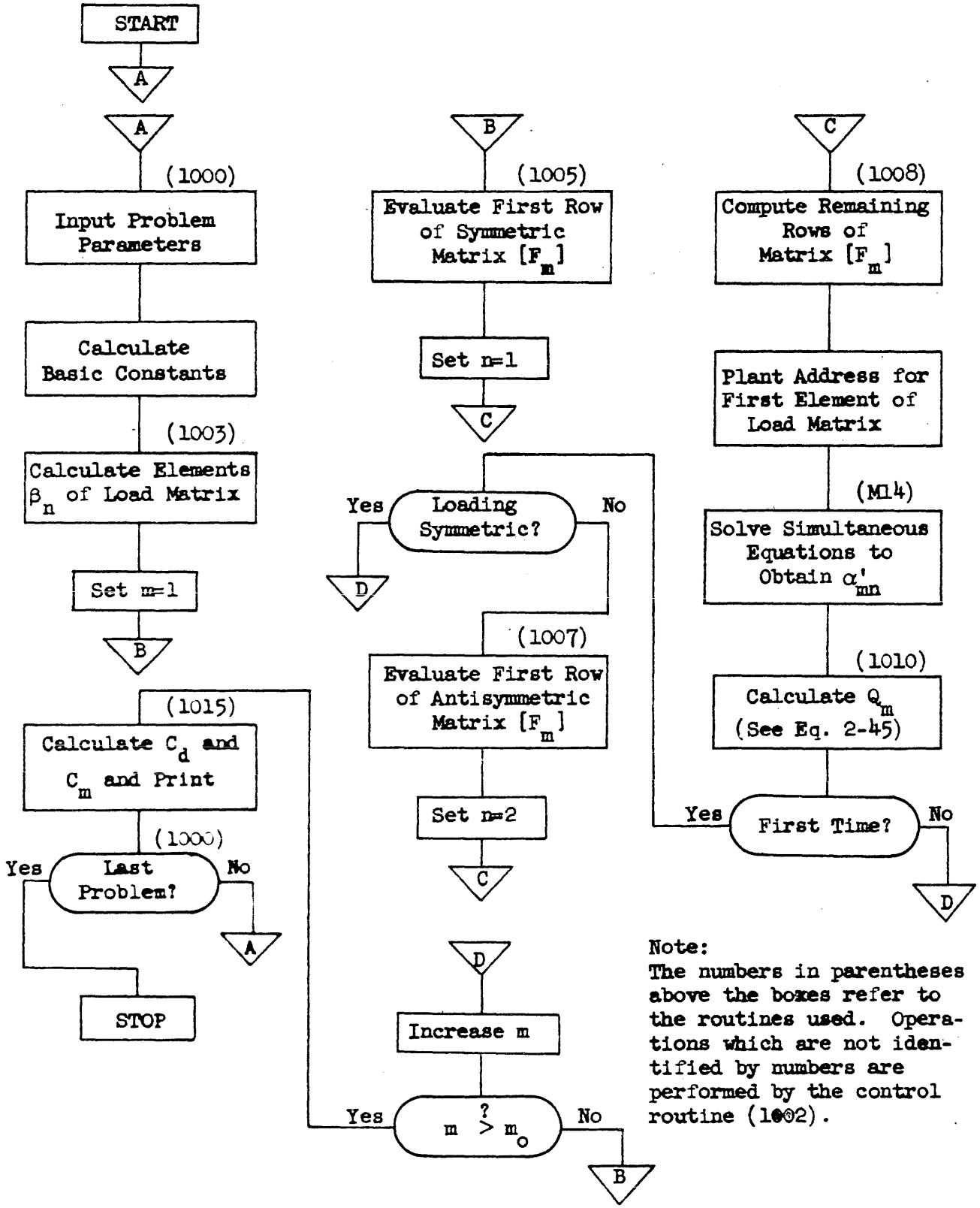

FIG. 4 FLOW DIAGRAM OF COMPLETE PROGRAM FOR INFLUENCE SURFACES

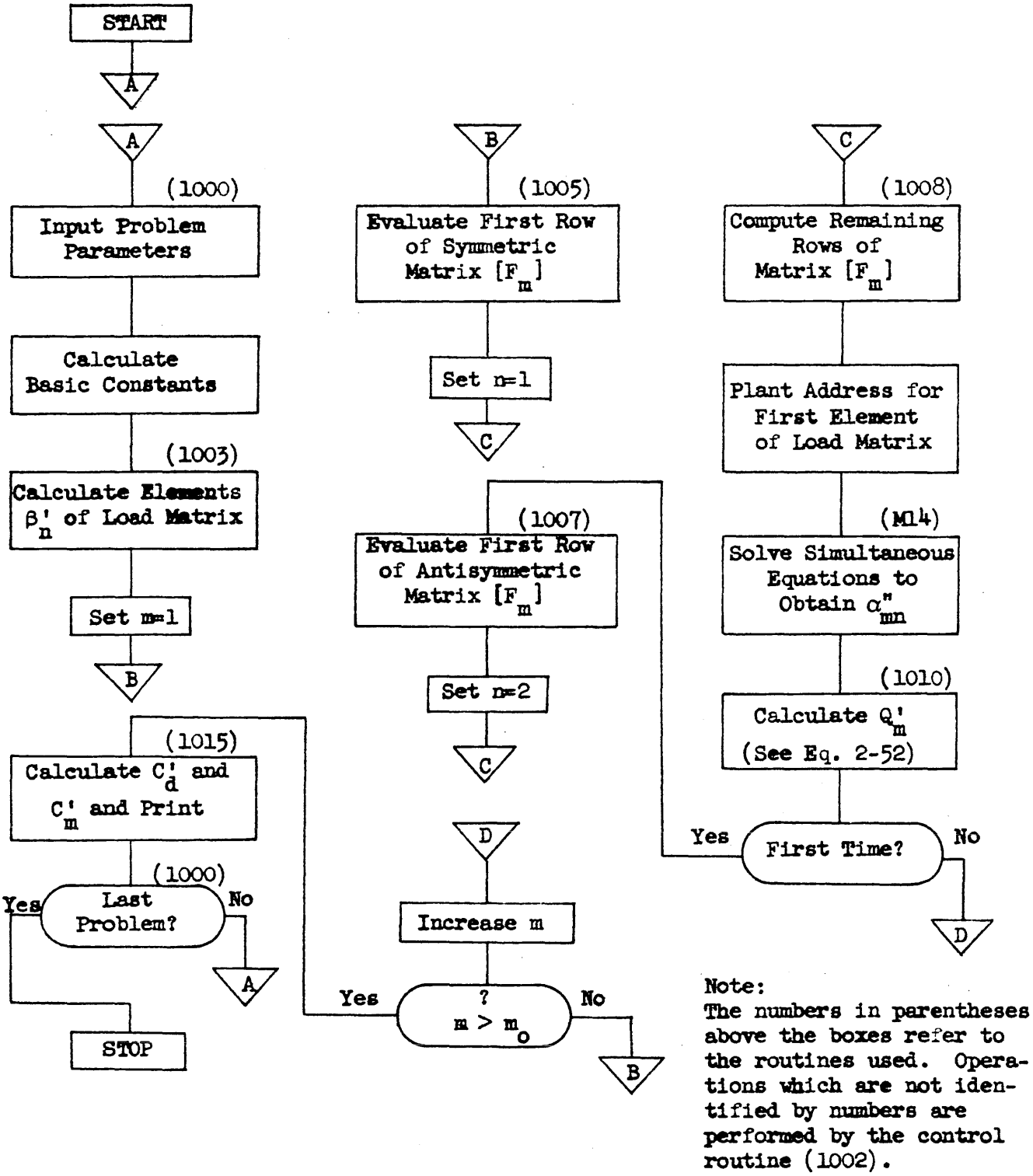

Note:
The numbers in parentheses above the boxes refer to the routines used. Operations which are not identified by numbers are performed by the control routine (1002).

FIG. 5 FLOW DIAGRAM OF COMPLETE PROGRAM FOR TRUCK LOADING

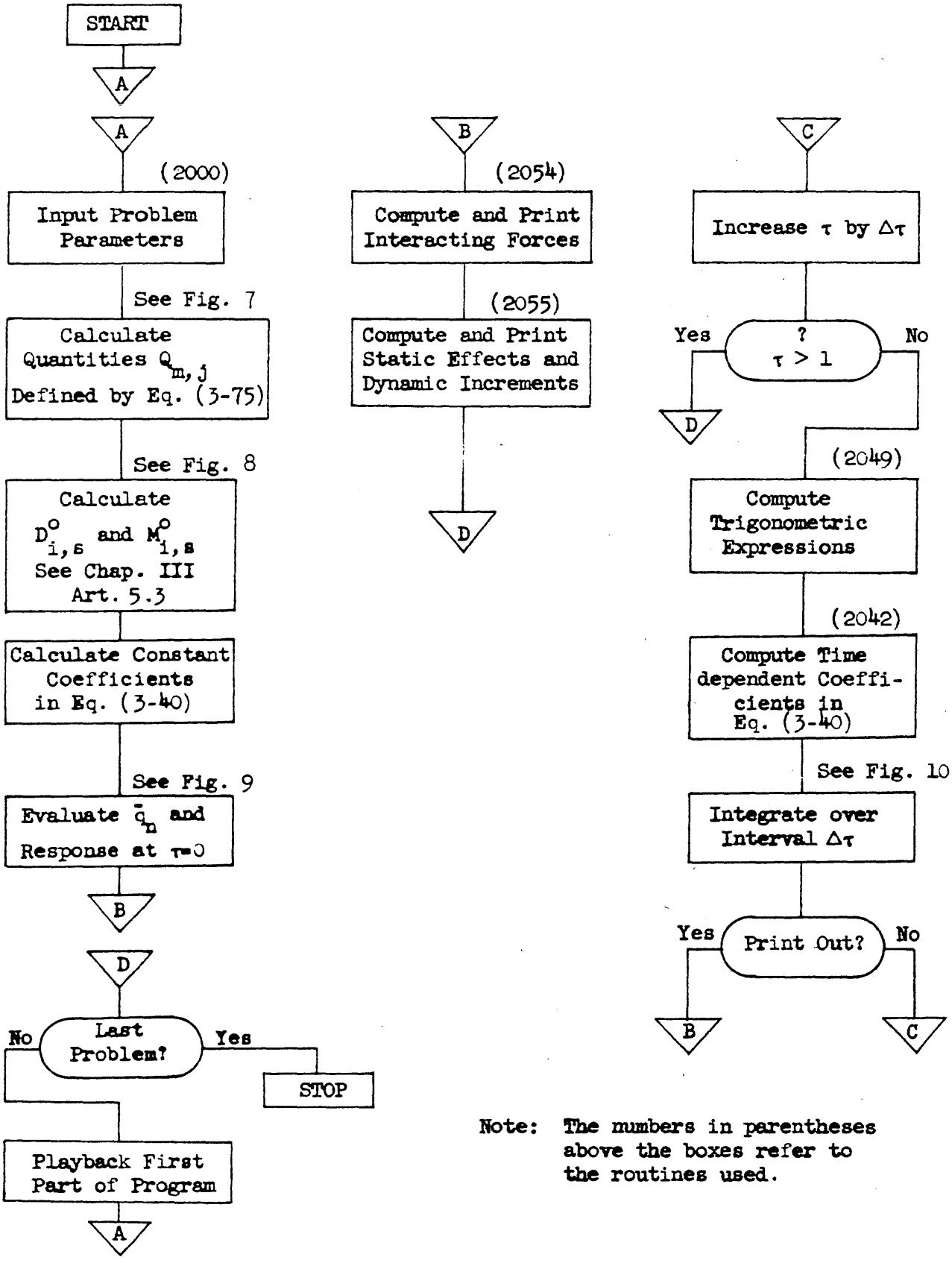

Note: The numbers in parentheses above the boxes refer to the routines used.

FIG. 6 GENERAL FLOW DIAGRAM OF COMPLETE PROGRAM FOR DYNAMIC PROBLEM

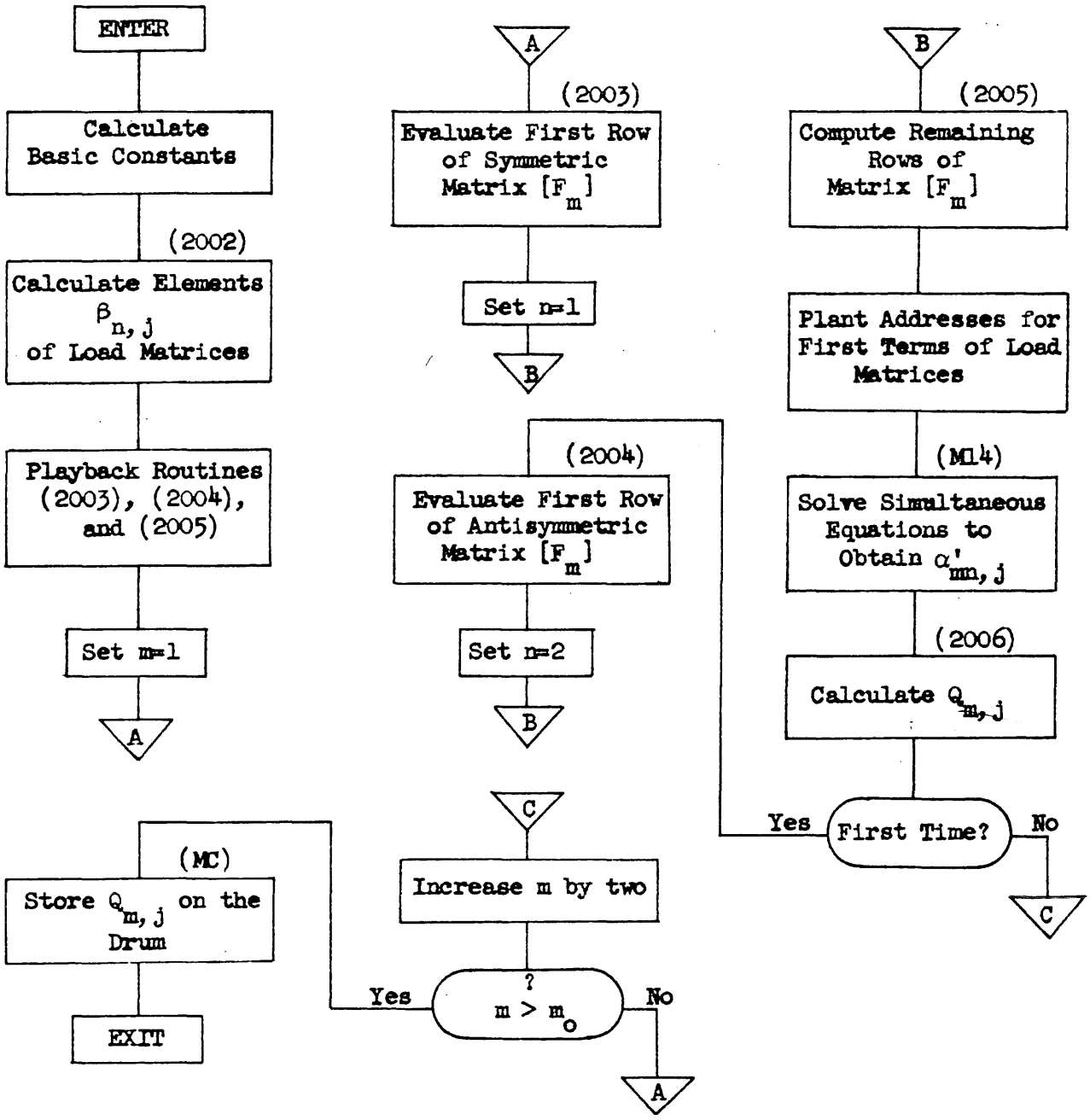

Note: Operations which are not identified by numbers are performed by the control routine (2001).

FIG. 7 FLOW DIAGRAM FOR COMPUTATION OF QUANTITIES $Q_{m,j}$

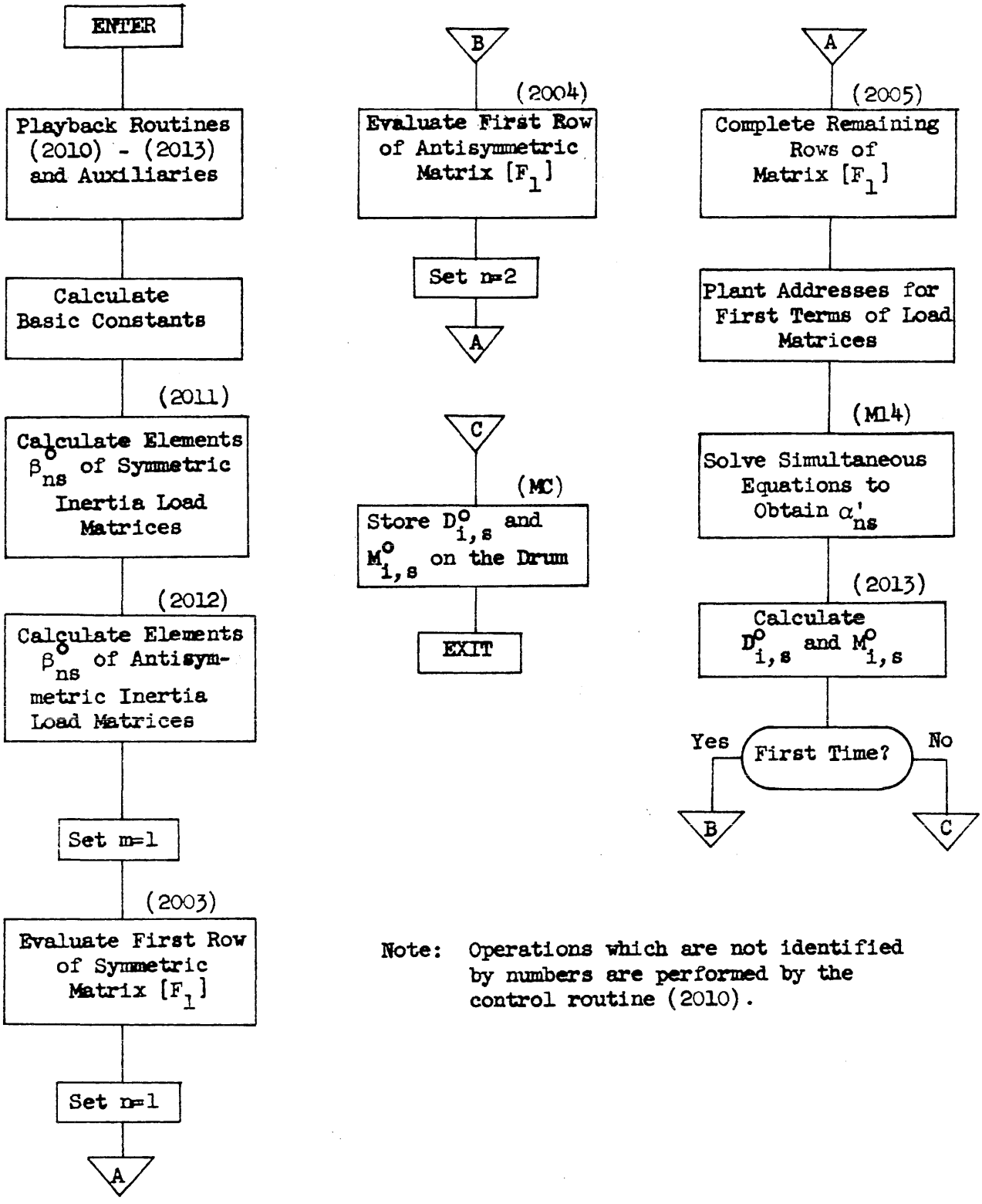

Note: Operations which are not identified by numbers are performed by the control routine (2010).

FIG. 8 FLOW DIAGRAM FOR COMPUTATION OF $D^{o}_{i,s}$ AND $M^{o}_{i,s}$

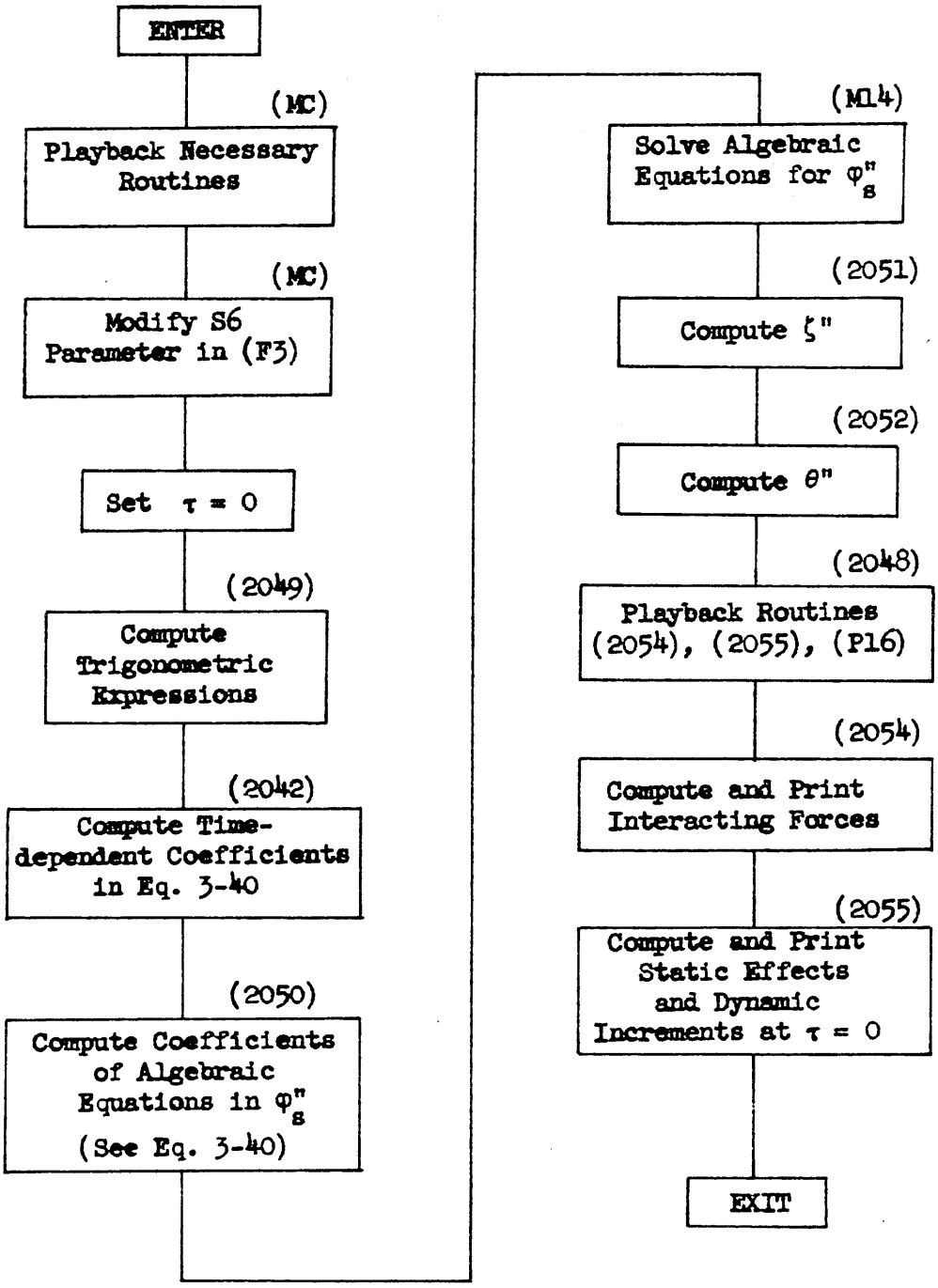

FIG. 9 FLOW DIAGRAM FOR COMPUTATION OF INITIAL RESPONSE

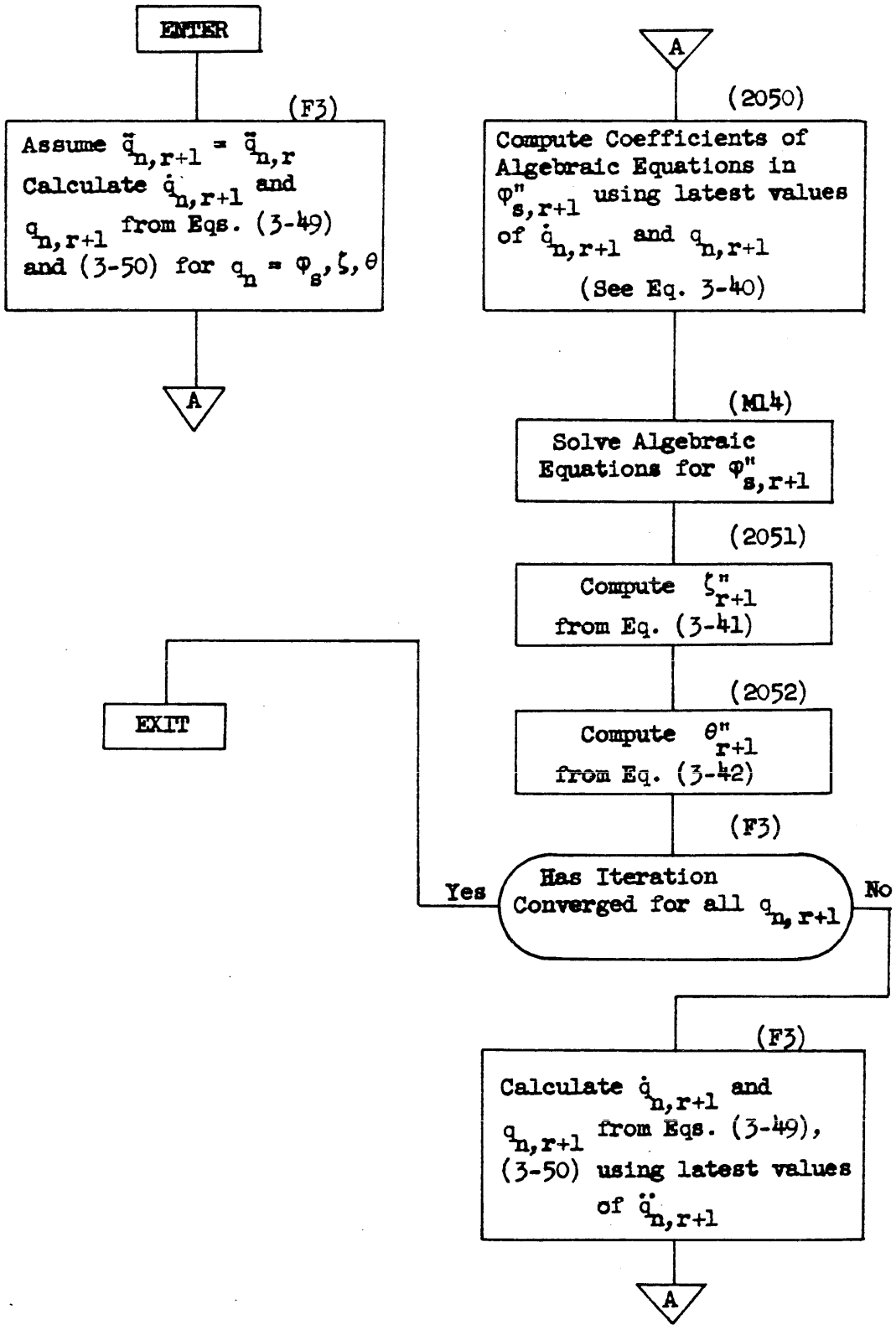

FIG. 10 FLOW DIAGRAM FOR INTEGRATION OVER INTERVAL $\Delta\tau$

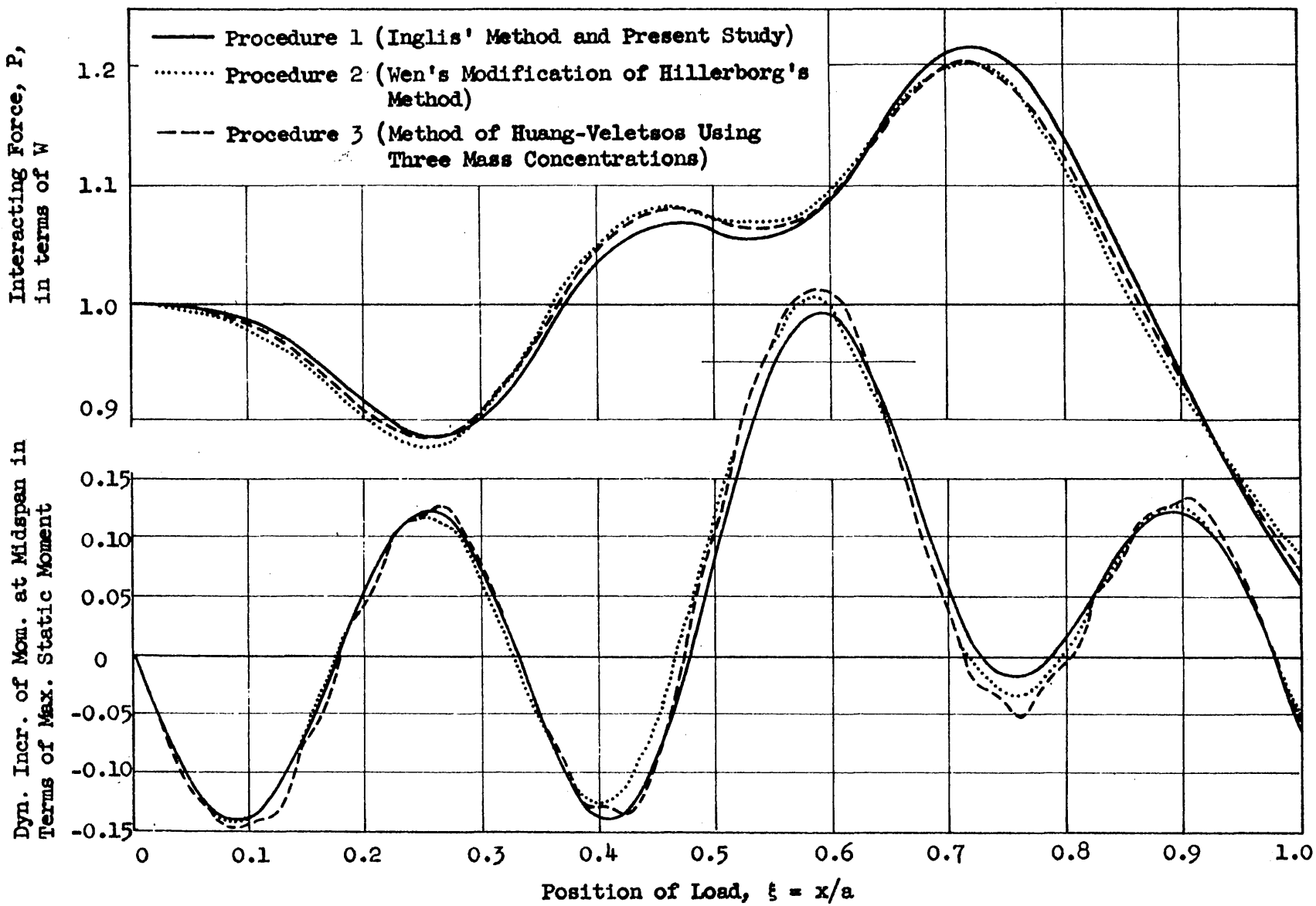

FIG. 11 COMPARISON OF RESULTS OBTAINED BY IDEALIZING THE BRIDGE AS A BEAM
Single Axle; Smoothly Rolling; $\alpha = 0.18$, $\nu = 0.5$, $f_v/f_b = 0.5$

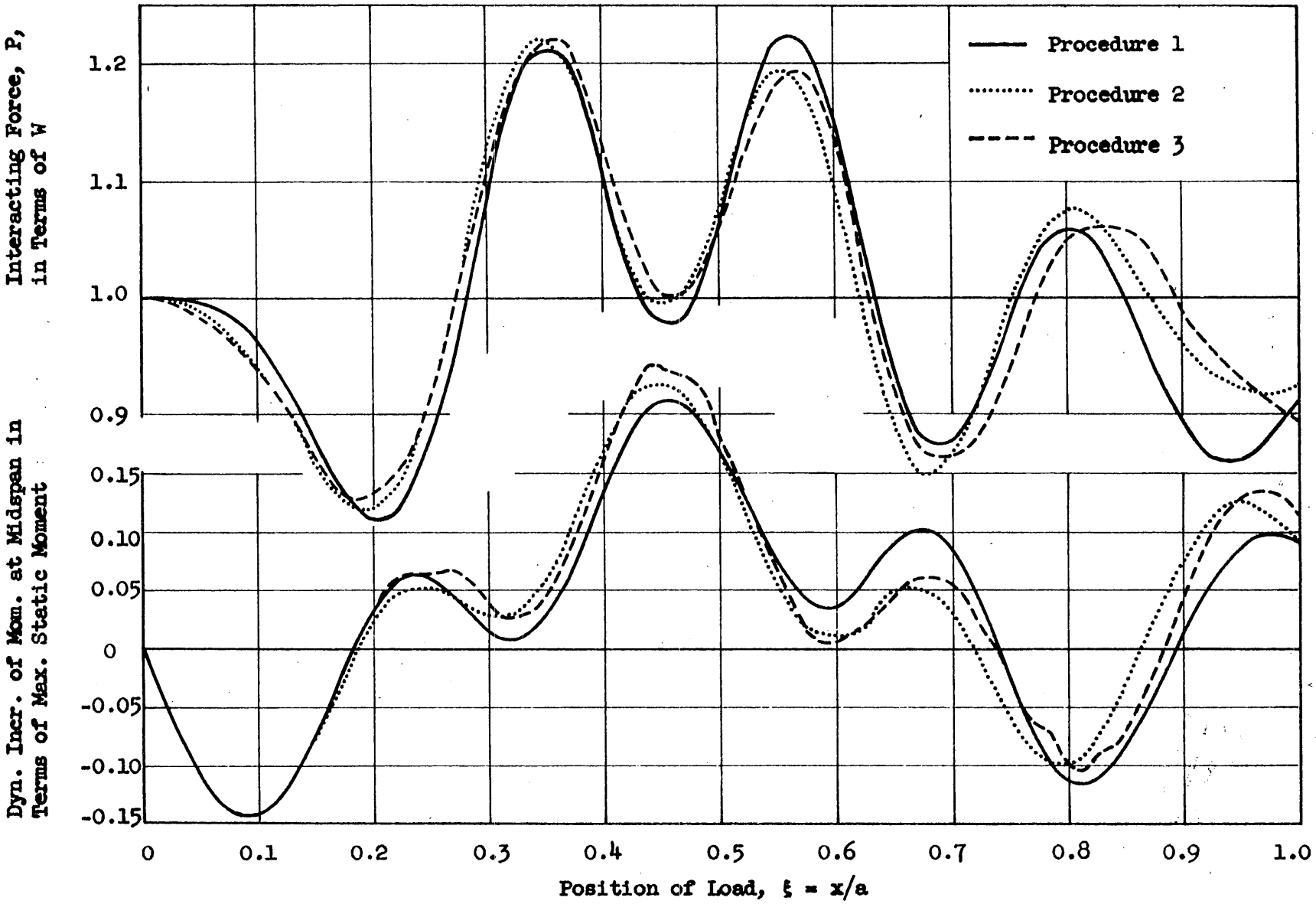

FIG. 12 COMPARISON OF RESULTS OBTAINED BY IDEALIZING THE BRIDGE AS A BEAM
Single Axle; Smoothly Rolling; $\alpha = 0.18$, $\nu = 0.5$, $f_v/f_b = 1.0$

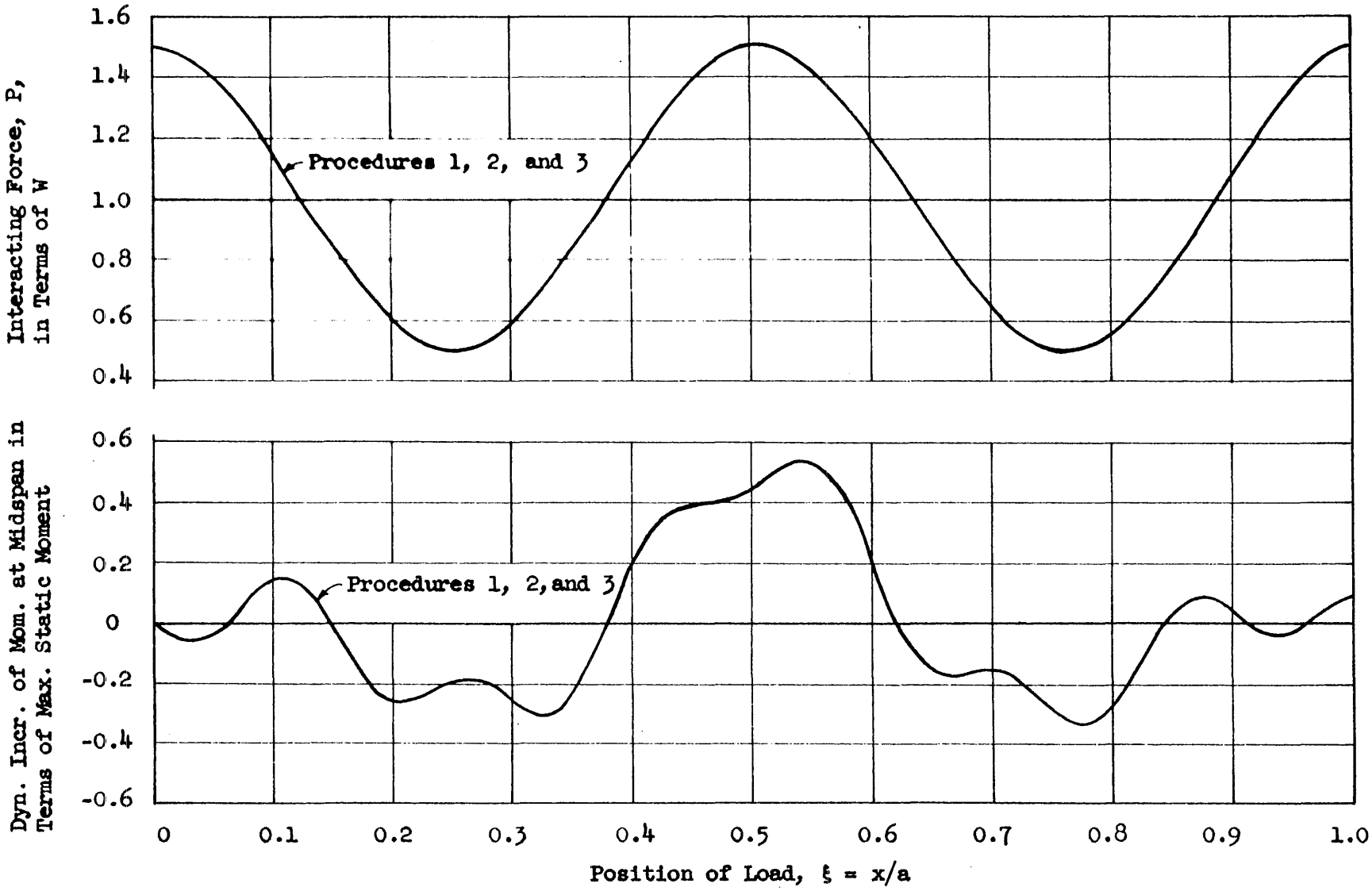

FIG. 13 COMPARISON OF RESULTS OBTAINED BY IDEALIZING THE BRIDGE AS A BEAM
Single Axle; $P_{initial} = 1.5\ W$; $\alpha = 0.075$; $\nu = 0.2$; $f_v/f_b = 0.3$

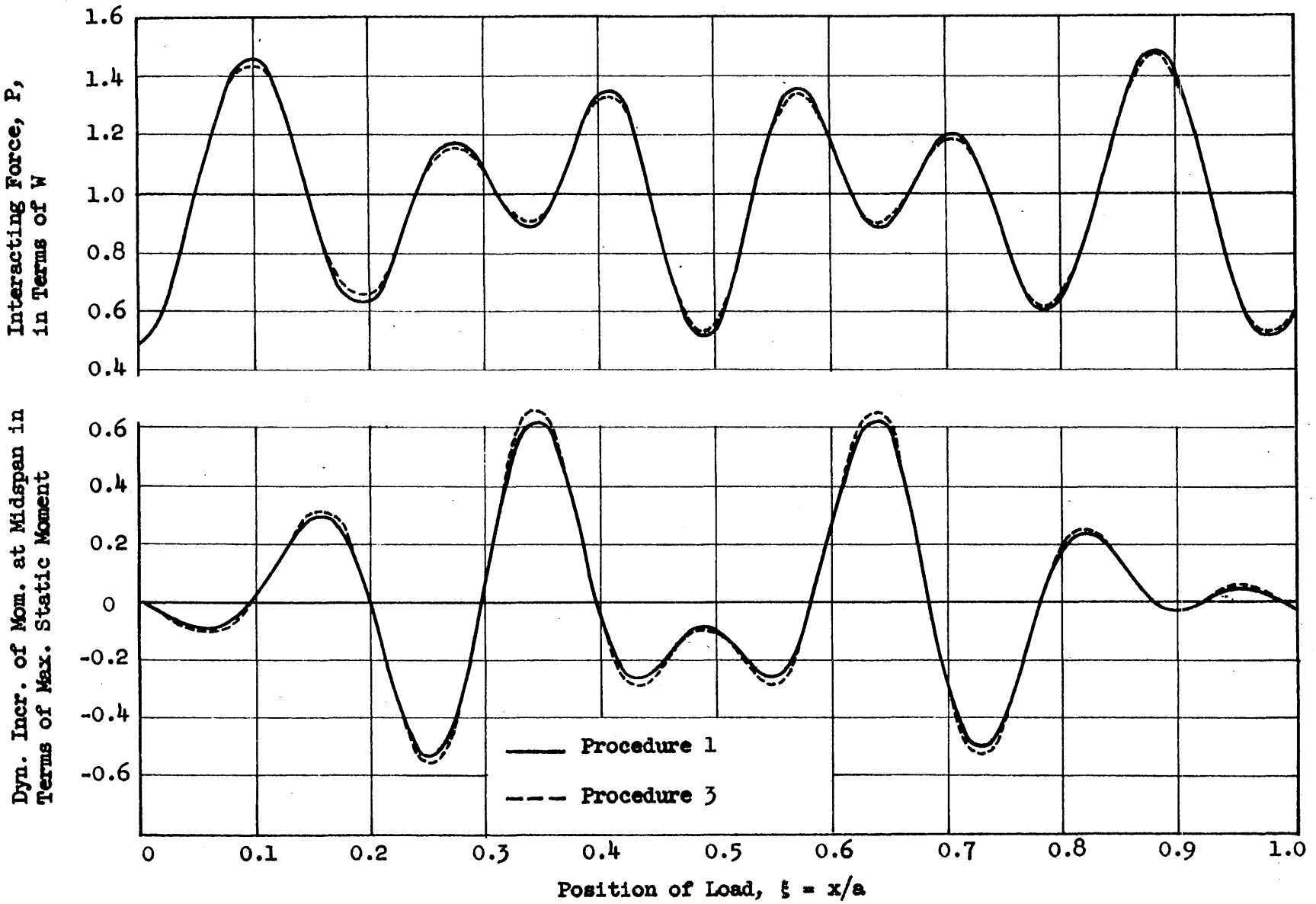

FIG. 14 COMPARISON OF RESULTS OBTAINED BY IDEALIZING THE BRIDGE AS A BEAM
Single Axle; $P_{initial} = 0.5\ W$; $\alpha = 0.10$; $\nu = 0.2$; $f_v/f_b = 1.0$

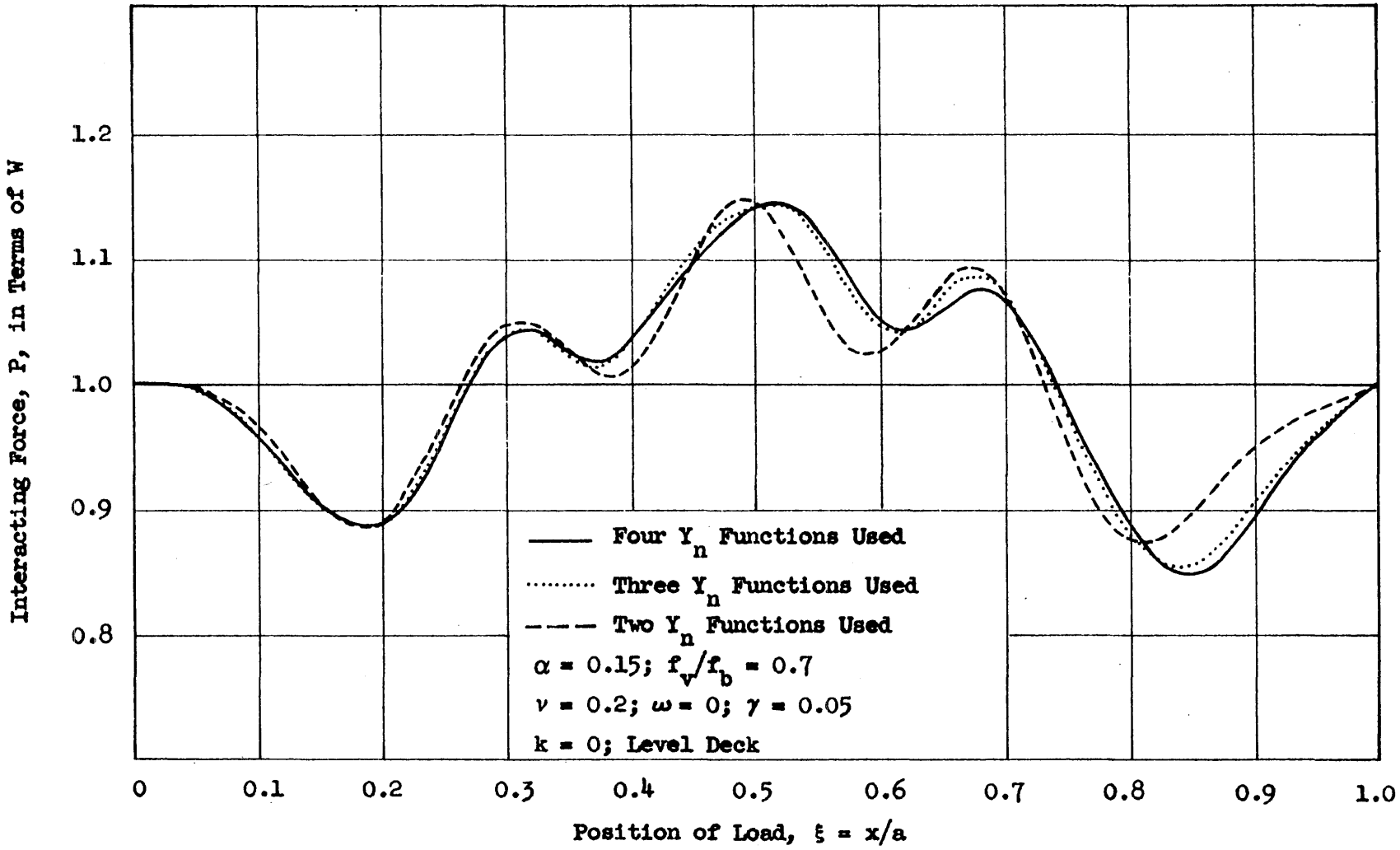

FIG. 15 HISTORY CURVES FOR INTERACTING FORCE -- EFFECT OF NUMBER OF Y_n FUNCTIONS USED
Load over Beam A; c = 0.4; λ = 12.5

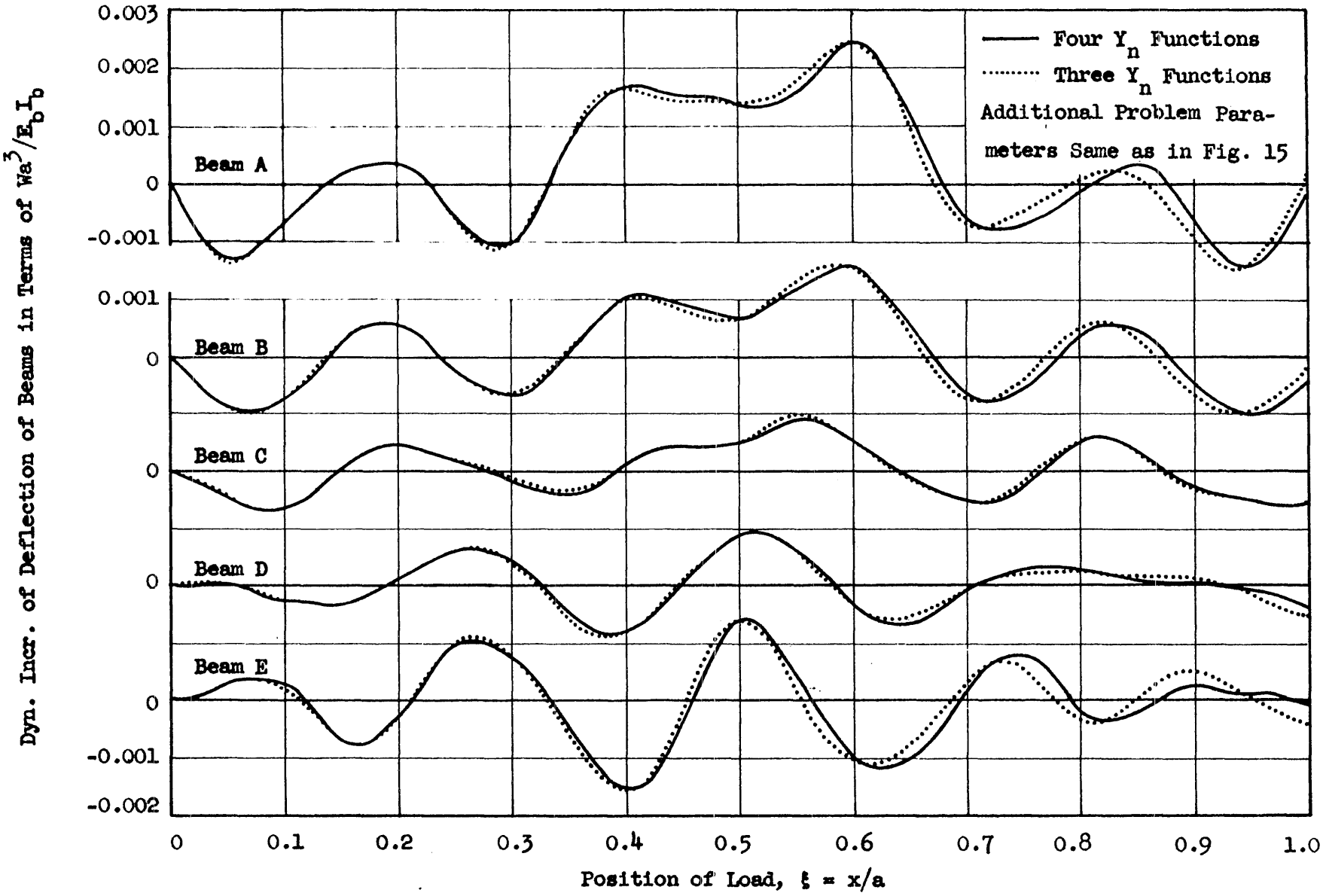

FIG. 16 HISTORY CURVES FOR DYNAMIC INCREMENT OF DEFLECTION OF BEAMS AT MIDSPAN -- EFFECT OF NUMBER OF Y_n FUNCTIONS USED; Load over Beam A; c = 0.4; λ = 12.5

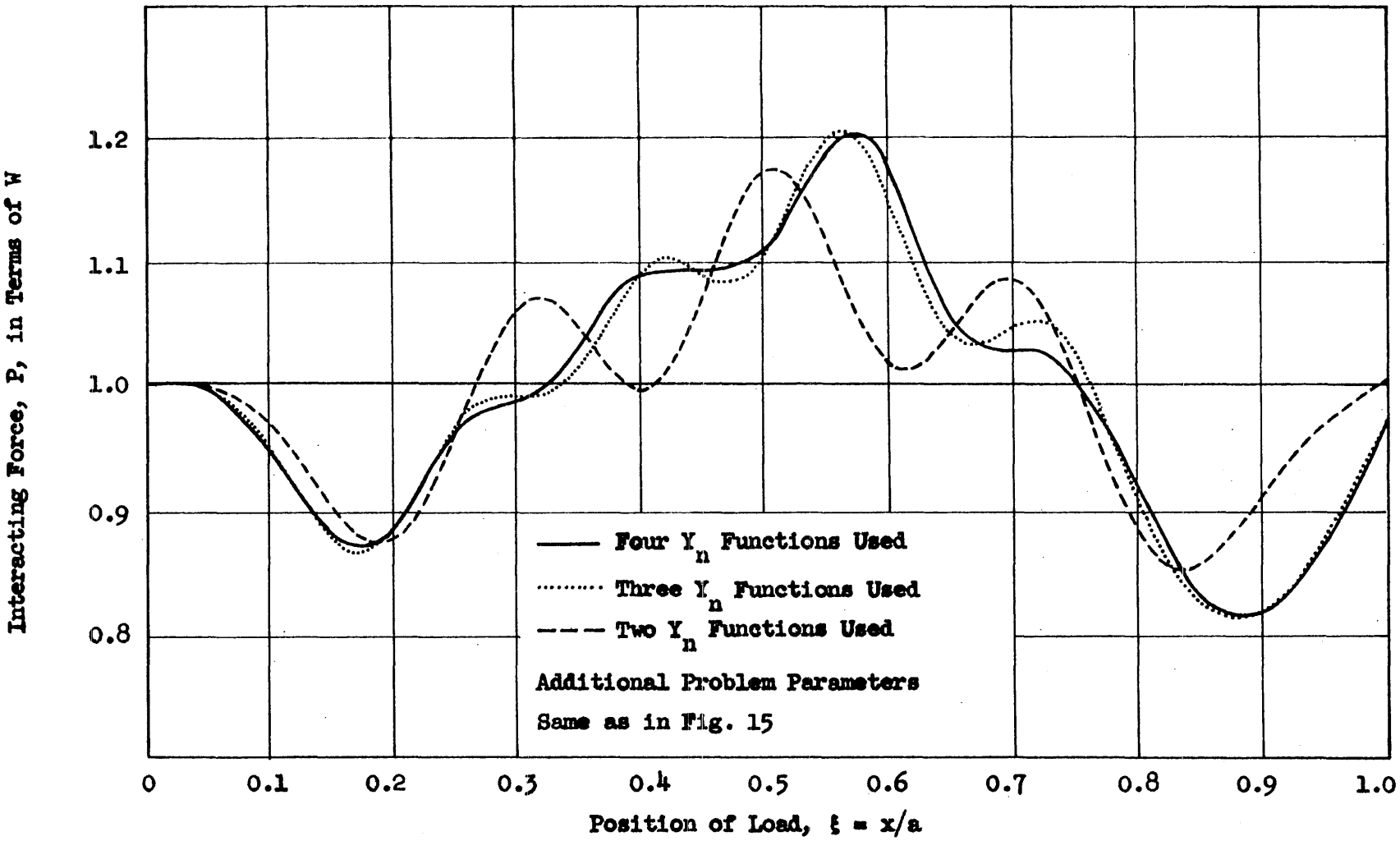

FIG. 17 HISTORY CURVES FOR INTERACTING FORCE -- EFFECT OF NUMBER OF Y_n FUNCTIONS USED
Load over Beam A; $c = 0.4$; $\lambda = 50$

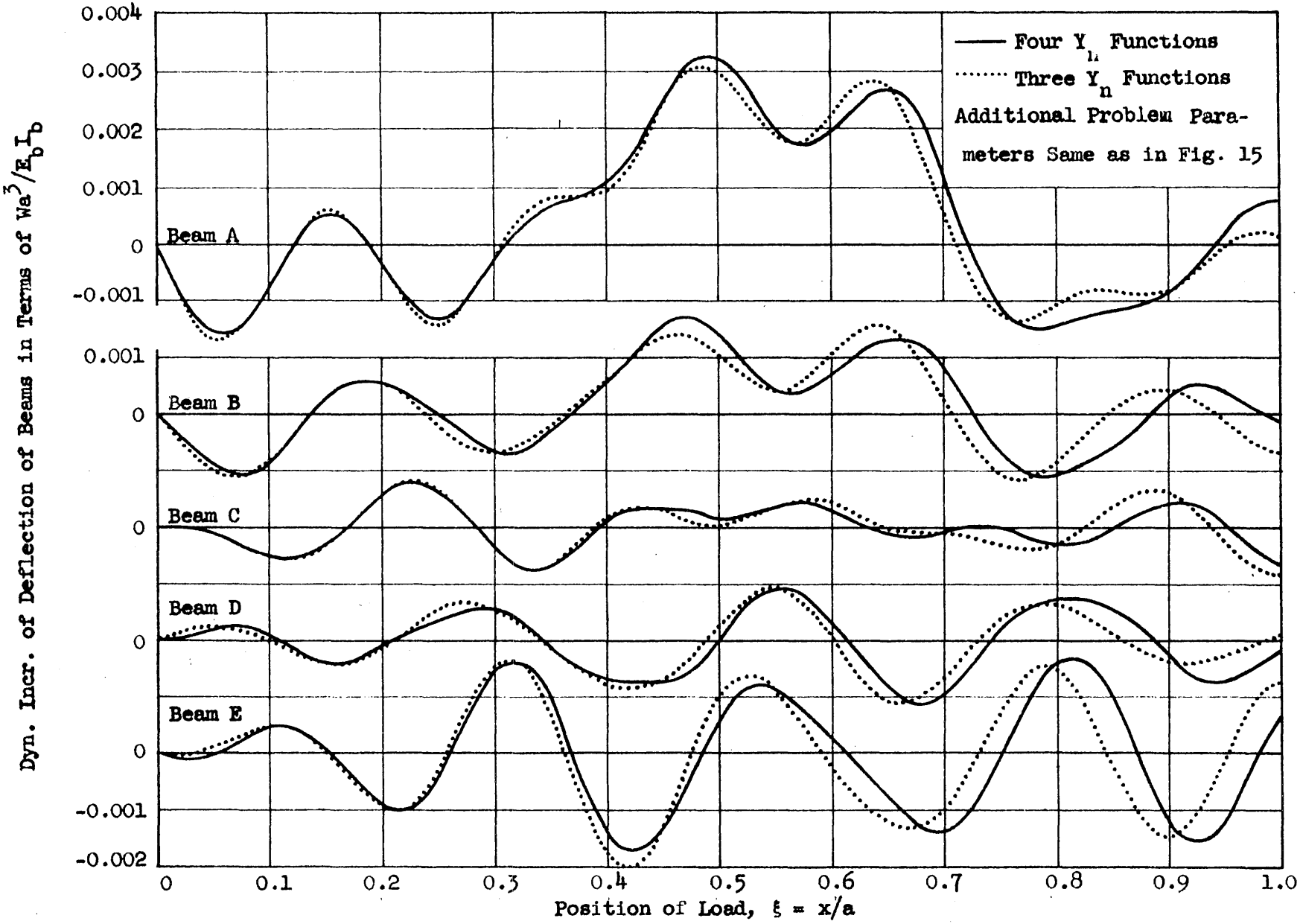

FIG. 18 HISTORY CURVES FOR DYNAMIC INCREMENT OF DEFLECTION OF BEAMS AT MIDSPAN -- EFFECT OF NUMBER OF Y_n FUNCTIONS USED; Load over Beam A; $c = 0.4$; $\lambda = 50$

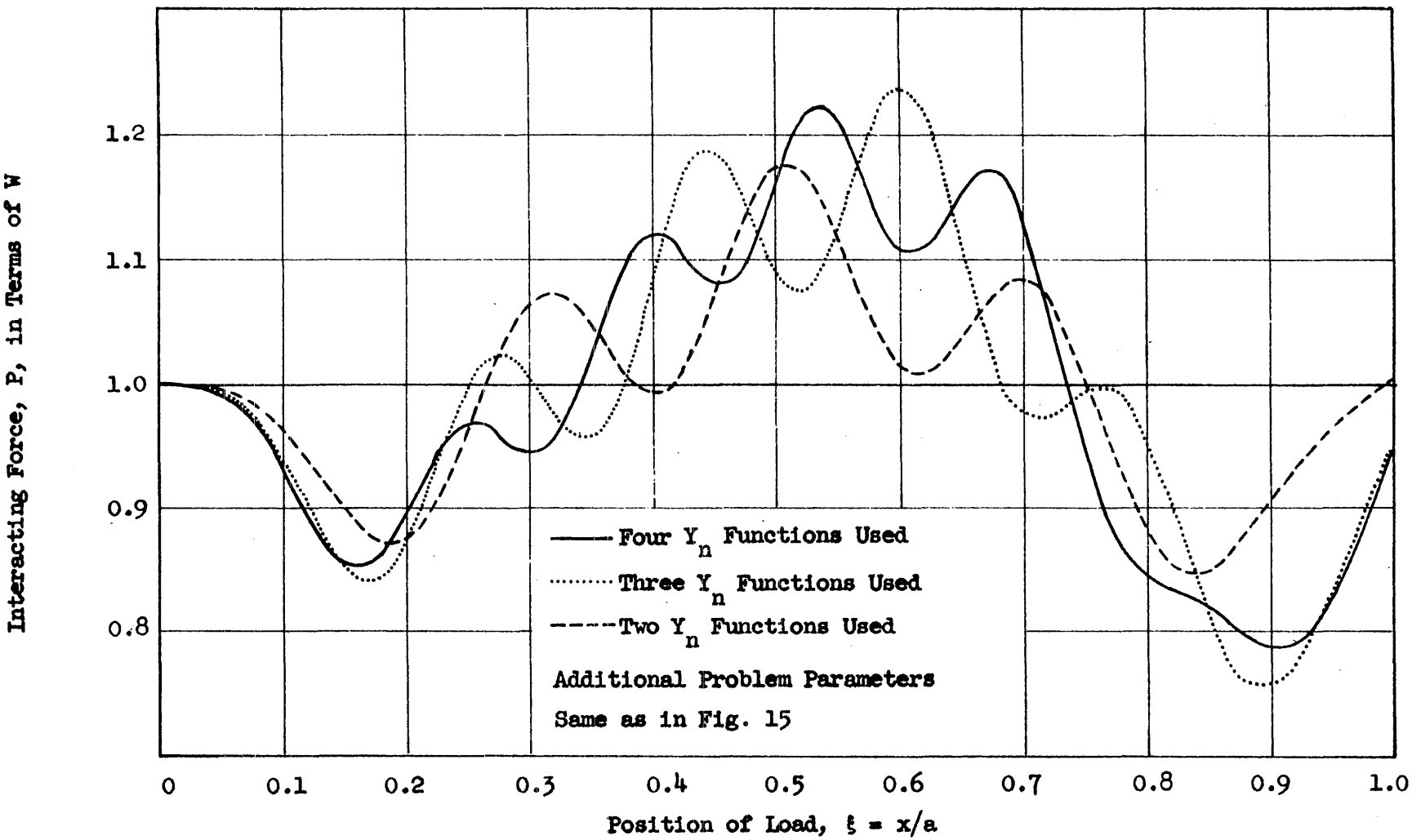

FIG. 19 HISTORY CURVES FOR INTERACTING FORCE -- EFFECT OF NUMBER OF Y_n FUNCTIONS USED
Load over Beam A; c = 0.8; λ = 25

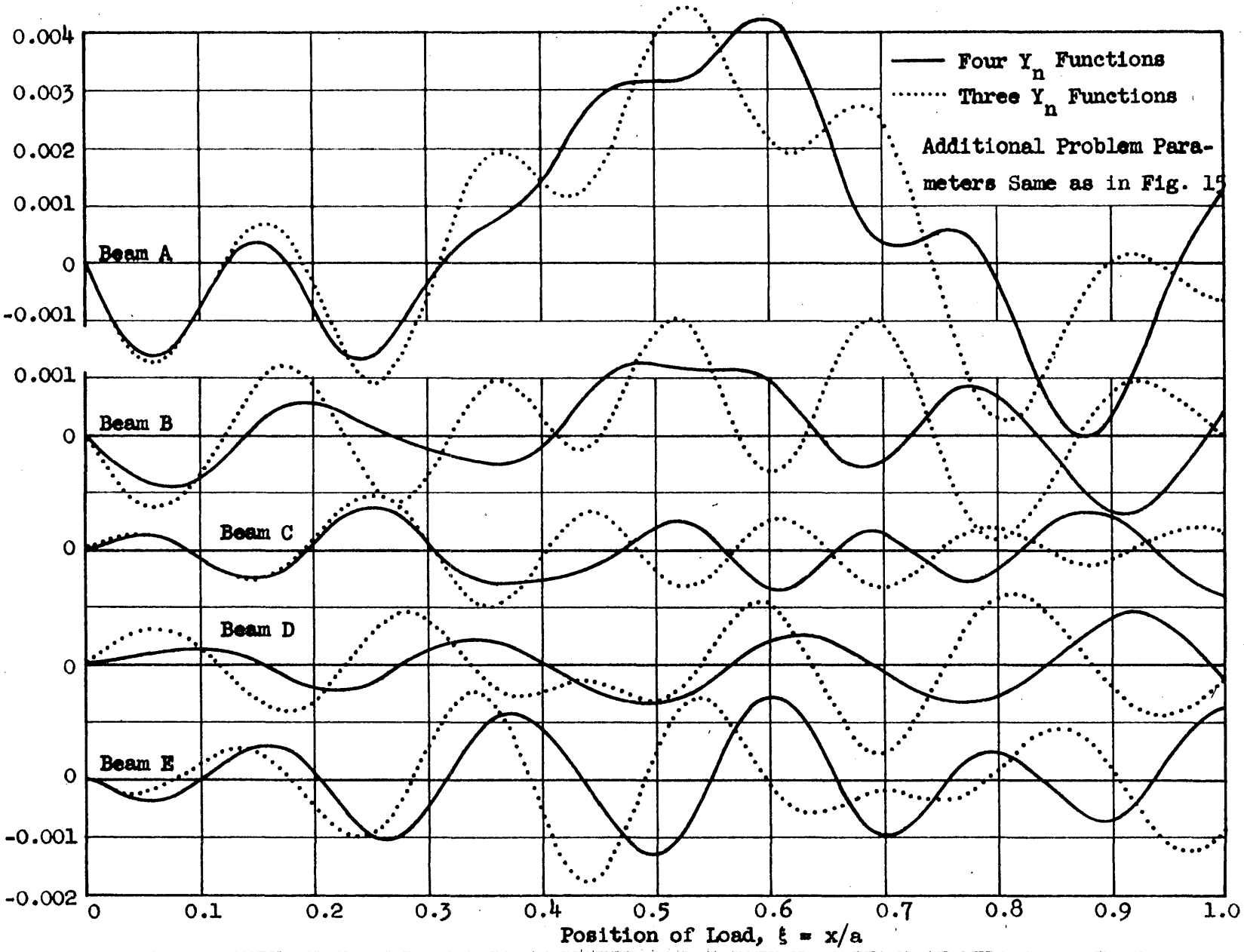

FIG. 20 HISTORY CURVES FOR DYNAMIC INCREMENT OF DEFLECTION OF BEAMS AT MIDSPAN -- EFFECT OF NUMBER OF Y_n FUNCTIONS USED; Load over Beam A; $c = 0.8$; $\lambda = 25$

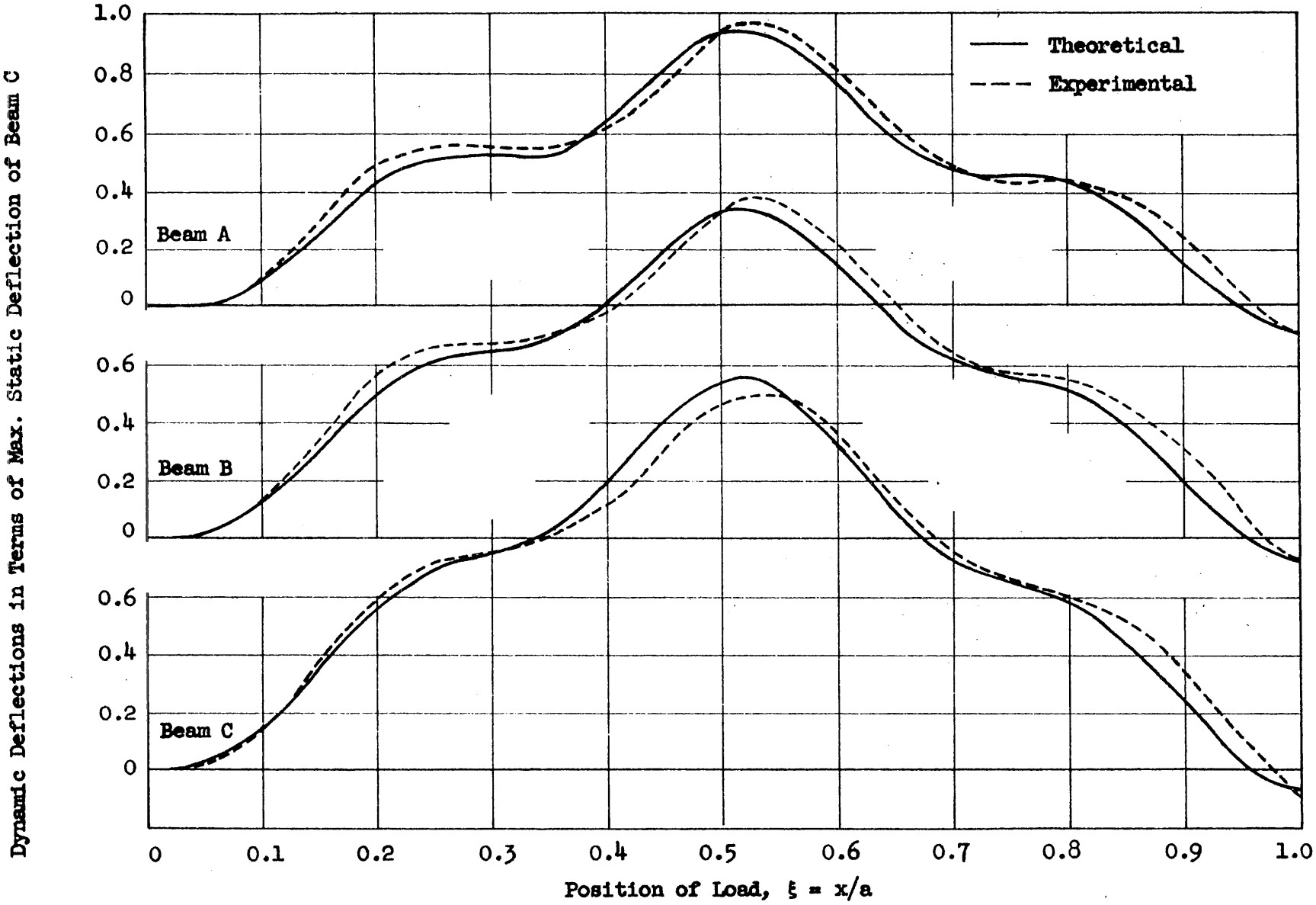

FIG. 21 COMPARISON OF THEORETICAL AND EXPERIMENTAL DEFLECTION CURVES
Load over Beam C

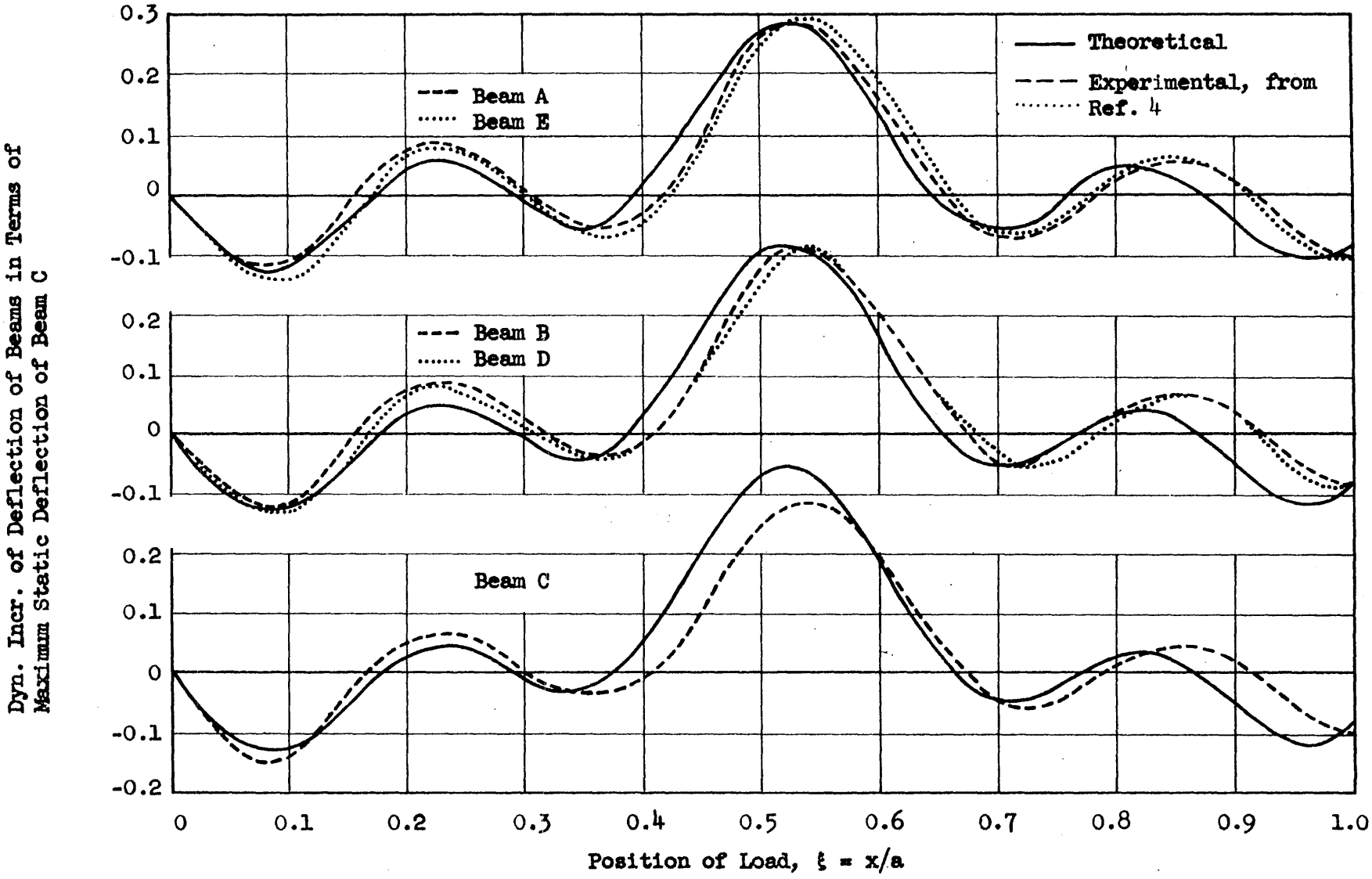

FIG. 22 COMPARISON OF THEORETICAL AND EXPERIMENTAL CURVES FOR DYNAMIC INCREMENT OF DEFLECTION
Load over Beam C

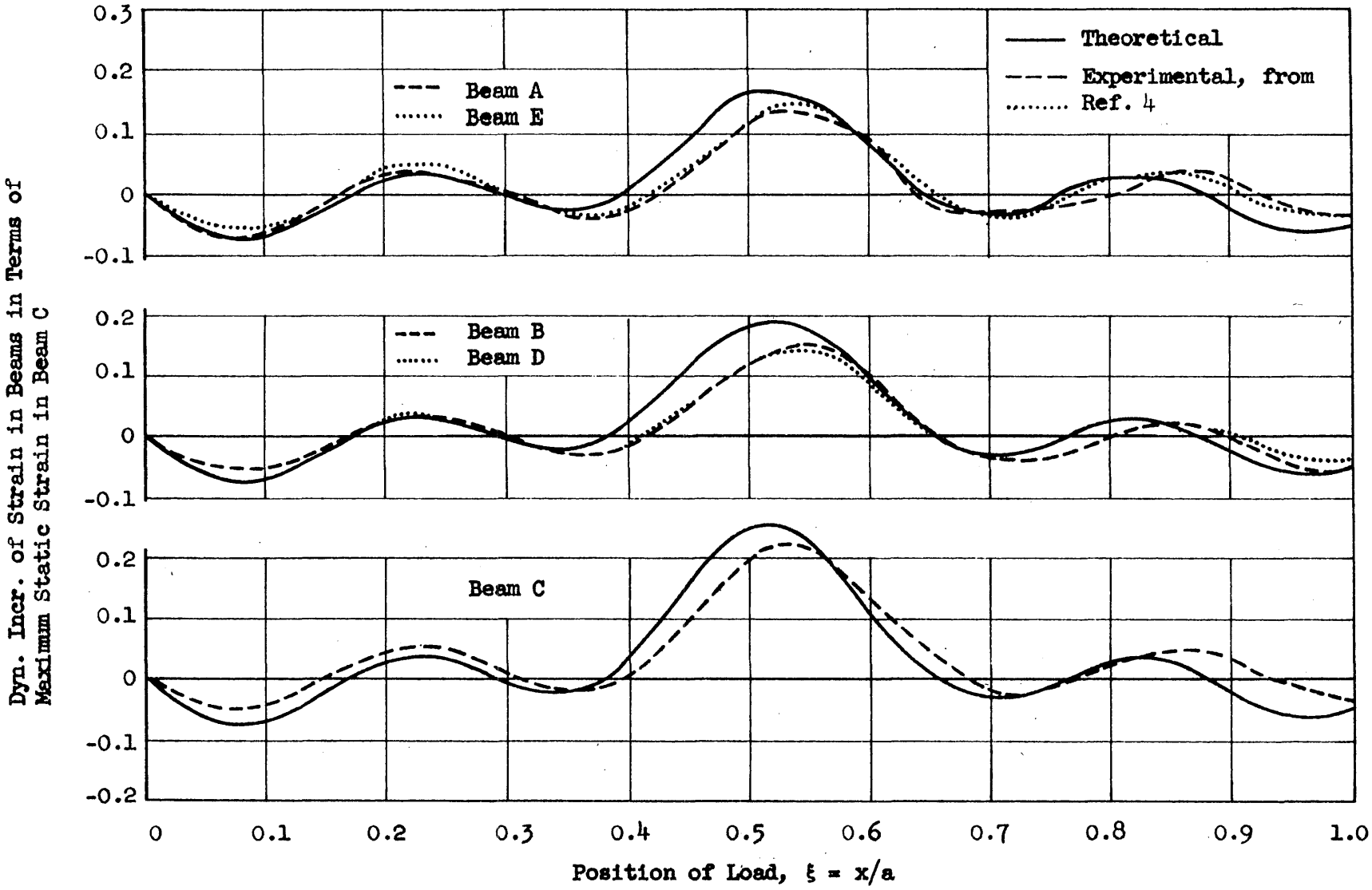

FIG. 23 COMPARISON OF THEORETICAL AND EXPERIMENTAL CURVES FOR DYNAMIC INCREMENT OF STRAIN
Load over Beam C

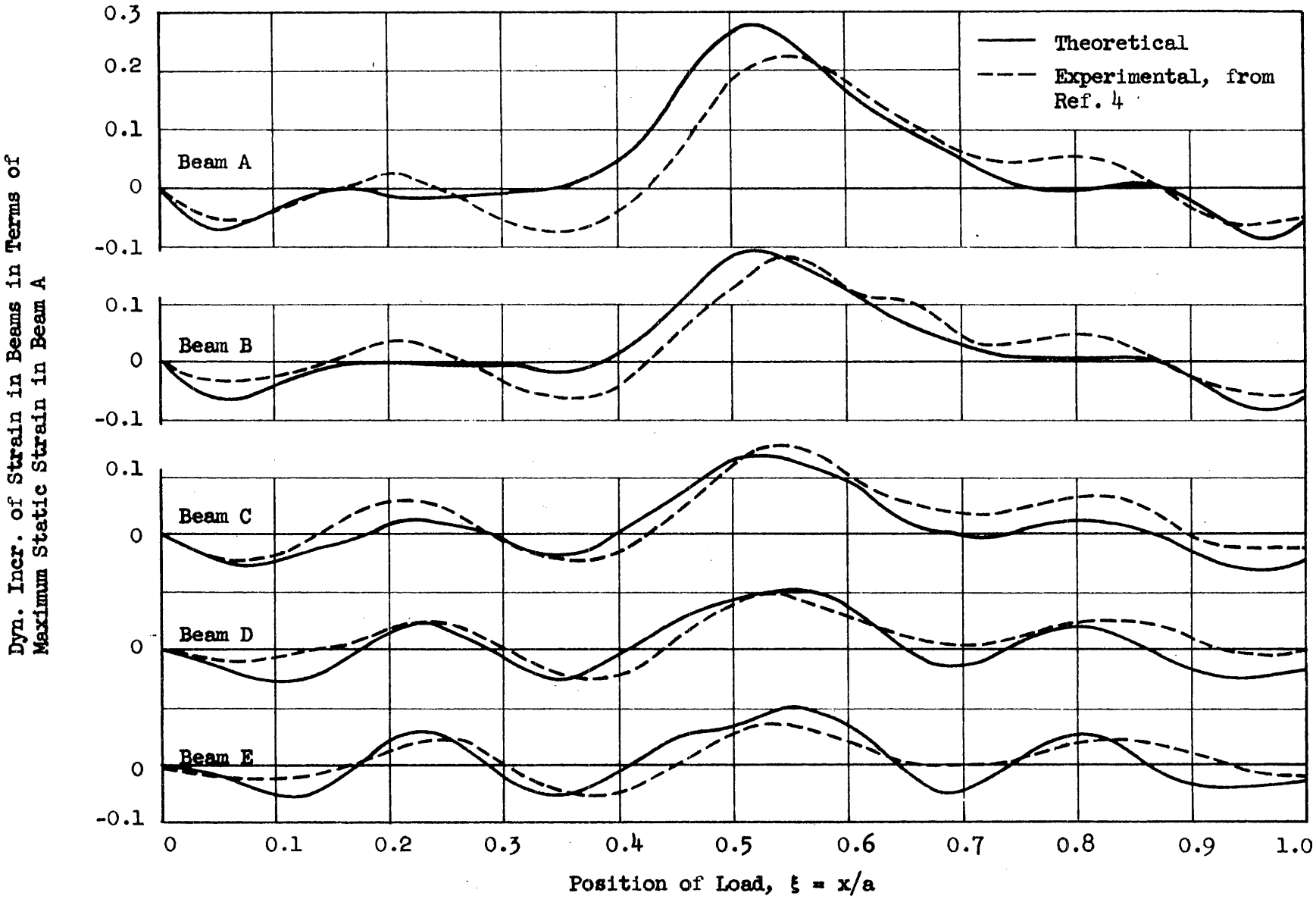

FIG. 24 COMPARISON OF THEORETICAL AND EXPERIMENTAL CURVES FOR DYNAMIC INCREMENT OF STRAIN
Load over Beam A

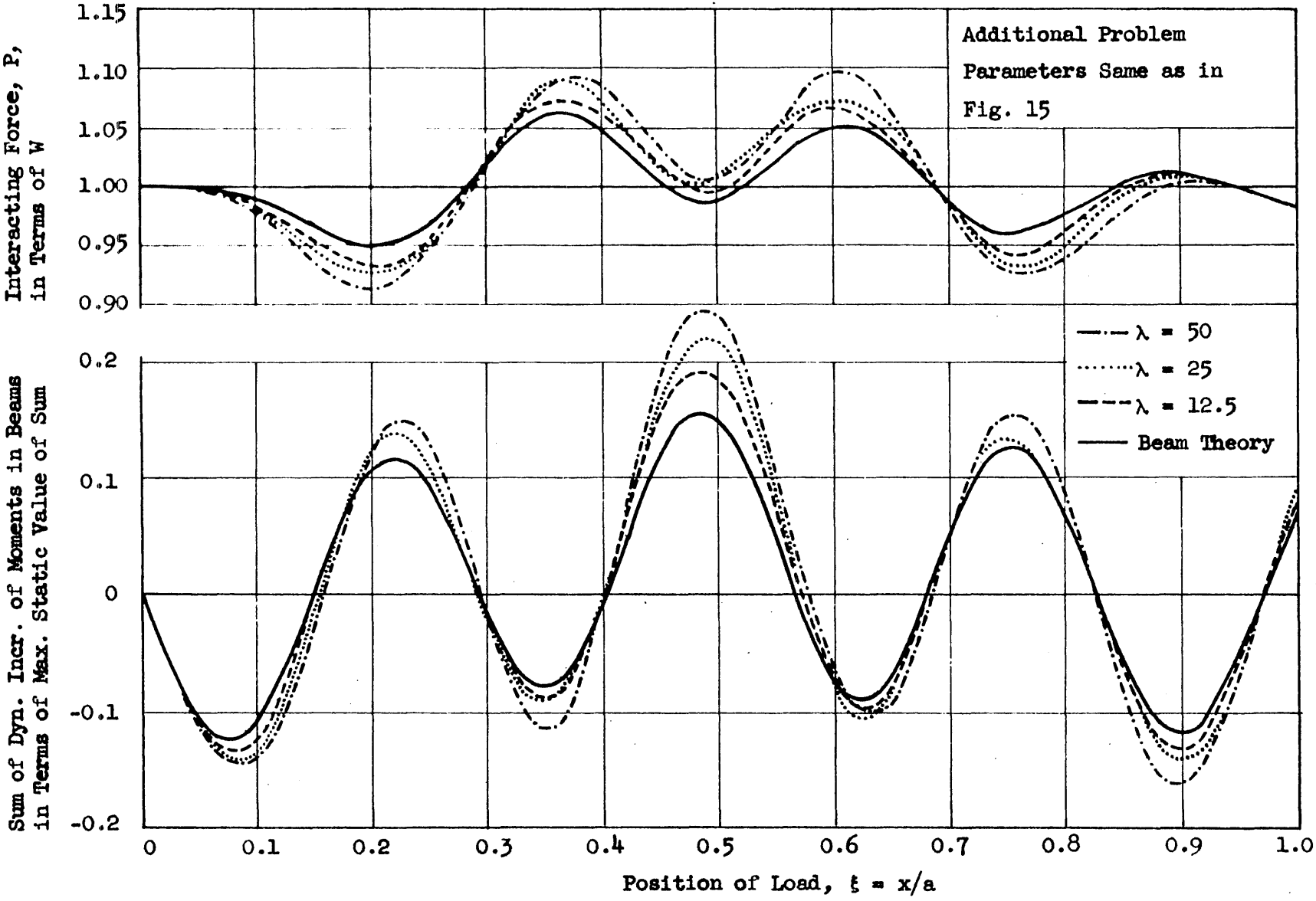

FIG. 25 HISTORY CURVES FOR INTERACTING FORCE AND SUM OF MOMENTS IN BEAMS -- EFFECT OF λ
Load over Beam C; c = 0.4

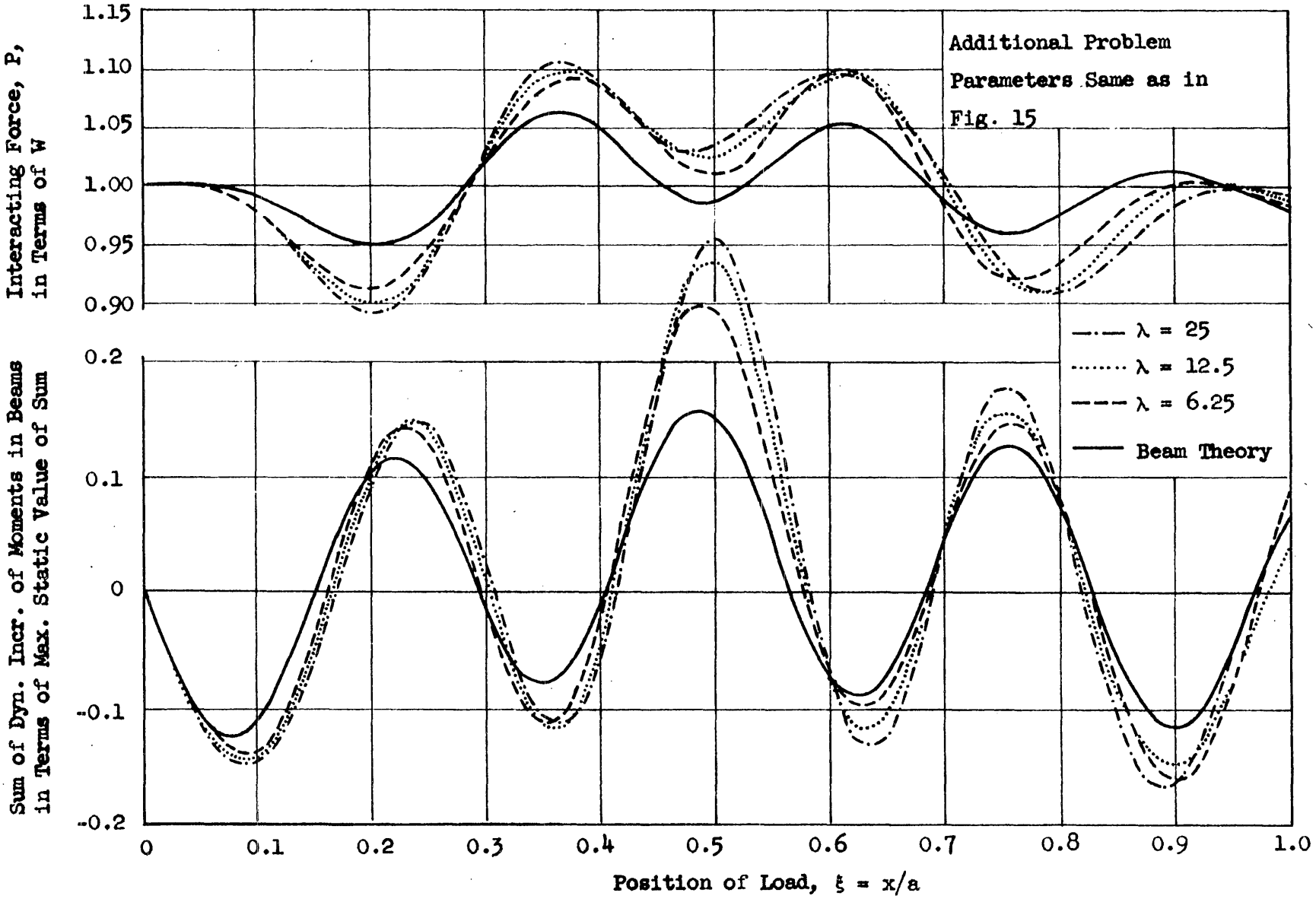

FIG. 26 HISTORY CURVES FOR INTERACTING FORCE AND SUM OF MOMENTS IN BEAMS -- EFFECT OF λ
Load over Beam C; c = 0.8

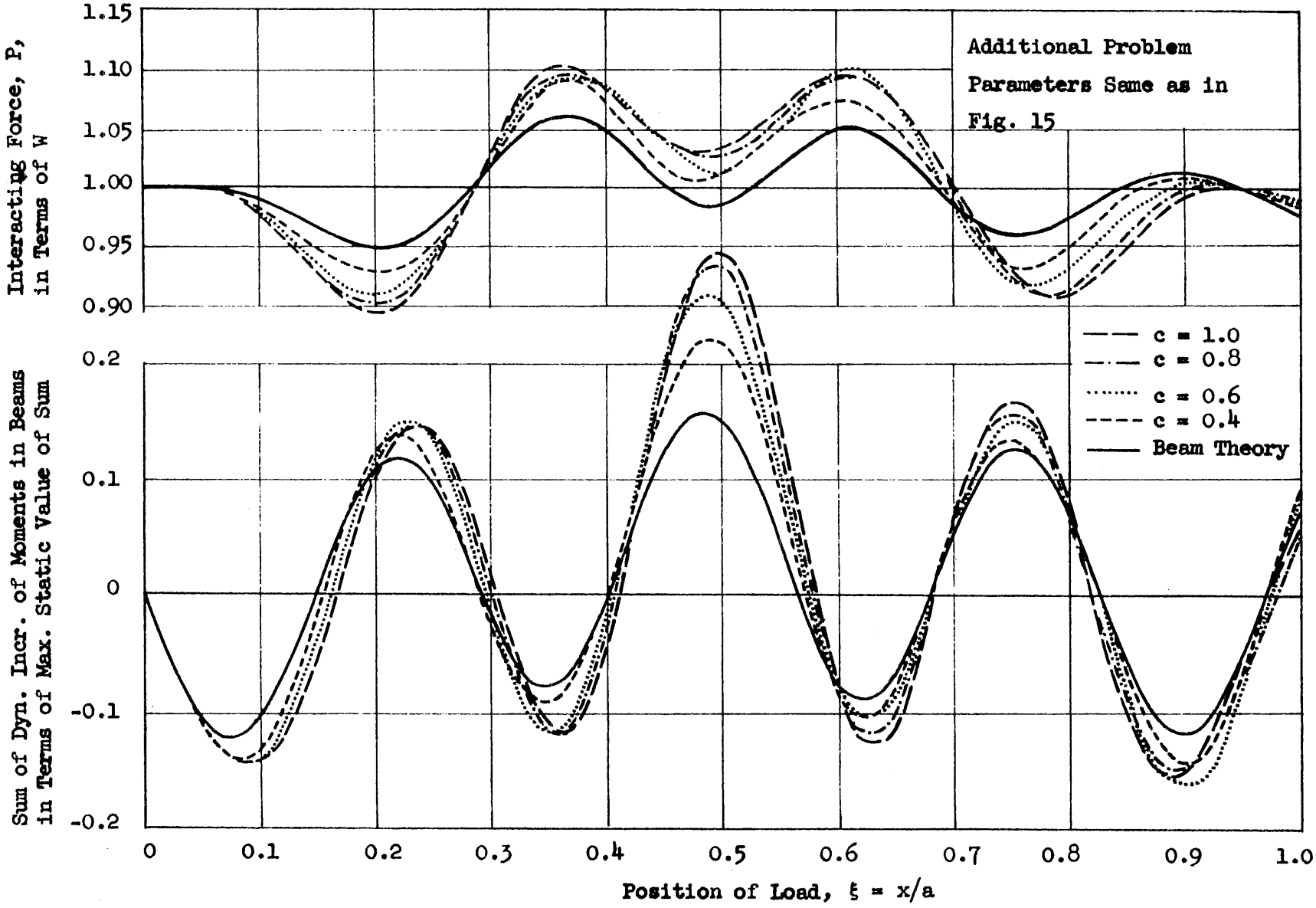

FIG. 27 HISTORY CURVES FOR INTERACTING FORCE AND SUM OF MOMENTS IN BEAMS -- EFFECT OF C
Load over Beam C; H = λc = 10

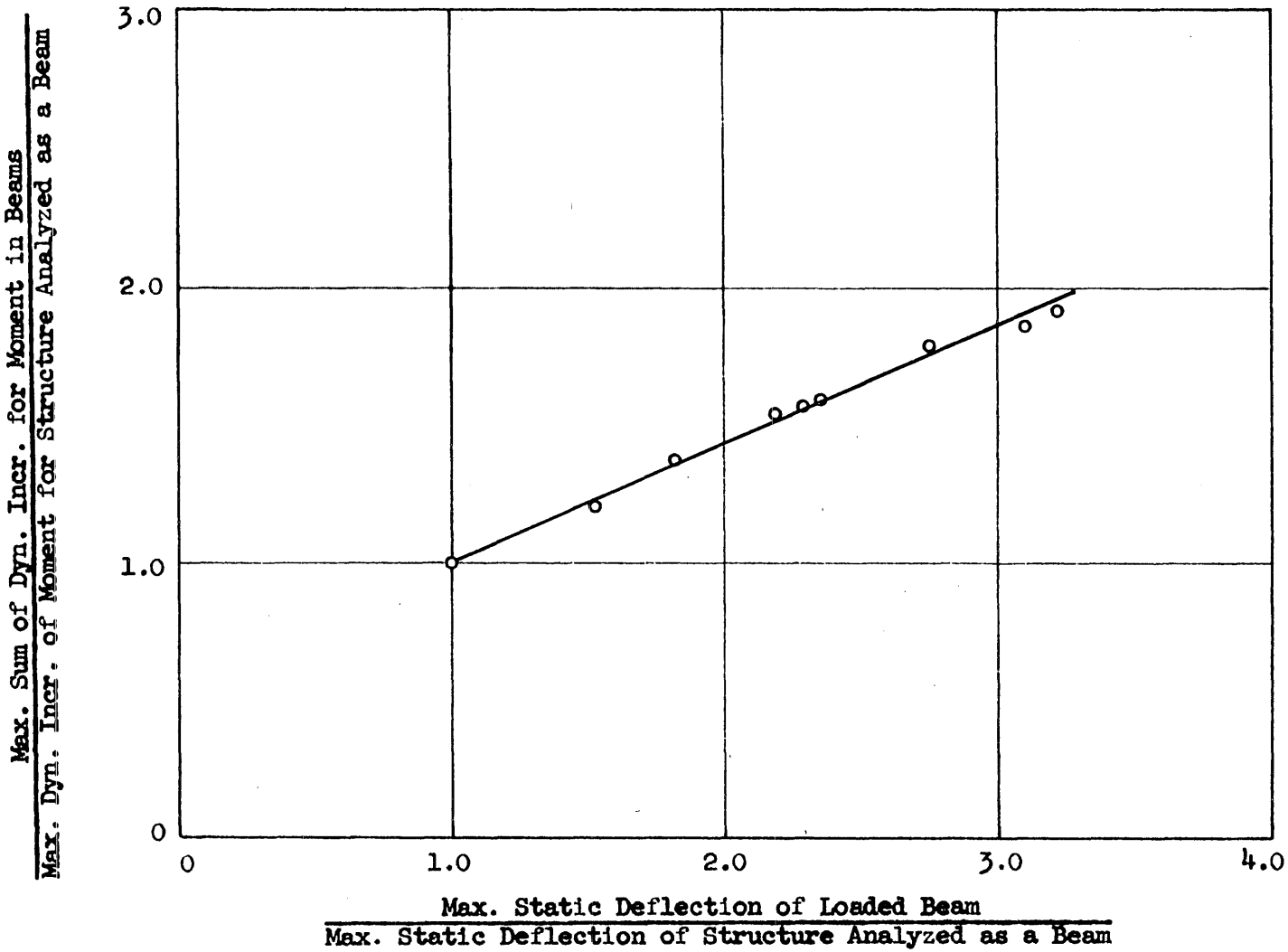

FIG. 28 RELATIONSHIP BETWEEN PEAK VALUES OF RESPONSE FOR ACTUAL STRUCTURE AND EQUIVALENT BEAM
Load over Beam C

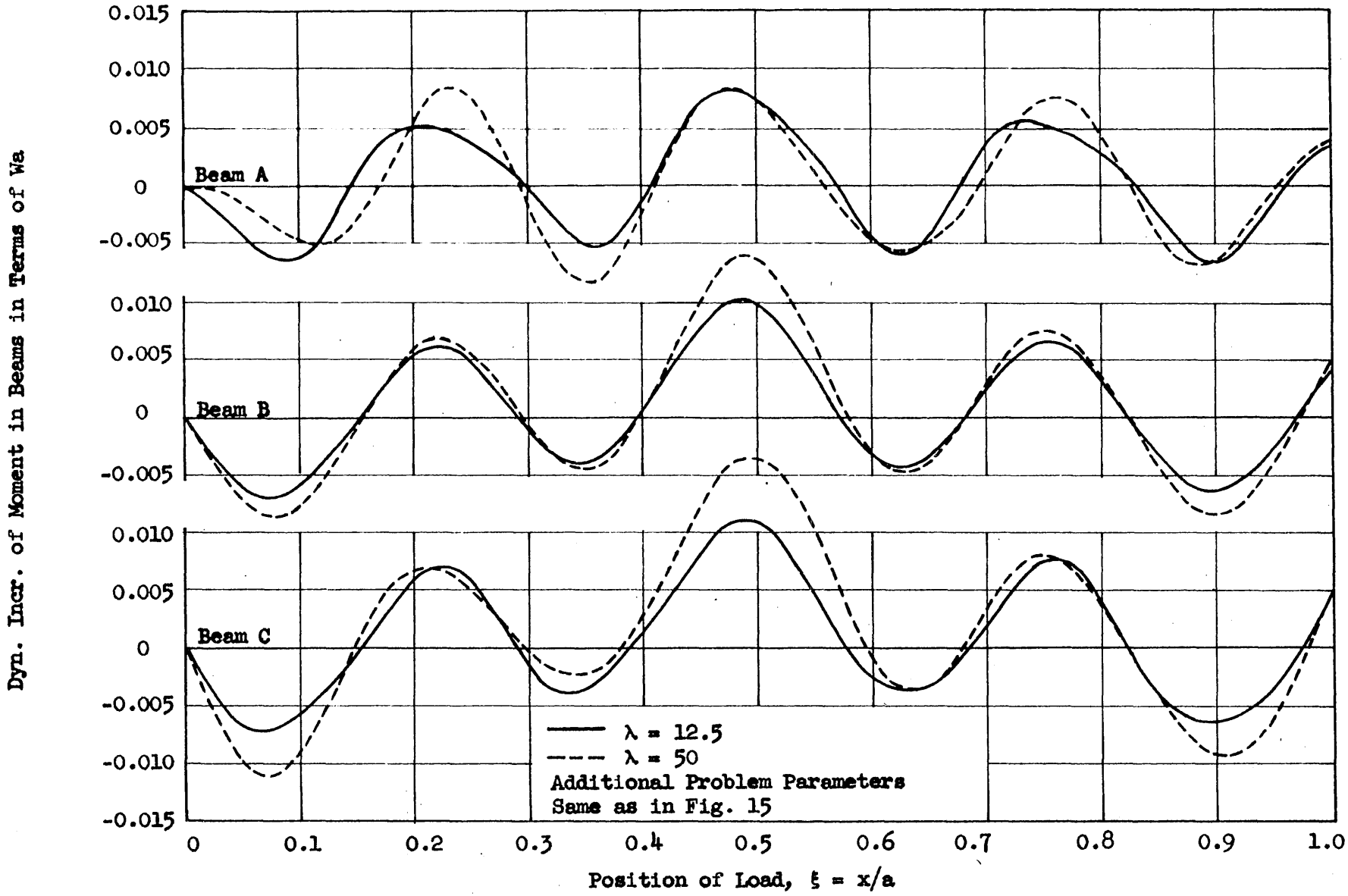

FIG. 29 HISTORY CURVES FOR DYNAMIC INCREMENT OF MOMENT IN BEAMS AT MIDSPAN -- EFFECT OF λ
Load over Beam C; c = 0.4

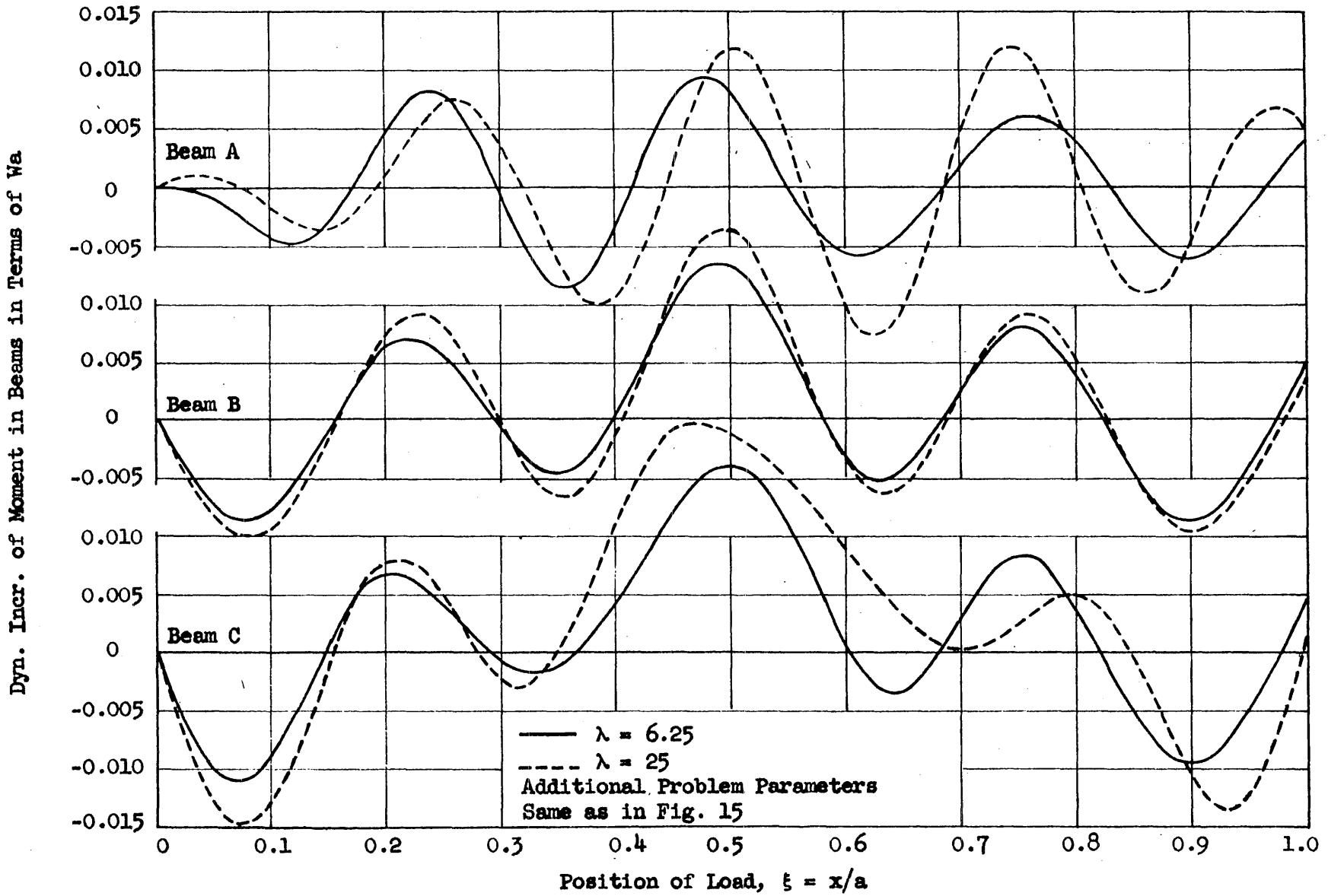

FIG. 30 HISTORY CURVES FOR DYNAMIC INCREMENT OF MOMENT IN BEAMS AT MIDSPAN -- EFFECT OF λ
Load over Beam C; c = 0.8

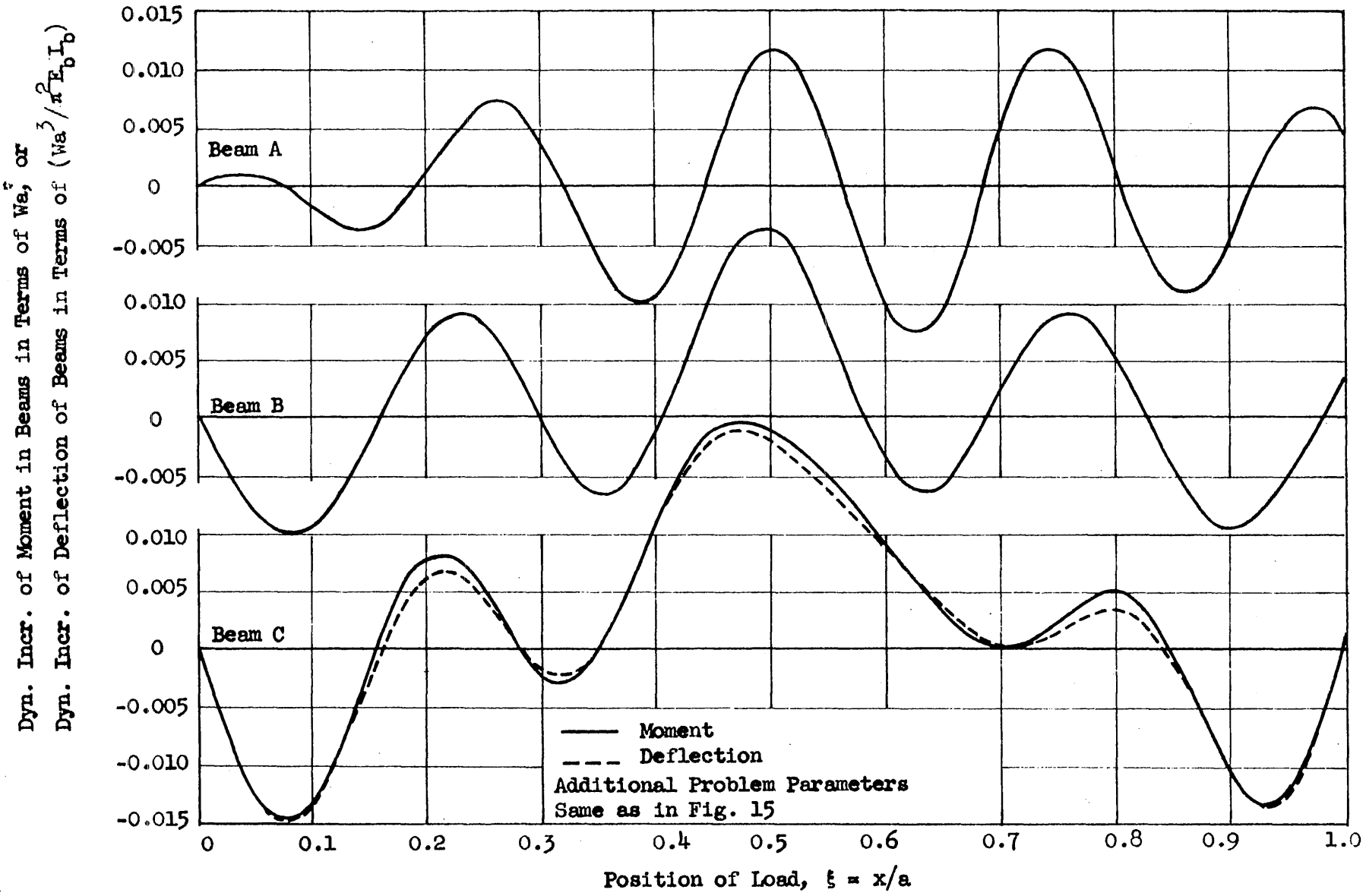

FIG. 31 CORRELATION BETWEEN DYNAMIC INCREMENTS FOR MOMENT AND DEFLECTION OF BEAMS AT MIDSPAN
Load over Beam C; c = 0.8; λ = 25

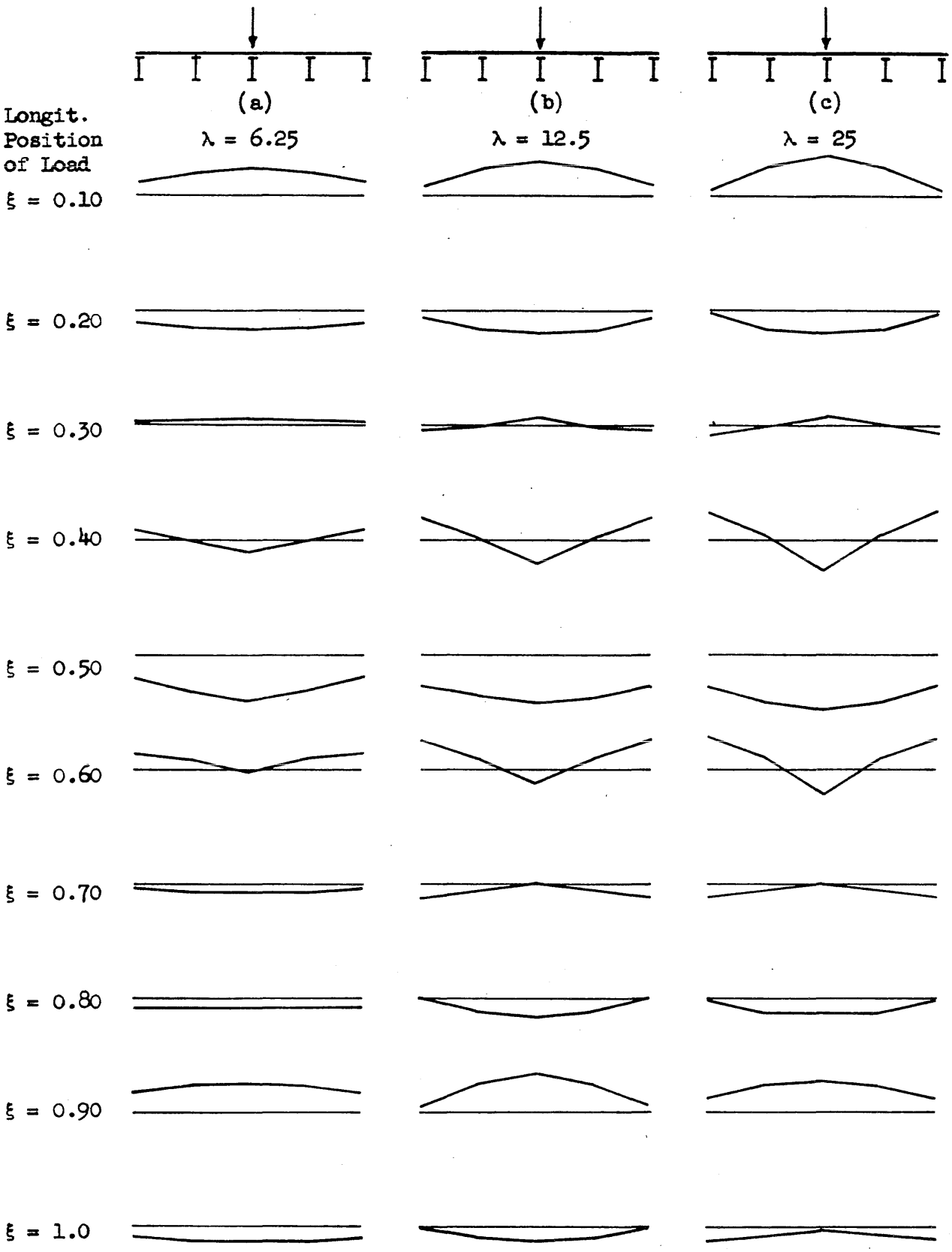

FIG. 32 INSTANTANEOUS TRANSVERSE DISTRIBUTION OF DYNAMIC INCREMENT OF MOMENT IN BEAMS -- EFFECT OF λ; Load over Beam C; c = 0.8

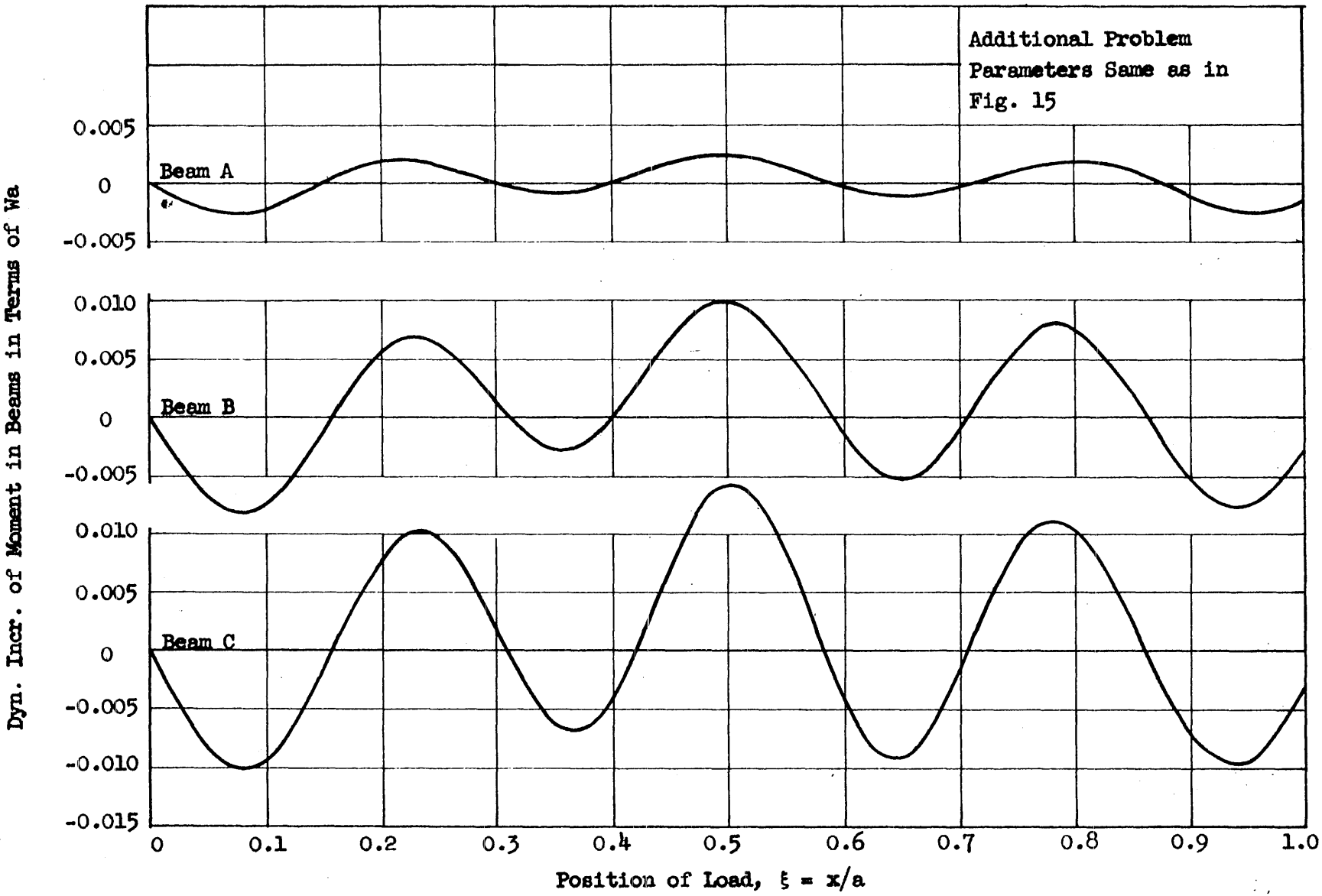

FIG. 33 HISTORY CURVES FOR DYNAMIC INCREMENT OF MOMENT IN BEAMS AT MIDSPAN
Loads over Beams B and D; c = 0.8; λ = 25

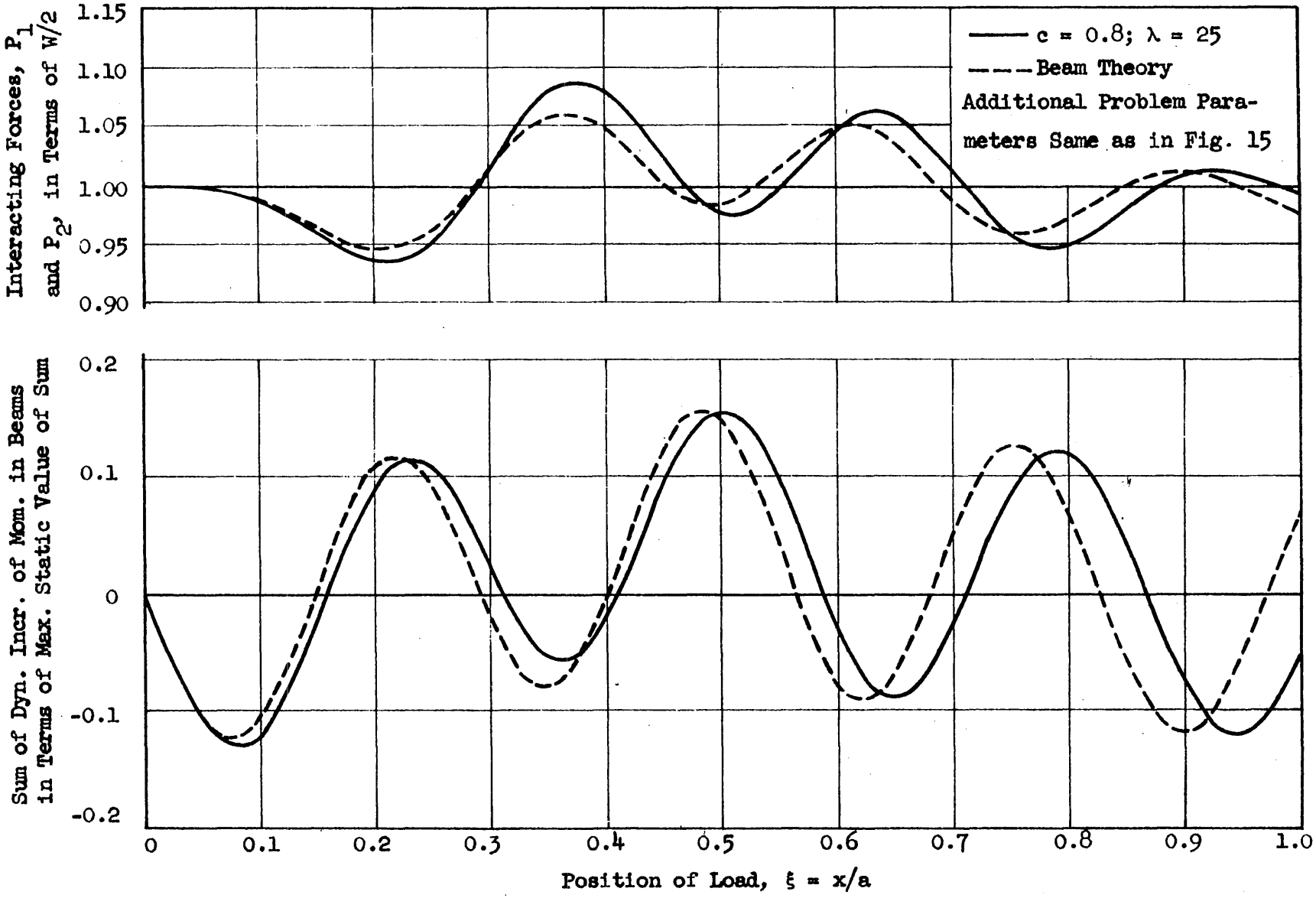

FIG. 34 HISTORY CURVES FOR INTERACTING FORCE AND SUM OF MOMENTS IN BEAMS
Loads over Beams B and D

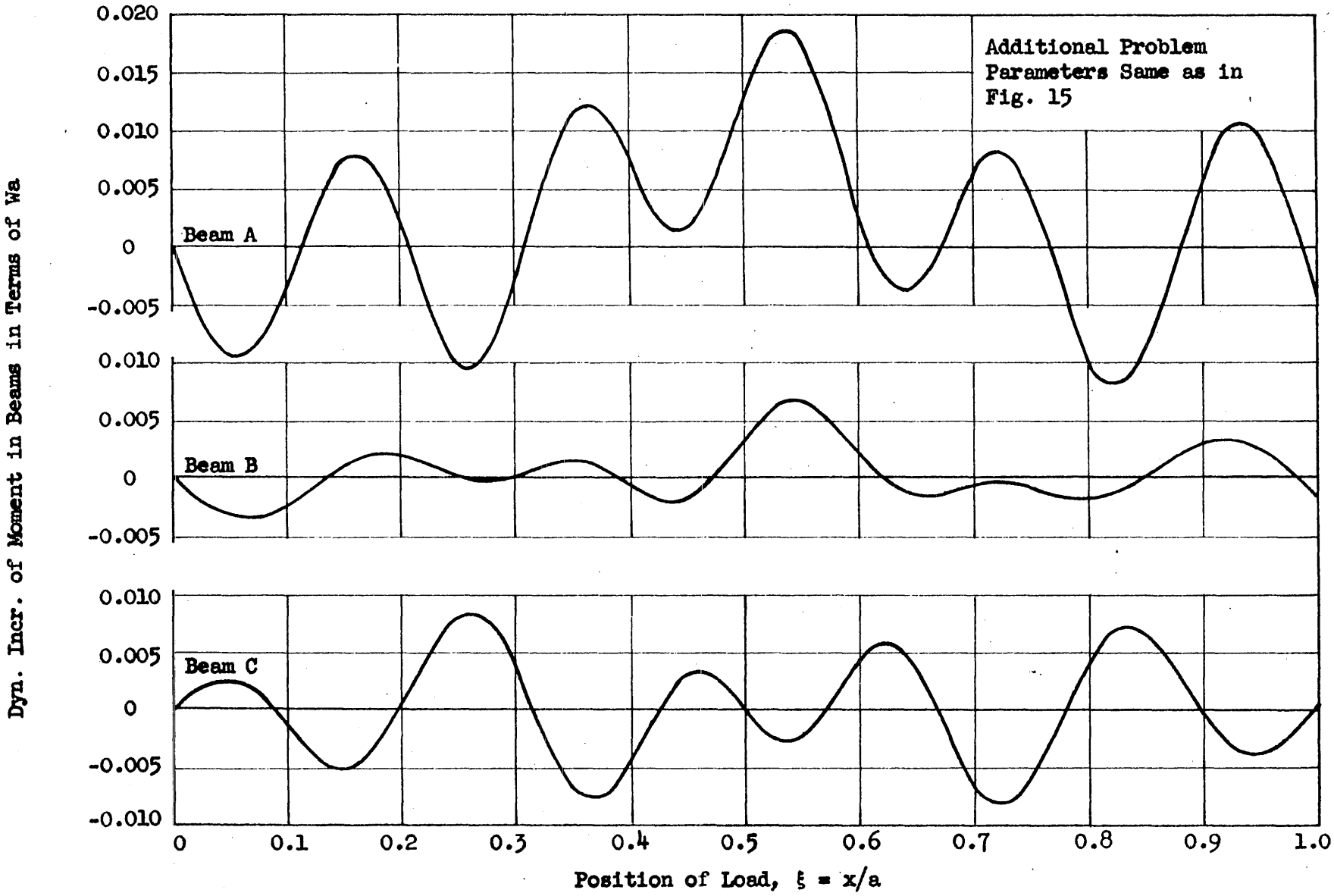

FIG. 35 HISTORY CURVES FOR DYNAMIC INCREMENT OF MOMENT IN BEAMS AT MIDSPAN
Loads over Beams A and E; c = 0.8; λ = 25

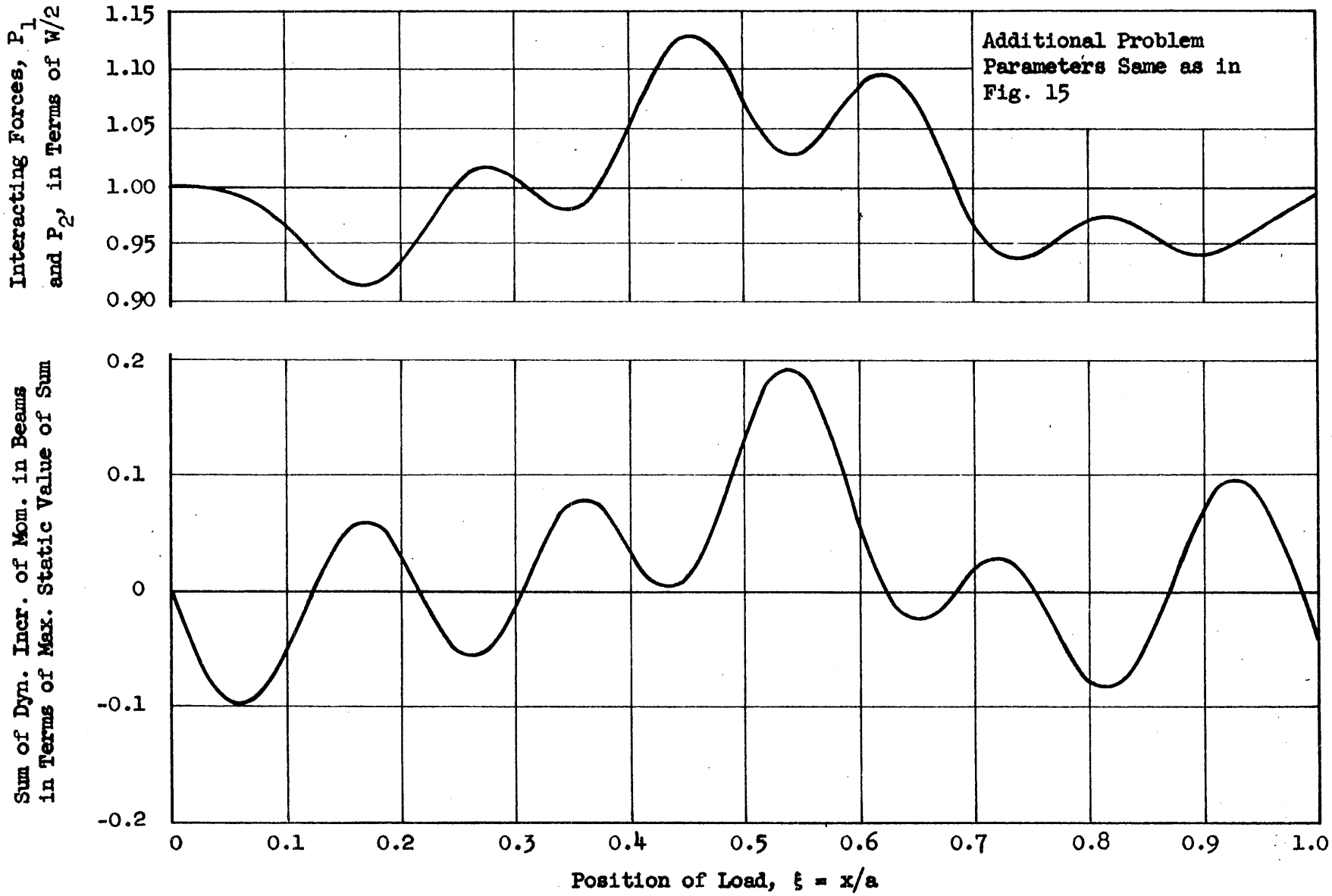

FIG. 36 HISTORY CURVES FOR INTERACTING FORCE AND SUM OF MOMENTS IN BEAMS
Loads over Beams A and E; c = 0.8; λ = 25

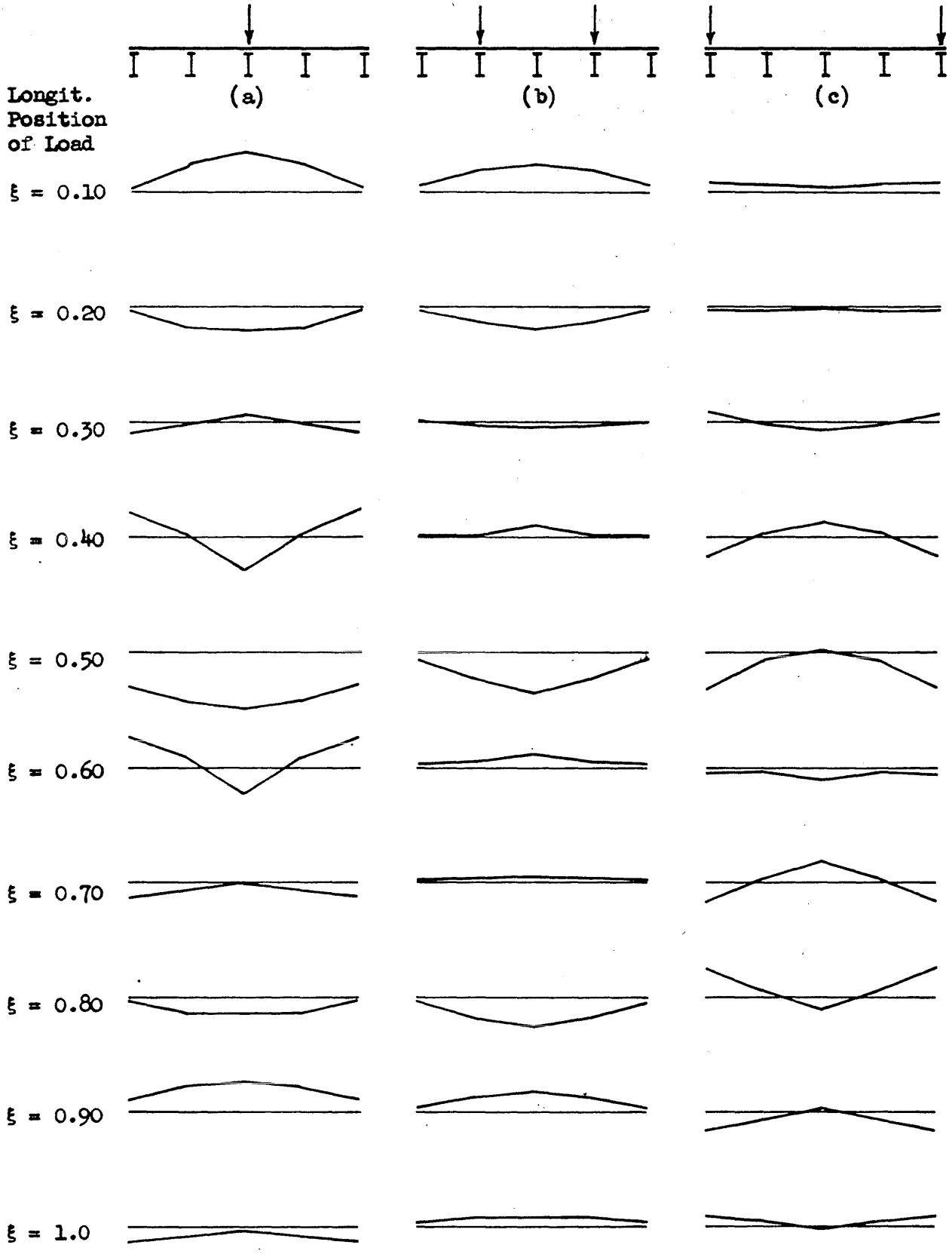

FIG. 37 INSTANTANEOUS TRANSVERSE DISTRIBUTION OF DYNAMIC INCREMENT OF MOMENT IN BEAMS -- EFFECT OF TRANSVERSE POSITION OF LOADS; $c = 0.8$, $\lambda = 25$

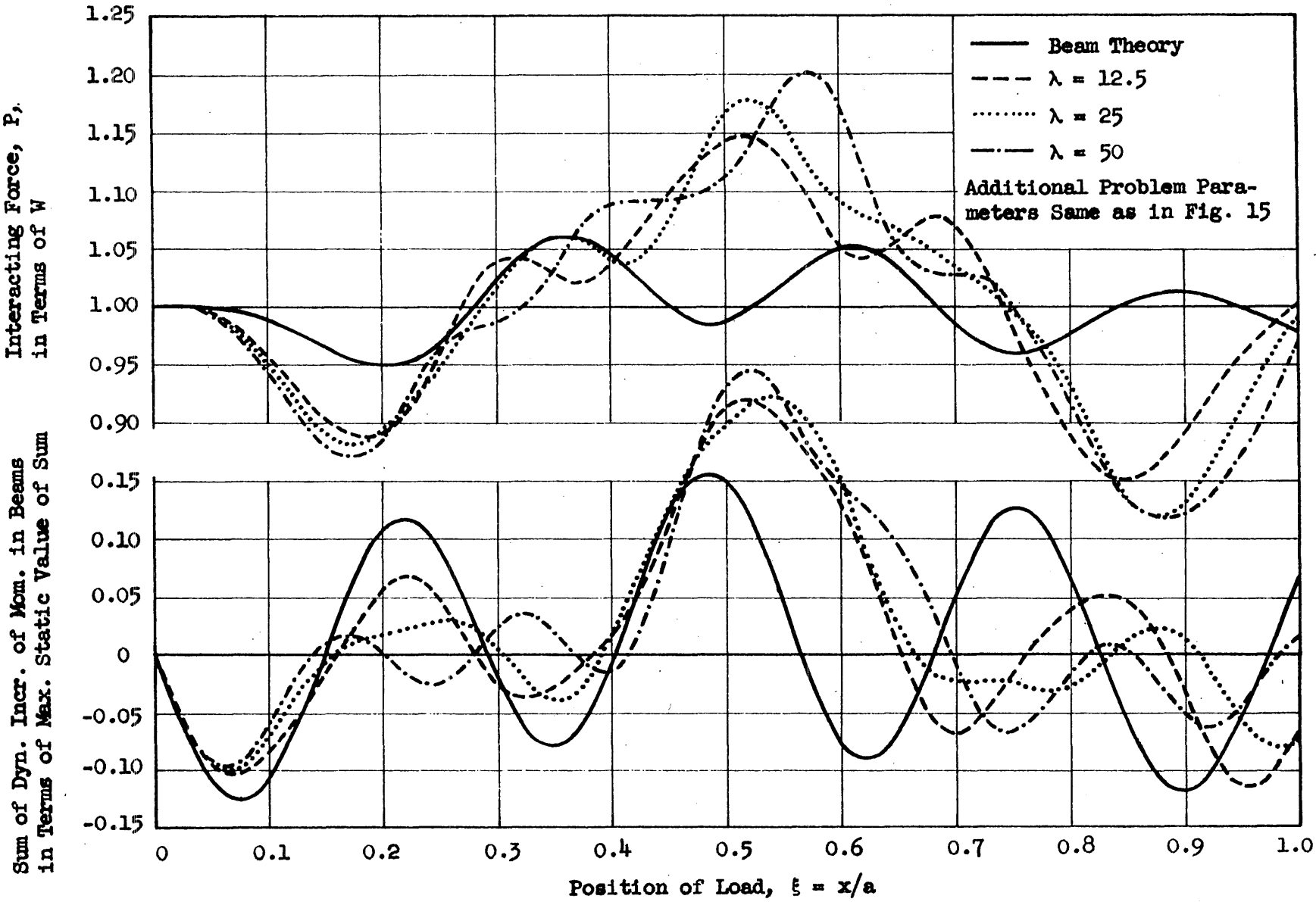

FIG. 38 HISTORY CURVES FOR INTERACTING FORCE AND SUM OF MOMENTS IN BEAMS -- EFFECT OF λ
Load over Beam A; c = 0.4

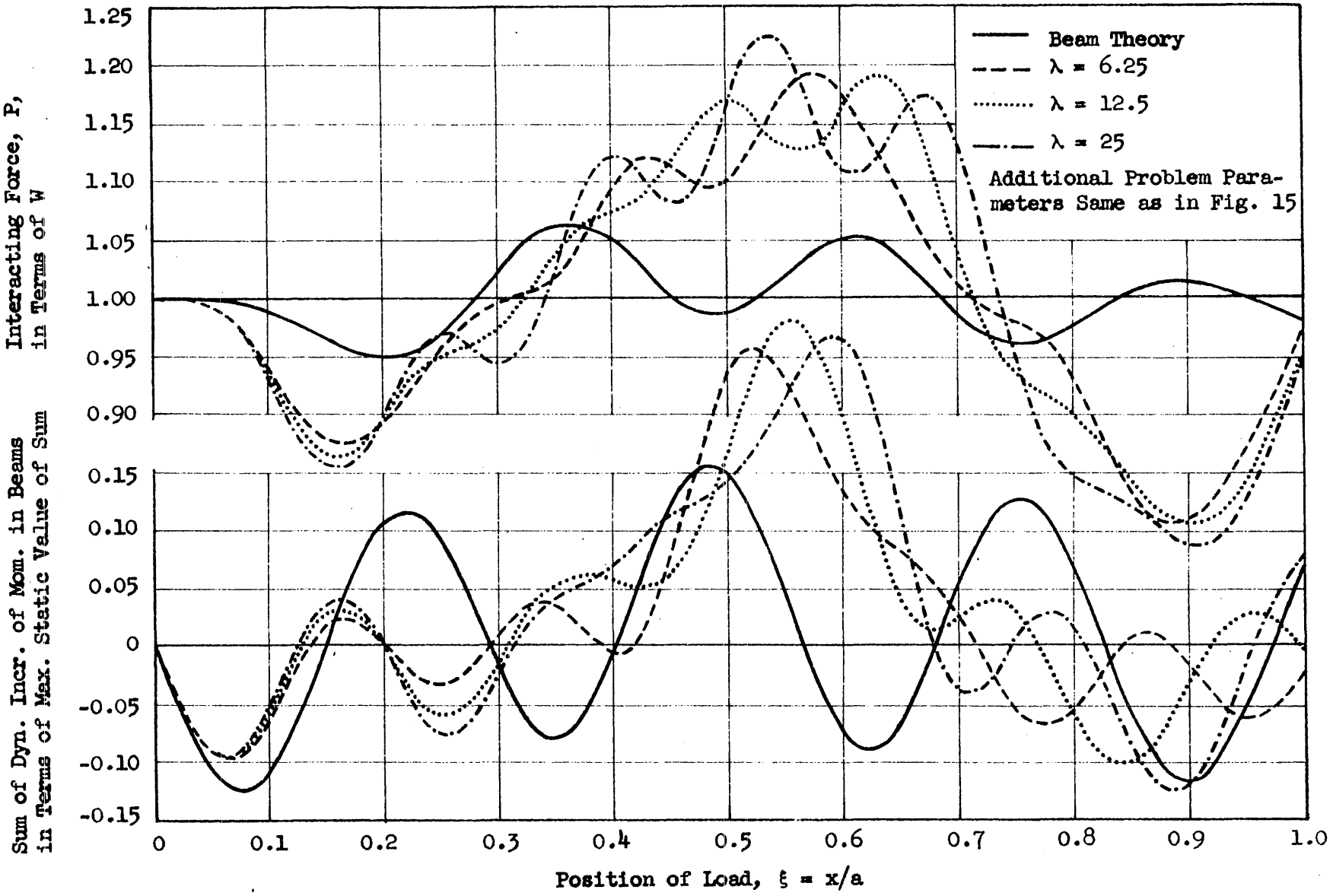

FIG. 39 HISTORY CURVES FOR INTERACTING FORCE AND SUM OF MOMENTS IN BEAMS -- EFFECT OF λ
Load over Beam A; c = 0.8

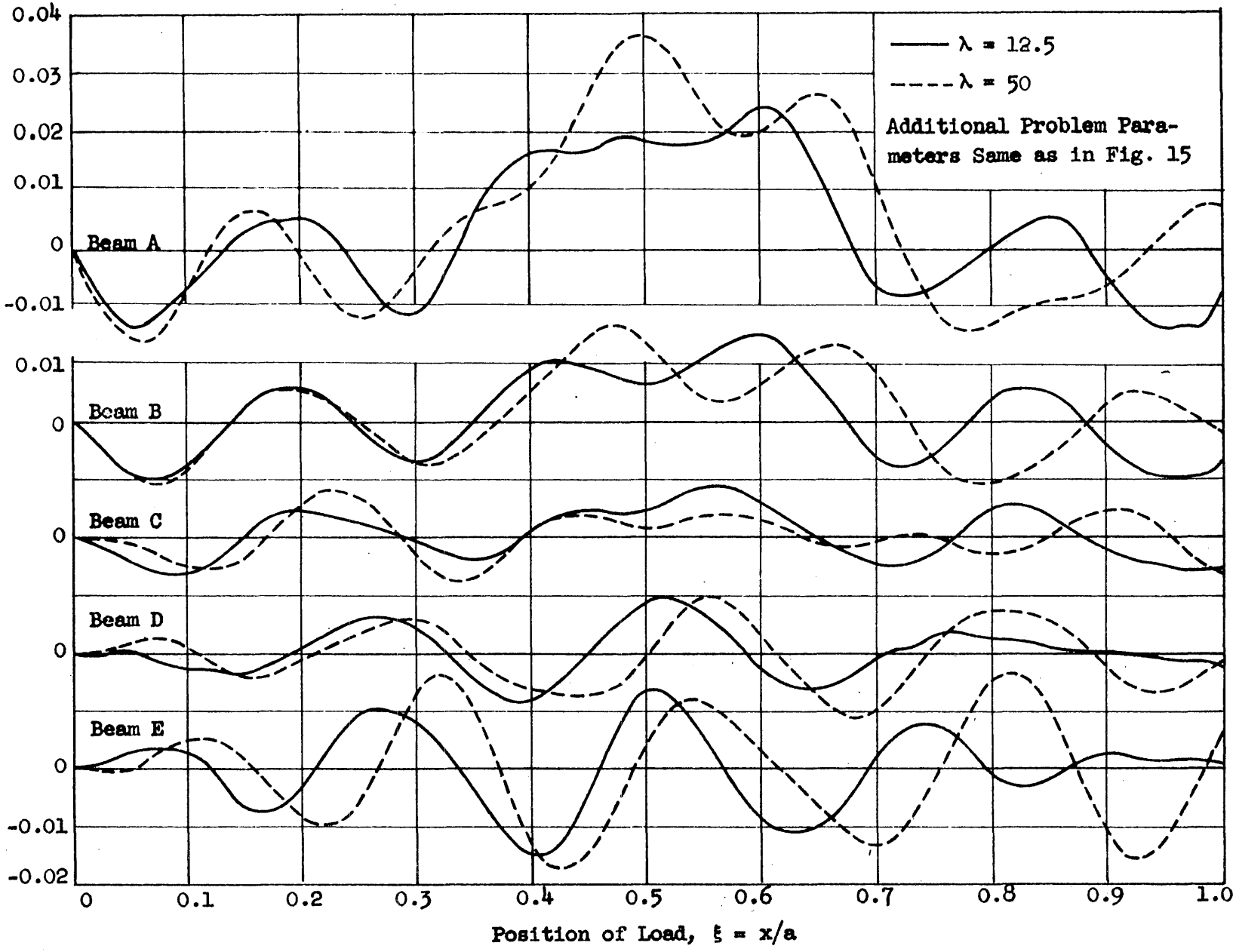

FIG. 40 HISTORY CURVES FOR DYNAMIC INCREMENT OF MOMENT IN BEAMS AT MIDSPAN -- EFFECT OF λ
Load over Beam A; c = 0.4

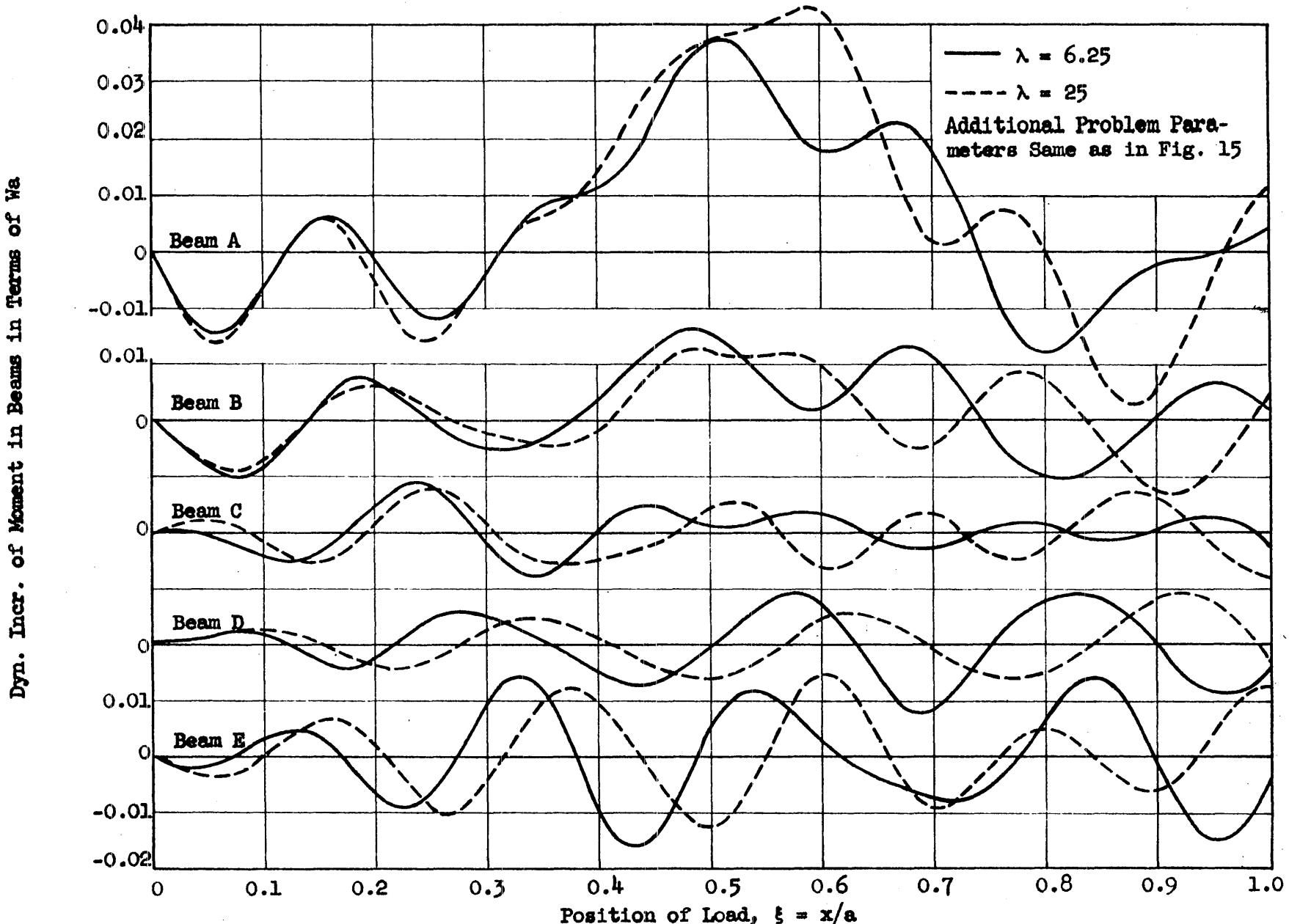

FIG. 41 HISTORY CURVES FOR DYNAMIC INCREMENT OF MOMENT IN BEAMS AT MIDSPAN -- EFFECT OF λ
Load over Beam A; c = 0.8

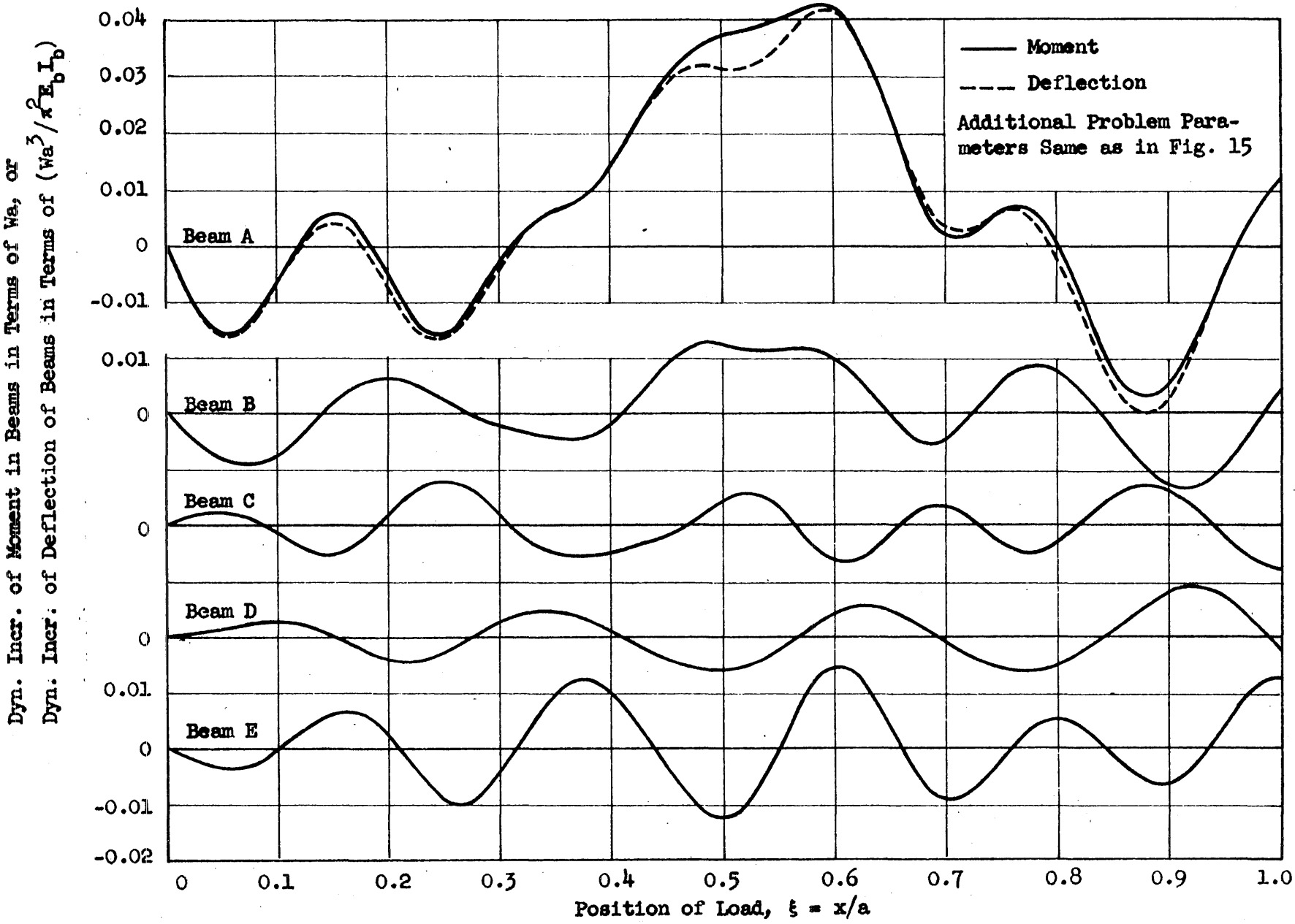

FIG. 42 CORRELATION BETWEEN DYNAMIC INCREMENTS FOR MOMENT AND DEFLECTION OF BEAMS AT MIDSPAN
Load over Beam A; c = 0.8; λ = 25

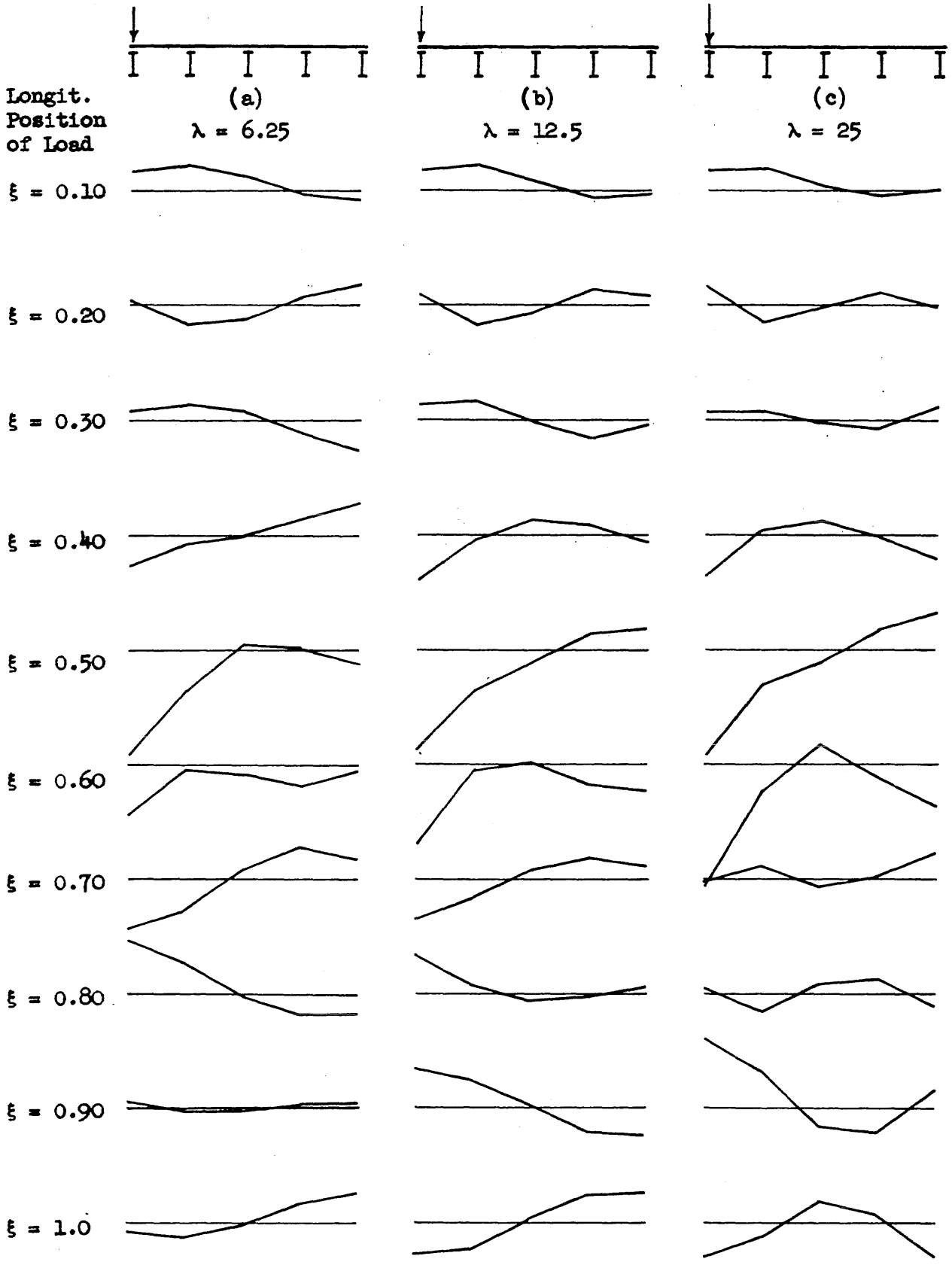

FIG. 43 INSTANTANEOUS TRANSVERSE DISTRIBUTION OF DYNAMIC INCREMENT OF MOMENT IN BEAMS -- EFFECT OF λ; Load over Beam A; c = 0.8

APPENDIX

DERIVATION OF GOVERNING DIFFERENTIAL EQUATIONS

A1. Lagrange's Equation for f_n

It can be verified that

$$\frac{\partial V_s}{\partial f_m} = \frac{\pi^4 D}{a^4}\,\frac{ab}{2}\,w_o^2 \sum_s A_{ns}\,(f_s+\delta_s) \tag{A-1}$$

$$\frac{\partial V_b}{\partial f_m} = \frac{\pi^4 D}{a^4}\,\frac{ab}{2}\,w_o^2 \sum_{i=0}^{p}\left[\lambda_i \sum_s (Y_n)_i (Y_s)_i (f_s+\delta_s) + \frac{k_i}{\pi^2 c^2}\sum_s (Y_n')_i (Y_s')_i (f_s+\delta_s)\right] \tag{A-2}$$

$$\frac{\partial V_{sp}}{\partial f_m} = k\sum_{j=1}^{2}\left[z+z_s-(w_i)_j+(-1)^j u b_1 - w_o \sin\frac{\pi v t}{a}\sum_s f_s (Y_s)_j\right]\left[-w_o (Y_n)_j \sin\frac{\pi v t}{a}\right] \tag{A-3}$$

By substituting

$$k\,z_s = \frac{gM}{2}$$

into Eq. (A-3), one obtains

$$\frac{\partial V_{sp}}{\partial f_m} = -w_o \sin\frac{\pi v t}{a}\sum_{j=1}^{2}(Y_n)_j\left\{\frac{gM}{2}+k\left[z-(w_i)_j - w_o \sin\frac{\pi v t}{a}\sum_s f_s (Y_s)_j + (-1)^j u b_1\right]\right\} \tag{A-4}$$

It can also be verified that

$$\frac{\partial U_s}{\partial f_n} = -\frac{2}{\pi}\,\mu g a b w_o \int_0^1 Y_n\, d\eta \tag{A-5}$$

$$\frac{\partial U_b}{\partial f_m} = -\frac{2}{\pi}\,a g w_o \sum_{i=0}^{p}(m_b)_i (Y_n)_i \tag{A-6}$$

$$\frac{\partial U_{sp}}{\partial f_m} = 0 \tag{A-7}$$

$$\frac{\partial U_w}{\partial f_m} = -mg w_o \sin\frac{\pi v t}{a}\sum_{j=1}^{2}(Y_n)_j \tag{A-8}$$

$$\frac{\partial T_s}{\partial f_n} = \frac{\partial T_b}{\partial f_n} = \frac{\partial T_{sp}}{\partial f_n} = 0 \tag{A-9}$$

$$\frac{\partial T_u}{\partial f_n} = m w_o \frac{\pi v}{a} \cos\frac{\pi v t}{a} \sum_{j=1}^{2} (Y_n)_j \left\{ \frac{v}{a} \left(\frac{\partial w_i}{\partial \xi}\right)_j + w_o \sum_s \left[f_s' \sin\frac{\pi v t}{a} + \frac{\pi v}{a} f_s \cos\frac{\pi v t}{a} \right] (Y_s)_j \right\} \tag{A-10}$$

$$\frac{d}{dt}\left(\frac{\partial T_s}{\partial f_n'}\right) = \frac{1}{2} \mu a b w_o^2 \sum_s f_s'' \int_0^1 Y_n Y_s \, d\eta \tag{A-11}$$

$$\frac{d}{dt}\left(\frac{\partial T_b}{\partial f_n'}\right) = \frac{1}{2} a w_o^2 \sum_{i=0}^{p} (m_b)_i \sum_s f_s'' (Y_n)_i (Y_s)_i \tag{A-12}$$

$$\frac{d}{dt}\left(\frac{\partial T_{sp}}{\partial f_n'}\right) = 0 \tag{A-13}$$

$$\frac{d}{dt}\left(\frac{\partial T_u}{\partial f_n'}\right) = m w_o \left[\frac{\pi v}{a} \cos\frac{\pi v t}{a} \sum_{j=1}^{2} (Y_n)_j \left\{ \frac{v}{a} \left(\frac{\partial w_i}{\partial \xi}\right)_j + w_o \sum_s \left[f_s' \sin\frac{\pi v t}{a} + \frac{\pi v}{a} f_s \cos\frac{\pi v t}{a} \right] (Y_s)_j \right\} + \sin\frac{\pi v t}{a} \sum_{j=1}^{2} (Y_n)_j \left\{ \left(\frac{v}{a}\right)^2 \left(\frac{\partial^2 w_i}{\partial \xi^2}\right)_j + w_o \left[f_s'' \sin\frac{\pi v t}{a} + 2\frac{\pi v}{a} f_s' \cos\frac{\pi v t}{a} - \left(\frac{\pi v}{a}\right)^2 f_s \sin\frac{\pi v t}{a} \right] (Y_s)_j \right\} \right] \tag{A-14}$$

By substituting Eqs. (A-1) through (A-14) into Eq. (3-2), dividing the resulting equation by w_o, and rearranging the terms, one obtains the following equation for the generalized coordinate f_n:

$$w_o \sum_s f_s'' \left[\frac{\mu ab}{2} \int_o^l Y_m Y_s \, d\eta + \frac{a}{2} \sum_{i=o}^{p} (m_b)_i (Y_m)_i (Y_s)_i + m \sin^2 \frac{\pi v t}{a} \sum_{j=1}^{2} (Y_m)_j (Y_s)_j \right]$$

$$+ w_o \sum_s f_s' \left[2m \left(\frac{\pi v}{a} \right) \sum_{j=1}^{2} (Y_m)_j (Y_s)_j \right] \sin \frac{\pi v t}{a} \cos \frac{\pi v t}{a}$$

$$+ w_o \sum_s f_s \left\{ \frac{\pi^4 D}{a^4} \frac{ab}{2} \left[A_{ns} + \sum_{i=o}^{p} \lambda_i (Y_m)_i (Y_s)_i + \sum_{i=o}^{p} \frac{k_i}{\pi^2 c^2} (Y_m')_i (Y_s')_i \right] \right.$$

$$\left. + k \sin^2 \frac{\pi v t}{a} \sum_{j=1}^{2} (Y_m)_j (Y_s)_j - m \left(\frac{\pi v}{a} \right)^2 \sin^2 \frac{\pi v t}{a} \sum_{j=1}^{2} (Y_m)_j (Y_s)_j \right\}$$

$$+ w_o \sum_s \delta_s \left\{ \frac{\pi^4 D}{a^4} \frac{ab}{2} \left[A_{ns} + \sum_{i=o}^{p} \lambda_i (Y_m)_i (Y_s)_i + \sum_{i=o}^{p} \frac{k_i}{\pi^2 c^2} (Y_m')_i (Y_s')_i \right] \right\}$$

$$- \sin \frac{\pi v t}{a} \sum_{j=1}^{2} (Y_m)_j \left[\frac{gM}{2} + k \left(z - (w_i)_j + (-1)^j u b_1 \right) \right]$$

$$- \frac{2}{\pi} \mu abg \int_o^l Y_n \, d\eta - \frac{2}{\pi} ag \sum_{i=o}^{p} (m_b)_i (Y_m)_i - mg \sin \frac{\pi v t}{a} \sum_{j=1}^{2} (Y_m)_j$$

$$+ m \left(\frac{v}{a} \right)^2 \sin \frac{\pi v t}{a} \sum_{j=1}^{2} (Y_m)_j \left(\frac{\partial^2 w_i}{\partial \xi^2} \right)_j = 0 \qquad \text{(A-15)}$$

Eq. (2-16), written in detail for the deflection of the bridge under its own weight, becomes for m = 1:

$$\sum_s (w_o \delta_s) \left[A_{ns} + \sum_{i=o}^{p} \lambda_i (Y_m)_i (Y_s)_i + \sum_{i=o}^{p} \frac{k_i}{\pi^2 c^2} (Y_m')_i (Y_s')_i \right]$$

$$= \frac{a^4}{\pi^4 D} \frac{2}{ab} \left[\frac{2}{\pi} \mu g ab \int_o^l Y_m \, d\eta + \frac{2}{\pi} ag \sum_{i=o}^{p} (m_b)_i (Y_m)_i \right] \qquad \text{(A-16)}$$

or

$$w_o \sum_s \delta_s \left\{ \frac{\pi^4 D}{a^4} \frac{ab}{2} \left[A_{ns} + \sum_{i=o}^{p} \lambda_i (Y_n)_i (Y_s)_i + \sum_{i=o}^{p} \frac{k_i}{\pi^2 c^2} (Y_n')_i (Y_s')_i \right] \right\}$$

$$- \frac{2}{\pi} \mu abg \int_o^1 Y_n \, d\eta - \frac{2}{\pi} ag \sum_{i=o}^{p} (m_b)_i (Y_n)_i = o \qquad \text{(A-17)}$$

By substituting Eq. (A-17) into Eq. (A-15) one obtains the equation (3-32) which was presented in the text.

A2. Lagrange's Equation for z

It can be shown that

$$\frac{\partial V_{sp}}{\partial z} = k \sum_{j=1}^{2} \left[z + z_s - (w + w_i)_j + (-1)^j u b_1 \right] \qquad \text{(A-18)}$$

$$\frac{\partial U_{sp}}{\partial z} = - Mg \qquad \text{(A-19)}$$

$$\frac{d}{dt} \left(\frac{\partial T_{sp}}{\partial z'} \right) = M z'' \qquad \text{(A-20)}$$

and that all other terms entering the Lagrange's equation for z are equal to zero. By substituting Eqs. (A-18) through (A-20) into Eq. (3-2), one obtains

$$k \sum_{j=1}^{2} \left[z + z_s - (w + w_i)_j + (-1)^j u b_1 \right] - Mg + M z'' = o \qquad \text{(A-21)}$$

Eq. (3-33) is obtained from Eq. (A-21) by noting that

$$k z_s = \frac{Mg}{2} \quad \text{and} \quad \sum_{j=1}^{2} (-1)^j u b_1 = o$$

A3. Lagrange's Equation for u

It can be shown that

$$\frac{\partial V_{sp}}{\partial u} = k b_1 \sum_{j=1}^{2} (-1)^j \left[z + z_s - (w + w_1)_j + (-1)^j u b_1 \right] \qquad \text{(A-22)}$$

$$\frac{d}{dt}\left(\frac{\partial T_{sp}}{\partial u'}\right) = J u'' \qquad \text{(A-23)}$$

and that all other terms entering the Lagrange's equation for u are equal to zero. By substituting Eqs. (A-22) and (A-23) into Eq. (3-2), one obtains

$$k b_1 \sum_{j=1}^{2} (-1)^j \left[z + z_s - (w + w_1)_j + (-1)^j u b_1 \right] + J u'' = 0 \qquad \text{(A-24)}$$

Eq. (3-34) is obtained from Eq. (A-24) by noting that

$$\sum_{j=1}^{2} (z + z_s)(-1)^j = 0$$